Aus dem

Department für Frauengesundheit Tübingen

Forschungsinstitut für Frauengesundheit

The molecular determinates of endometrial physiology in reproductive failure

Inaugural-Dissertation
zur Erlangung des Doktorgrades
der Medizin

der Medizinischen Fakultät
der Eberhard Karls Universität
zu Tübingen

vorgelegt von

Yang, Zhiqi

2025

Dekan:	Professor Dr. B. Pichler
1. Berichterstatter:	Dr. M. S. Salker
2. Berichterstatter:	Privatdozentin Dr. L. Pelzl
3. Berichterstatter:	Dr. Viet Loan Dao Thi
Tag der Disputation:	29.07.2025

Table of Contents

List of Tables

List of Figures

List of Abbreviations

$[Ca^{2+}]_i$	Cytosolic Ca^{2+} concentration
ACTB	β-actin
AR	Androgen receptor
ASK1	Apoptosis signal-regulating kinase 1
ATP	Adenosine triphosphate
CACNA1C	L-type voltage gated Ca^{2+} channel
cAMP	Cyclic adenosine monophosphate
CAT	Catalase
COX2	Cyclooxygenase-2
CPM	Counts per million
Ct	Cycle threshold
DCC	Dextran coated charcoal
DCFDA	2',7'−dichlorofluorescin diacetate
DMSO	Dimethyl sulfoxide
E_2	Estradiol
EBAF	Endometrial bleeding associated factor
ECM	Embryo culture media
ECM	Extracellular matrix
EEC	Endometrial epithelial cells
EMT	Epithelial-mesenchymal transition
ENaC	Epithelial sodium channel
eNOS	Endothelial nitric oxide synthase
EnSCs	Human endometrial stromal cells
ERs	Estrogen receptors

ETC	Mitochondrial electron transport chain
FACS	Fluorescence-activated cell sorting analysis
FBS	Fetal bovine serum
FDR	False discovery rate
FSH	Follicle stimulating hormone
GEO	Gene Expression Omnibus
GLRX	Glutaredoxin
GLUT	Glucose transporter molecules
GnRH	Gonadotropin releasing hormone
GO	Gene Ontology
GPCRs	G protein-coupled receptors
GPX	Glutathione peroxidase
GSH	Glutathione
GSSG	Glutathione disulfide
H_2O_2	Hydrogen peroxide
HB-EGF	Heparin-binding epidermal growth factor
HCD	Higher energy collisional dissociation
hCG	Human chorionic gonadotropin
IF	Immunofluorescence
Ig	Immunoglobulin
IGFBP-1	Insulin-like growth factor binding protein-1
IHC	Immunohistochemistry
ISK	Ishikawa cells
ITGA5	Integrin subunit alpha 5
IVF	*In vitro* fertilization
KEGG	Kyoto Encyclopedia of Genes and Genomes

LEFTY2	Left-right determination factor 2
LH	Luteinizing hormone
LIF	Leukemia inhibitory factor
MMP14	Matrix metallopeptidase 14
MPA	Medroxyprogesterone acetate
NaCl	Sodium chloride
NOX	NADPH oxidases
O_2^-	Superoxide
OH^-	Hydroxyl radical
OS	Oxidative stress
P_4	Progesterone
PARK7	Parkinson disease protein 7
PD	Parkinson's disease
PE	Preeclampsia
PFA	Paraformaldehyde
PGE_2	Prostaglandin E_2
PI	Propidium Iodide
PKA	Protein kinase A
PRL	Prolactin
PRs	Progesterone receptors
qRT-PCR	Quantitative real-time polymerase chain reaction
ROS	Reactive oxygen species
RT	Room temperature
SASP	Senescence-associated secretory phenotype
SDS	Sodium dodecyl sulfate
SO_2H	Sulfinic

SO_3H	Sulfonic
SOCE	Store operated Ca^{2+} entry
SOD	Superoxide dismutase
SOH	Sulfenic
TF	Tissue factor
TGF	Transforming growth factor
TGF	Transforming growth factor
TMX3	Thioredoxin related transmembrane protein 3
TXNRD1	Thioredoxin reductase 1
UMAP	Uniform manifold approximation and projection
WNT4	WNT family member 4
WT	Wild-type
wt-DJ-1	pGW1-Myc-DJ-1-wt

1. Introduction

1.1 Endometrial Anatomy and Physiology

1.1.1 The Human Endometrium and the Menstrual Cycle

The reproductive system in females is important for providing the appropriate environment for fertilization, ensuring the uterus is primed for implantation, supporting early embryo development, and nourishing the growing fetus until birth (Colvin & Abdullatif, 2013). It consists of ovaries, fallopian tubes, uterus, vagina, and external genitalia (Colvin & Abdullatif, 2013). Furthermore, the uterus is a pivotal organ in which the menstrual cycle and pregnancy occur. The uterus consists of three different layers: the proximal part - endometrium, the middle part - myometrium, and the distal part - perimetrium (Maybin & Critchley, 2015). Out of these, the endometrium is an essential component of the female uterus, as it contributes significantly to processes such as menstruation, implantation and pregnancy (Maybin & Critchley, 2015). Structurally, endometrium is composed of epithelial cells, both luminal and glandular, surrounded by stromal cells, immune cells, and endothelial cells that make up the uterine vasculature (Holdsworth-Carson et al., 2023; J. Wang et al., 2024). In the terms of morphology, it is divided into stratum basalis and stratum functionalis, with stratum functionalis undergoing cyclical changes in thickness and structure under the influence of ovarian steroids (**Figure 1-1**) (Jarrell, 2018; Mihm et al., 2011). Furthermore, physiologically, the endometrium facilitates menstruation in the absence of pregnancy, prepares for implantation, and supports pregnancy when implantation occurs (Critchley et al., 2020).

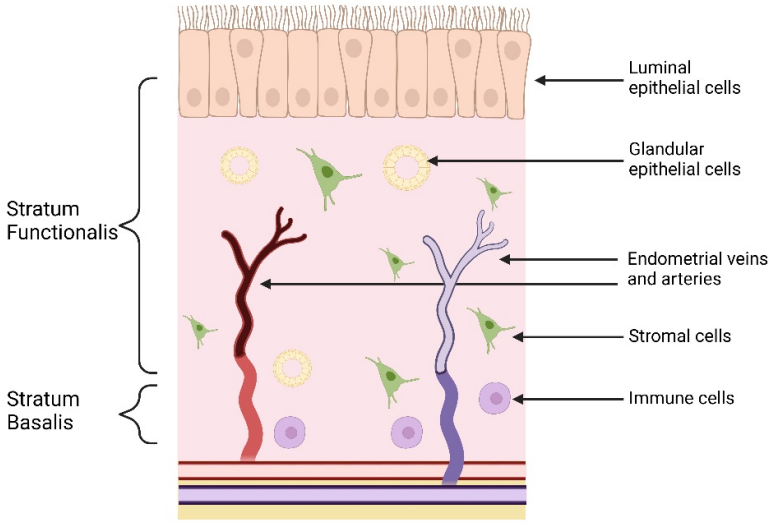

Figure 1-1: Physiological Structures within the Endometrium.

This diagram illustrates the histological structure of the endometrium, which contains two functional layers: the stratum functionalis and the stratum basalis. Key cellular components are labelled, including luminal epithelial cells, glandular epithelial cells, immune cells, stromal cells, and endometrial veins and arteries. Figure adapted from previous studies (Jarrell, 2018; Mihm et al., 2011). Created with BioRender.com.

The endometrium undergoes dynamic cyclical remodeling regulated by hormones, which maintain its functionality and reproductive health (**Figure 1-2**) (Gellersen & Brosens, 2014). This remodeling is conducted by intricate hormonal regulation, primarily orchestrated by the hypothalamus, which releases gonadotropin-releasing hormone (GnRH). GnRH stimulates the pituitary gland, and further produce follicle-stimulating hormone (FSH) and luteinizing hormone (LH), which play critical roles in ovarian and endometrial dynamics (Deligdisch-Schor & Mares Miceli, 2020; Olivennes et al., 2002). During the estradiol (E_2)-driven follicular phase (proliferative phase), FSH promotes ovarian follicle development, leading to rising E_2 levels (Wu et al., 2022). This increasing can further drive the rise in the number of epithelial cells in the endometrium, preparing the uterine lining for potential implantation. Conversely, LH triggers oocyte maturation, ovulation, and the release of ovum from ovary (Deligdisch-Schor & Mares Miceli, 2020). Following ovulation, the cycle progresses into the luteal phase (secretory phase), during which progesterone (P_4) secretion by the ovary inhibits E_2-driven proliferation, initiates

stromal cell decidualization, and facilitates the transformation of the endometrium into a receptive tissue suitable for implantation and pregnancy (Mihm et al., 2011; Okada et al., 2018). Morphologically, the receptive endometrium displays features such as an edematous stroma, pseudostratified, columnar, and polarized luminal epithelium, highly secretory glands, as well as the presence of pinopodes on luminal epithelial cells (Ashary et al., 2018; Lessey & Young, 2019; Nikas & Aghajanova, 2002). The two main types of estrogen receptors (ER) — α and β, along with progesterone receptors (PRs), are responsible for mediating the effects of E_2 and P_4 (Li & O'Malley, 2003). Notably, two isoforms of PR, PR-B (the full-length form) and PR-A (the short form), are encoded by a single gene. Among these, PR-A plays a dominant role in the decidualization of endometrial stromal cells (EnSCs) not only *in vitro*, but also in the biological environment. These coordinated hormonal interactions underscore the complexity of the menstrual cycle and its critical role in reproduction (Cope & Monsivais, 2022).

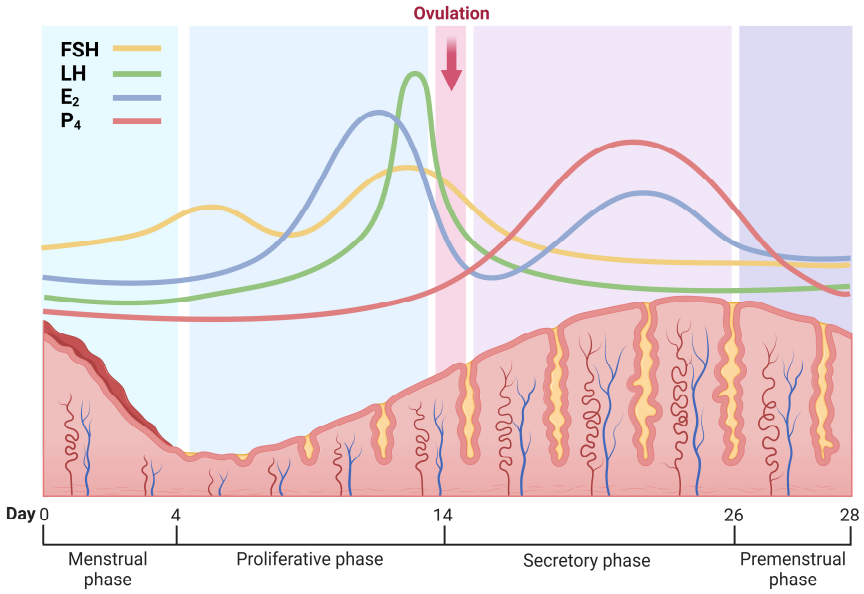

Figure 1-2: The Pituitary and Ovarian Hormonal Fluctuations during Menstrual Cycle.

During the proliferative phase of menstrual cycle, FSH enhances the growth of ovarian follicles, which results in an increasing level of E_2. The first peak in E_2 results in a rise of LH and ovulation, which indicates the beginning of the secretory phase. Endometrial decidualization is initiated by P_4, and is essential for the establishment of an appropriated implantation environment. In the absence of implantation, P_4 levels drop can trigger menstruation. Figure adapted from a previous study (Gellersen & Brosens, 2014). Created with BioRender.com.

These interconnected systems and hormonal regulations govern fertility, reproduction, and the stages of a woman's life, from menarche to menopause. Menarche is defined as the first menstrual period in a female adolescent. It commonly occurs between the ages of 10 and 16, with an average onset age of 12.4 years (Marques et al., 2022). It marks the beginning of the reproductive years, which is characterized by regular menstrual cycles driven by hormonal changes (Marques et al., 2022). The menstrual cycle includes phases of follicular development, ovulation, and the luteal phase, during which the endometrium is prepared for a potential pregnancy (Munro et al., 2018). This cycle usually lasts about 24 to 38 days, but can vary among individuals (Munro et al., 2018). With increasing age in women, the ovaries' ability to produce ova and hormones declines. Ultimately, menstrual cycles terminate at menopause, which typically occurs around age 51, implying the end of a woman's reproductive capacity (Coast et al., 2019). Therefore, understanding the female reproductive system is essential for addressing health concerns and supporting women's reproductive health throughout their lifespan.

1.1.2 Decidualization

Decidualization is a complex morphological and biochemical reprogramming process, in which the endometrium prepares itself to support a potential pregnancy (Gellersen et al., 2007). This transformation is critical for embryo implantation, placentation, and pregnancy maintenance. It involves postovulatory endometrial remodeling, including vascular reorganization, secretion of various cytokines, growth factors and adhesion molecules, EnSCs differentiation, and the assembly of immune cells including natural killer cells, macrophages, and dendritic cells (Gellersen & Brosens, 2014). During decidualization, human endometrial stromal cells (EnSCs) exhibit extensive proliferation and differentiation abilities. The EnSCs undergo morphological changes, during which EnSCs become rounded and acquire myofibroblast-like characteristics. They also secrete different kinds of proteins, such as prolactin (PRL), as well as insulin-like growth factor binding protein-1 (IGFBP-1) (**Figure 1-3**)(Gellersen et al., 2007; Ramathal et al., 2010). In humans, the process of decidualization initiates about 6 days post-ovulation during each

menstrual cycle. This process takes place independently of whether a blastocyst is implanting (Ochoa-Bernal & Fazleabas, 2020). This phenomenon, known as spontaneous decidualization, is unique to humans and a few other higher primates, such as chimpanzees and baboons. Conversely, most other mammals exhibit induced decidualization, where the process is triggered only in response to embryo implantation (Gellersen & Brosens, 2014).

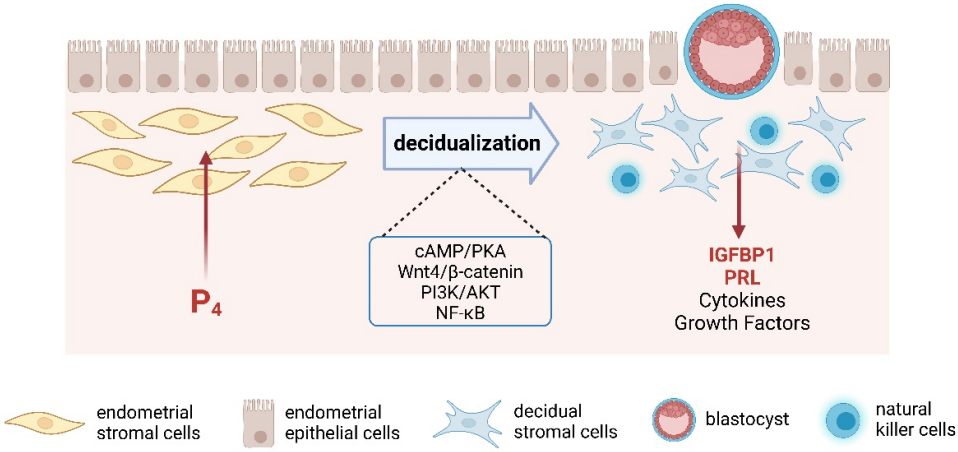

Figure 1-3: Morphological Changes during Decidualization.

Decidualization is a morphological and biochemical reprograming process. During decidualization, EnSCs exhibit extensive proliferation and differentiation abilities, and these EnSCs becomes rounded, uterine natural killer cells accumulate and vessels start remodelling. Figure adapted from previous studies (Gellersen et al., 2007; Ramathal et al., 2010). Created with BioRender.com.

Decidualization is initiated by hormonal signals, primarily progesterone acting *via* the progesterone receptor (PR), in the context of estrogen priming (Okada et al., 2018). The effects of progesterone are amplified by cyclic AMP (cAMP), a ubiquitous second messenger molecule synthesized from adenosine triphosphate (ATP) by the enzyme adenylate cyclase (Ould Amer & Hebert-Chatelain, 2018). This synthesis is triggered when ligands bind to G protein-coupled receptors (GPCRs) on the cell membrane (Dunn et al., 2003). cAMP activates protein kinase A (PKA), which further cause the phosphorylation of transcription factors such as cAMP response element-binding protein (CREB) (Peng et al., 2021). This activation enhances chromatin remodeling and drives the expression of key decidualization genes, including IGFBP-1 and PRL (Tang, Mazella, et al.,

2005). Medroxyprogesterone acetate (MPA), a synthetic progestin, can mimic the effects of natural progesterone by binding to PR. It promotes the expression of decidualization genes, and support stromal cell differentiation (Cloke et al., 2008). Additionally, MPA has affinity for the glucocorticoid receptor (GR), which plays a role in immune modulation and tissue remodeling during decidualization (Bamberger et al., 1999). GR activation regulates immune responses by limiting excessive inflammation and suppressing pro-inflammatory cytokines such as TNF-α and IL-6, creating an immune-tolerant environment (Bereshchenko et al., 2018; Whirledge et al., 2015). Cross-talk between PR and GR pathways further modulates gene expression and cellular differentiation, with MPA acting as a dual modulator through its interaction with both receptors (Pecci et al., 2022). Furthermore, during pregnancy, the decidua is exposed to elevated levels of human chorionic gonadotropin (hCG), which is a glycoprotein hormone primarily produced by the syncytiotrophoblast cells of the developing placenta. hCG predominantly signals through the cAMP pathway, promoting further decidualization and supporting the maintenance of early pregnancy by modulating immune responses and facilitating vascular remodeling (Kasahara et al., 2001). Alongside this, the PI3K-AKT pathway, stimulated by growth factors like IGF-1, supports cell survival and metabolic reprogramming (Yin et al., 2012). Correspondingly, Wnt4, regulated by BMP2 and linked to FoxO1 cytoplasmic shuttling, is vital for stromal cell survival and differentiation (Carson et al., 2002). Functional inhibition of β-catenin impairs BMP2-Wnt4-induced decidualization, highlighting the Bmp2-Wnt4/β-catenin-FoxO1 pathway's significance in mouse and human endometrial stromal cells (Arango et al., 2005; Zhang & Yan, 2016). Additionally, the NF-κB pathway, triggered by cytokines, plays a critical role in modulating inflammation and recruiting immune cells (Gomez-Chavez et al., 2021).

Cytokines and growth factors also play essential roles in the regulation of decidualization, orchestrating immune modulation, cellular differentiation, and tissue remodeling (Guzeloglu-Kayisli et al., 2009). Pro-inflammatory cytokines, such as interleukin-6 (IL-6), support decidual cell differentiation and regulate immune cell recruitment, while IL-11 enhances trophoblast invasion and modulates the maternal immune response (Karpovich et al., 2005; Lockwood et al., 2010). Both the

differentiation of EnSCs and the creation of a receptive endometrial environment rely on leukemia inhibitory factor (LIF), which plays an essential role in both decidualization and implantation (Lass et al., 2001). Tumor necrosis factor-alpha (TNF-α) also contributes to cellular remodeling and immune cell recruitment, although excessive TNF-α levels can be detrimental to pregnancy by promoting inflammation (Kim et al., 2020). In contrast, anti-inflammatory cytokines like transforming growth factor-beta (TGF-β) and interleukin-10 (IL-10) maintain a balance between immune responses and immune tolerance, promoting a favorable environment for pregnancy. TGF-β inhibits excessive inflammation, while IL-10 keeps an anti-inflammatory state, preventing immune rejection of the conceptus (Guerin et al., 2009). Growth factors, including vascular endothelial growth factor (VEGF), epidermal growth factor (EGF) and insulin-like growth factor 1 (IGF-1), stimulate angiogenesis and stromal cell proliferation, contributing to the development of a well-vascularized and differentiated decidual tissue necessary for early pregnancy (Guzeloglu-Kayisli et al., 2009).

1.1.3 Window of Implantation

Embryo implantation is a complex process that relies on the presence of both an implantation-ready blastocyst and an endometrium in a receptive state (Muter et al., 2023). However, implantation is possible only within a limited timeframe, which is known as the window of implantation. It lasts 3 to 5 days in most of primates and only a few hours in rodents during their menstrual cycle (de Ziegler et al., 1998). This window is characterized by rising E_2 levels, which work in conjunction with P_4 during the midluteal phase (cycle days 20–24), creating optimal conditions for implantation and pregnancy (Cha et al., 2012). Successful embryo implantation requires precise synchronization between the development of the embryo and the endometrial receptivity, in which embryo-maternal communication is important for maternal recognition and implantation (Governini et al., 2021). This interaction is tightly regulated by a series of molecular, hormonal, and immunological signals to ensure proper communication and interation (Massimiani et al., 2019).

The endometrial epithelial cells (EECs) that line the uterine lumen are the primary responders to signals secreted by the blastocyst (Hennes et al., 2023). These EECs detect and transfer embryonic signals into subsequent signaling pathways, and further enhance endometrial receptivity to the invading blastocyst (Whitby et al., 2020). The blastocyst secretes signaling molecules, including growth factors like heparin-binding epidermal growth factor (HB-EGF) and cytokines, including LIF, which play crucial roles in preparing the endometrium for implantation. In response, EECs express adhesion molecules such as integrins and selectins, facilitating the attachment of the embryo to the endometrium (Aghajanova, 2004; Kim et al., 2023). Moreover, EECs communicate with the underlying EnSCs to sustain and promote the decidualization process, which provides nutrients to the invading blastocyst and modulates local immune responses, creating a supportive environment for successful implantation (Hantak et al., 2014).

1.2 Factors Influencing the Reproductive Potential of the Endometrium

1.2.1 The Role of Reactive Oxygen Species in Decidualization

Reactive oxygen species (ROS), products generated by aerobic respiration and metabolism, are essential at physiological levels for the activation of specific proteins, including MAPKs (Mitogen-activated protein kinases), phosphatases, transcription factors and enzymes. Redox signaling, which plays a vital role in processes like cell proliferation, differentiation, migration, and transcriptional responses, is driven by these molecules (Finkel, 2011). ROS are generated from various sources, including NADPH oxidases (NOX), uncoupled endothelial nitric oxide synthase (eNOS), cytochrome P-450 oxygenase and cyclooxygenase, and the mitochondrial electron transport chain (ETC) (de Almeida et al., 2022). While mitochondria are commonly known for ATP production, ROS are increasingly recognized as essential mitochondrial signals that play a pivotal role in cellular adaptation and stress resistance, beyond their association with cellular dysfunction and disease (Palma et al., 2024). Among ROS sources, NOX enzymes are now widely acknowledged as key regulators of intracellular ROS homeostasis and significant producers of cellular ROS (Pecchillo Cimmino et al., 2023). In particular, NOX4, which

associates with the protein p22phox on internal membranes, constitutively produces large amounts of H_2O_2 (Martyn et al., 2006).

Among the many factors influencing decidualization, oxidative stress (OS) has gained significant attention. OS is characterized by increased levels of ROS, including superoxide (O_2^-), hydrogen peroxide (H_2O_2) and hydroxyl radical (OH^-) (Gao et al., 2022; Ruder et al., 2008). cAMP has been shown to enhance endogenous ROS production after 12 h of stimulation, coinciding with a great increase in PRL and IGFBP1 expression during decidualization (Al-Sabbagh et al., 2011). In this context, the p22phox/NOX4 complex has been identified as the primary source of ROS, mediating cAMP-dependent decidualization in EnSCs (Al-Sabbagh et al., 2011). However, excessive ROS impairs the decidualization process, leading to stromal cell apoptosis and a reduction in implantation sites (Hussain et al., 2021; Liang et al., 2021).

Antioxidant enzymes play critical roles in mitigating ROS and maintaining redox balance during decidualization. Superoxide dismutase (SOD) catalyzes the dismutation of O_2^- into H_2O_2, which is subsequently converted to water (H_2O) by catalase (CAT) and glutathione peroxidase (GPX) (Agarwal et al., 2008). Reduced glutathione (GSH), a natural nonenzymatic antioxidant, functions in free radical scavenging, anti-oxidation, and electrophile elimination to maintain redox homeostasis (Liu et al., 2022). During OS, GSH is oxidised to glutathione disulfide (GSSG), leading to a decreased GSH/GSSG ratio. Glutathione reductase (GR) reduces GSSG to GSH, allowing its reuse within cells (Diaz-Vivancos et al., 2015). GPX3 has also been identified as a major enzyme in reducing H_2O_2 during decidualization (Xu et al., 2014). Recent studies have linked disruptions in antioxidant pathways to impaired decidualization. For instance, inactivation of the yes-associated protein (YAP), which is essential for decidualization, results in an accumulation of intracellular ROS due to defects in the ribonucleotide reductase regulatory subunit M2 (Rrm2)/GR/GSH pathway. This accumulation leads to mitochondrial dysfunction and cellular apoptosis (Yu et al., 2022). Furthermore, HB-EGF has been shown to enhance the activities of SOD, CAT and GPX, restore GSH levels, and normalize the GSH/GSSG ratio following exposure to H_2O_2, although it does not affect NOX activity (Yu et al., 2019). These findings highlight the importance of antioxidant

enzymes in reducing ROS and maintaining oxygen balance, both of which are critical for successful decidualization.

1.2.2 Molecular Characteristics of DJ-1: Structure and Function

Given the significant role of ROS in cellular damage and the progression of decidualization, mechanisms that maintain oxidative stress balance are crucial. One such mechanism involves DJ-1, a protein known for its antioxidant properties (Dolgacheva et al., 2019). DJ-1 helps counteract oxidative stress by regulating redox balance, scavenging ROS, and protecting mitochondria, thereby safeguarding cells from damage (Hijioka et al., 2017).

DJ-1 is a protein that is expressed in distinct tissues throughout the body. It was initially identified and characterized as a mitogen-dependent oncogene product, which participate in a Ras-related signaling pathway (Nagakubo et al., 1997). In humans, DJ-1 is encoded by the Parkinson disease protein 7 (PARK7) gene, which has been identified as a causative gene of autosomal recessive early-onset Parkinson's disease (PD) (Bonifati et al., 2003). This multifunctional protein possesses both antioxidant and transcription-modulatory activities. Under basal conditions, DJ-1 is predominantly localized in the cytoplasm, it can translocate to the mitochondria and nucleus in response to OS (Junn et al., 2009). Mitochondrial DJ-1 plays a key role in providing short-term protection against OS before subsequently relocating to the nucleus (Zhou et al., 2020).

DJ-1 is composed of 189 amino acids, and its molecular weight is approximately 19.8 kDa (Honbou et al., 2003). It is part of the DJ-1/ThiJ/PfpI superfamily, a large and diverse group of proteins evolutionarily conserved across bacteria to humans (Buneeva & Medvedev, 2021; Smith & Wilson, 2017). Structurally, the DJ-1 monomer features a conserved α/β-fold characteristic of this superfamily, along with an additional C-terminal helix that mediates dimerization, a process essential for its *in vivo* functionality (Tao & Tong, 2003; Wilson et al., 2003). DJ-1 contains three cysteine residues (C46, C56, and C106), among which C106 is the most functionally significant. This residue is critical for DJ-1's ability to protect cells against OS (Bahmed et al., 2019). The three-dimensional

structure of DJ-1 reveals a compact globular domain with C106 positioned in its active site. Oxidation of the SH group at C106 regulates DJ-1's activity, as the degree of oxidation influences its function (Hijioka et al., 2017; Trempe & Fon, 2013). During oxidation, the SH-group of C106 undergoes successive conversion into sulfenic (SOH), sulfinic (SO_2H) and further sulfonic (SO_3H) acids forms (Buneeva & Medvedev, 2021). The functionality of DJ-1 is influenced by the oxidation state of its C106 residue (Wilson, 2011). Moderate oxidation of DJ-1-SO_2H promotes mitochondrial localization and cytoprotective functions, which involve apoptosis signal-regulating kinase 1 (ASK1). However, excessive oxidation of C106 to the SO_3H form results in accumulated and inactive DJ-1. This process has been associated with the pathological progression of PD, where OS is a key pathological feature (Kiss et al., 2017; Wilson, 2011).

1.2.3 The Role of DJ-1 in Physiological and Pathophysiological Processes

As an antioxidant protein, DJ-1 plays a significant role in plenty of physiological functions, including cell proliferation, apoptosis, mitochondrial homeostasis regulation, and glucose level regulation (**Figure 1-4**) (Neves et al., 2022). Given its multifunctionality, dysregulation of DJ-1 has been implicated in a wide range of diseases. Beyond its well-known roles in cancer and PD, studies have highlighted the significant involvement of DJ-1 in the pathogenesis of multiple OS-associated disorders affecting different organs and systems in the human body (Chunna & Pu, 2017; Eberhard & Lammert, 2017; Lind-Holm Mogensen et al., 2023; Pantcheva et al., 2014).

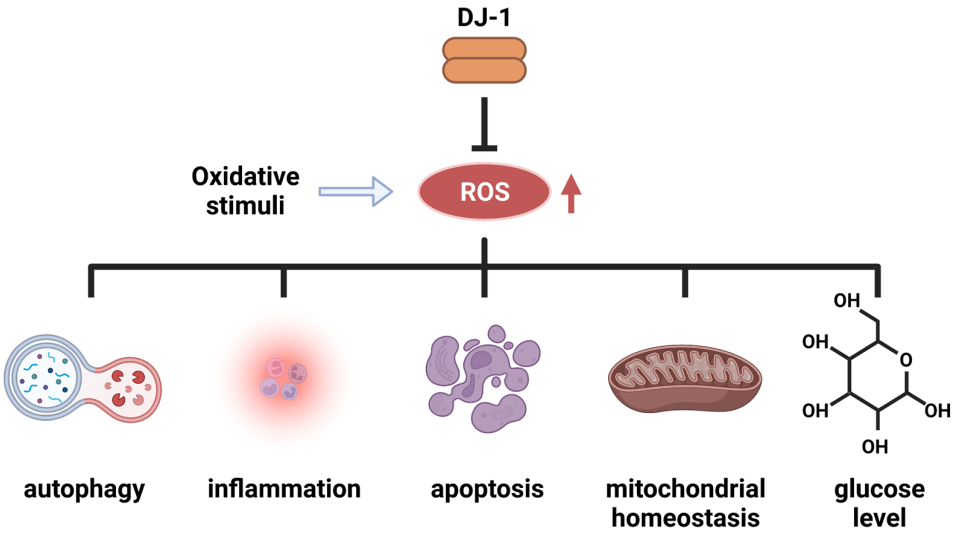

Figure 1-4: The Functions of DJ-1 in Physiological Processes.

Under the oxidative stimuli, DJ-1 can reduce the production of ROS, further regulate the physiological process including autophagy, inflammation, apoptosis, mitochondrial homeostasis and glucose level. Figure adapted from a previous study (Neves et al., 2022). Created with BioRender.com.

DJ-1 plays multifaceted roles in a variety of diseases, including PD, cancers, reproductive disorders, diabetes, lung diseases and stroke (**Figure 1-5**) (Aleyasin et al., 2007; Amatullah et al., 2021; Dolgacheva et al., 2019; Eberhard & Lammert, 2017; Guo et al., 2015; Kawate et al., 2017; Kwon et al., 2013; Sun et al., 2020). In PD, DJ-1 protects neurons from α-synuclein aggregation and oligomer-induced neurodegeneration by regulating redox balance and key transcription factors, including Nrf2, PI3K/PKB, and p53 signaling pathways, as well as protecting mitochondria (Dolgacheva et al., 2019). It has also been identified as an oncogene, demonstrating significant transforming activity in cooperation with H-Ras or c-Myc (Cao et al., 2015). Elevated DJ-1 expression has been observed in various cancers, such as melanoma, breast, ovarian, and colorectal cancers, implicating its role in cancer pathogenesis (Chen et al., 2021; Quesnel et al., 2024; Schumann et al., 2015; Scumaci et al., 2020). In endometrial cancer, Shu K et al. found that high DJ-1 expression may contribute to tumorigenesis by inhibiting apoptosis and enhancing cell proliferation (Shu et al., 2013). Furthermore, higher serum DJ-1 levels

have been detected in patients with endometrioid endometrial cancer, with even greater levels observed in cases of endometrial serous carcinoma (Morelli et al., 2014).

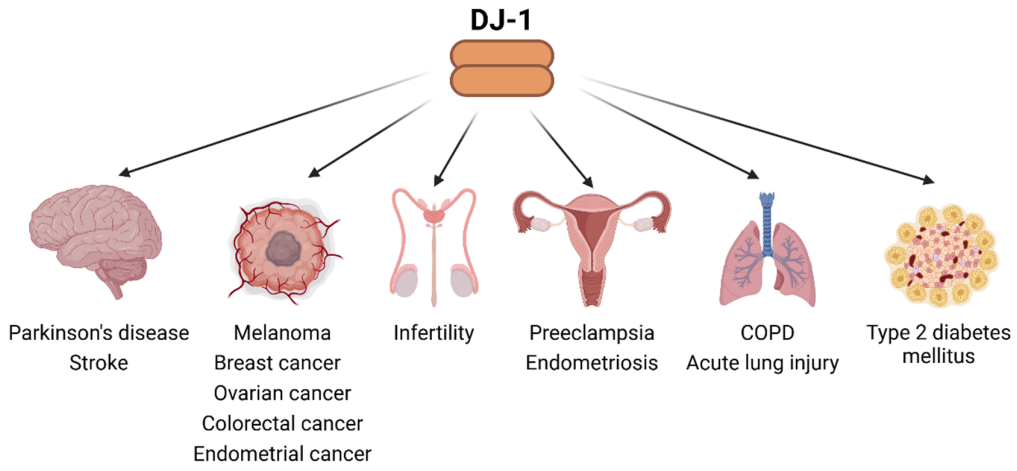

Figure 1-5: The Role of DJ-1 in Pathophysiological Processes.

DJ-1 is crucial for the pathological processes of multiple OS-associated diseases in different organs and systems in human. COPD: chronic obstructive pulmonary disease. Figure adapted from previous studies (Aleyasin et al., 2007; Amatullah et al., 2021; Dolgacheva et al., 2019; Eberhard & Lammert, 2017; Guo et al., 2015; Kawate et al., 2017; Kwon et al., 2013; Sun et al., 2020) . Created with BioRender.com.

Beyond its main role in PD and cancers, DJ-1 has also been recognized for its involvement in preeclampsia (PE). Studies suggest that DJ-1 levels are significantly elevated in the placental tissue, serum, and umbilical cord blood of both early- and late-onset PE patients, potentially as a compensatory response to uteroplacental hypoxia and oxidative stress (OS) (Kwon et al., 2013; Yang et al., 2020). In type 2 diabetes mellitus, OS plays a significant role in disease pathogenesis (Bensellam et al., 2012). Increasing DJ-1 levels protect insulin-producing beta cells and other vulnerable tissues, thereby mitigating diabetic complications (Eberhard & Lammert, 2017; Wang et al., 2020). Recent studies also highlight DJ-1's role in lung diseases. In chronic obstructive pulmonary disease, DJ-1 activates the Wnt3a/β-catenin and Nrf2 pathways in alveolar epithelial cells, reducing inflammatory response (Xiang et al., 2021; Zhou et al., 2021). In acute lung injury, DJ-1 deficiency exacerbates OS, elevates pro-inflammatory markers, and leads to edema and lung damage (Amatullah et al., 2021). Similarly, in stroke, which

results from interrupted blood flow to the brain, DJ-1 mitigates oxidative stress, potentially protecting neurons from damage after ischemic injury (Aleyasin et al., 2007).

In reproductive diseases, a study showed that DJ-1 deficiency in spermatozoa contributes to metabolic abnormalities in ornidazole-induced asthenozoospermia, as demonstrated using rat models (Sun et al., 2020). Emerging evidence also connects DJ-1 to abnormalities in the female reproductive system. For instance, DJ-1 is highly expressed in endometriotic cells and is associated with enhanced survival, migration, and invasion of endometrial cells, contributing to conditions such as endometriosis and adenomyosis (Rai & Shivaji, 2011). Moreover, a previous study found that DJ-1 impacts on the PI3K/Akt/p-mTOR signaling pathway, which regulates proliferation, migration, and angiogenesis in endometrial cells, thereby offering a potential theoretical target for the treatment of endometriosis and adenomyosis (Guo et al., 2015). However, studies investigating DJ-1's role in reproductive diseases linked to impaired endometrial decidualization remain limited.

1.2.4 The Roles of Calcium Channels and Trypsin in Early Pregnancy

Human blastocysts release a diverse array of signals, including interleukins, microRNAs, mucins, growth factors, hormones, and trypsin-like proteases, which reflect their developmental potential and play critical roles in the implantation process (Brosens et al., 2014; Hennes et al., 2023; Ruan et al., 2012). Among these, trypsin-like proteases are crucial for early embryonic development in various vertebrates, such as mice, rats, and rhesus monkeys (Jiang et al., 2011; Lin et al., 2006; Perona & Wassarman, 1986). As a type of serine protease, trypsin is produced by the murine blastocyst. It is particularly notable for its role in mediating communication between the EECs and the blastocyst (Shmygol & Brosens, 2021). A previous study demonstrated that, in mice, trypsin modulates epithelial cell function through the amiloride-sensitive epithelial sodium channel (ENaC) alpha subunit, inducing cell membrane depolarization. This depolarization triggers L-type voltage-gated Ca^{2+} channels, resulting in a sustained rise in cytosolic Ca^{2+} concentration ($[Ca^{2+}]_i$), which drives cyclooxygenase-2 (COX2)-

dependent prostaglandin E_2 (PGE_2) release. This cascade enhances the decidualization process (Ruan et al., 2012). Furthermore, murine studies have demonstrated that protease inhibitors targeting trypsin reduce implantation sites, increase fetal loss, and lower birth weight *in vivo* (Sun et al., 2007).

1.3 Infertility and Recurrent Pregnancy Loss

1.3.1 Infertility

Fertility refers to an individual's ability to conceive, whereas a woman's fecundity refers to the biological capacity for reproduction, determined by the monthly probability of conception (Vander Borght & Wyns, 2018). Infertility, a significant issue in reproductive health, is defined as a incapacity of a couple to conceive after 1 year of sexual intercourse without protection (Vander Borght & Wyns, 2018). Around 15% of people in the world is affected by infertility, with both male and female factors contributing almost equally (Bala et al., 2021). The causes of female infertility are vast ranging from endometriosis, ovulation and fallopian tube disorders (Ehsani et al., 2019). Furthermore, in many industrialised countries, lifestyle factors are also contribute to in(sub-)fertility including, obesity and metabolic syndrome, vaping/smoking and advanced maternal age (Emokpae & Brown, 2021). Despite these identifiable factors, approximately 30% of infertility cases remain unexplained (Dougherty et al., 2023). Failure of the endometrium to reach a receptive state is reported to be a main cause of infertility, and a great obstacle in assisted reproductive technology (Gellersen & Brosens, 2014). Furthermore, Large clinical studies have shown that the implantation rate significantly declines in women with reduced fertility, even when using donor oocytes from young women (Loid et al., 2024; Soares et al., 2005; Toner et al., 2002). These findings imply that the endometrium, or aberrant endometrial factors, contribute to the reduced successful implantation rates. However, the underlying mechanism of these pregnancy failures are poorly understood.

Among the molecular factors contributing to infertility, the Left-right determination factor 2 (LEFTY2) gene has emerged as a critical regulator of reproductive processes, playing a pivotal role in uterine receptivity, embryo implantation, and early

developmental events (Salker et al., 2018; Tang, Taylor, et al., 2005). Another important factor in implantation is LEFTY2, which belongs to the transforming growth factor (TGF)-β superfamily (Cornet et al., 2002; Ulloa & Tabibzadeh, 2001). LEFTY2 is initially synthesized as a precursor protein that undergoes cleavage to release its active C-terminal monomeric form (Ulloa & Tabibzadeh, 2001). Around 6 days after ovulation, the expression of LEFTY2 is predominantly observed in decidualizing human EnSCs, coinciding with the closure of the window of implantation (Gellersen & Brosens, 2014; Salker et al., 2018). An increase in LEFTY2 expression has been linked to unexplained infertility (Salker et al., 2011), abnormal uterine bleeding (Kothapalli et al., 1997) and implantation failure (Tabibzadeh, 2011; Tabibzadeh & Hemmati-Brivanlou, 2006). Moreover, a previous study has demonstrated that overexpression of LEFTY2 inhibits decidualization, effectively preventing implantation and pregnancy (Tang et al., 2010).

1.3.2 Recurrent Pregnancy Loss

After a woman overcomes infertility and achieves conception, the subsequent challenge may involve the ability to sustain the pregnancy, as recurrent pregnancy loss (RPL) can be a significant factor affecting reproductive outcomes. RPL is estimated to affect approximately 5% of couples and is the most common obstetric complication (Genovese & McQueen, 2023; Quenby et al., 2021). It is characterized by the recurrence of two or more consecutive pregnancy losses prior to 24 weeks of gestation (Dimitriadis et al., 2020). Several factors have been identified as contributors to RPL, including advanced maternal age, parental chromosomal abnormalities, hormonal and metabolic disturbances, maternal autoantibodies, specific uterine anomalies, infections, compromised sperm quality, and lifestyle-related factors (Busnelli et al., 2023; D'Ippolito et al., 2020; Garrisi et al., 2009; Pluchino et al., 2014; Turesheva et al., 2023; Zhu et al., 2023). Serum- and glucocorticoid-inducible kinase 1 (SGK1) is a protein essential for cellular stress responses and ion transport. Previous study showed that SGK1 deficiency is an indication of the mid-secretory endometrium in patients suffering from RPL. This deficiency may compromise the endometrium's ability to support early pregnancy,

leading to pregnancy loss (Salker et al., 2011). A study further highlights a potential cellular mechanism behind RPL. They found that endometrial stromal cells from women with RPL exhibited a failure to detect the differences between high-quality and low-quality embryos. This impaired sensing function of the stromal cells could increase the likelihood of low-quality embryo implantation, thereby contributing to RPL (Weimar et al., 2012).

Despite extensive investigative efforts, up to 50% of RPL cases remain unexplained, with no clearly identifiable etiology (Yu et al., 2023). Furthermore, with each additional miscarriage, the incidence of euploid loss increases while the possibility of a successful pregnancy declines (Ogasawara et al., 2000). Preimplantation genetic testing, progestational hormone supplementation, anticoagulant therapy, immunomodulatory treatments, and surgical correction of uterine abnormalities are among the clinical interventions utilized for patients with RPL (Yu et al., 2023). However, these approaches have demonstrated limited effectiveness in improving live birth rates, demonstrating that the underlying mechanisms are inadequately understood in many instances (Eshre Guideline Group on RPL et al., 2023).

1.3.3 Role of Decidualization in Modulating Endometrial Receptivity and Selectivity: Implications for Recurrent Pregnancy Loss and Infertility

Previous studies have posited the association between impaired decidualization and heightened susceptibility to subsequent reproductive failures (Lucas et al., 2020; Salker et al., 2010; Teklenburg et al., 2010). Reduced endometrial receptivity during the implantation window for embryos may be a key factor contributing to unexplained infertility and failed *in vitro* fertilization (IVF) cycles (Stevens Brentjens et al., 2022). Research has demonstrated that the endometrium can act as a 'bio-sensor' to assess the quality of embryos, thereby limiting maternal investment of nonviable embryos (Brosens & Gellersen, 2010; Macklon & Brosens, 2014; Teklenburg et al., 2010). The 'selection hypothesis' suggests that an excessive or pronounced decidual response can shorten the window of receptivity and enhance the elimination of embryos, thereby lowering the

risk of miscarriage but potentially preventing conception (Brosens et al., 2014). In contrast, several studies suggest that the endometrium in women with RPL exhibits a disordered and prolonged pro-inflammatory decidual response (Salker et al., 2012). This exaggerated initial inflammatory decidual response may extend the endometrial receptive window, leading to implantation occurring outside this phase and hindering the selectivity of the endometrium (Salker et al., 2010). Furthermore, the absence of quality control at implantation is clinically manifested as a brief time span for conception, referred to as 'superfertility', a characteristic often observed in many RPL patients (Bhandari et al., 2016; Teklenburg et al., 2010). Therefore, the human uterus has an intrinsic ability to adapt and can adjust its receptivity and selectivity traits (Gellersen & Brosens, 2014). However, the precise mechanistic underpinnings governing this relationship remain largely obscure.

1.4 Hypothesis and Aims

Despite emerging insights, the mechanisms by which the maternal decidua acquires the necessary molecular signature to support rapid expansion during early gestation remain poorly understood. Accumulated evidence highlights a strong association between impaired decidualization and an increased susceptibility to reproductive failures, including infertility and recurrent pregnancy loss (Salker et al., 2010). Physiological factors such as ROS level, cytoskeletal dynamics, and ion channel activity are known to play critical roles in ensuring healthy decidualization. DJ-1, a multifunctional protein with antioxidant properties, may contribute significantly to this process by regulating oxidative stress and cell mobility. Additionally, embryo-induced activation of calcium channels through trypsin secretion has been implicated in promoting key signaling events during implantation. However, the precise mechanistic pathways linking these factors to healthy decidualization and successful implantation remain largely undefined. In our study, we hypothesized two potential mechanisms:

1. The absence of DJ-1 in the endometrium could disrupt decidualization by altering ROS levels and cell motility, thereby contributing to RPL.

2. Embryo-derived trypsin-induced calcium entry could be modulated by the endometrial infertility factor LEFTY2, which may act as a critical regulator during implantation.

For the first hypothesis, the objectives are:

1. To investigate the role of DJ-1 in endometrial decidualization and RPL by analyzing its expression patterns in both human and murine endometrial tissues.
2. To elucidate the mechanisms by which DJ-1 regulates key aspects of decidualization, including ROS levels, cytoskeletal dynamics, and cellular motility.
3. To assess the potential therapeutic implications of DJ-1 overexpression in reversing impaired decidualization and reducing the risk of RPL.

For the second hypothesis, the aims are:

1. To evaluate whether embryo-derived trypsin is involved in embryonic development and implantation in human.
2. To examine the function of the infertility factor LEFTY2 in modulating trypsin-induced calcium entry in human endometrial epithelial cells, including a detailed exploration of the underlying molecular mechanisms.

By addressing these aims, this dissertation seeks to unravel the intricate molecular mechanisms underlying decidualization and implantation, offering insights into potential therapeutic strategies to improve reproductive outcomes and mitigate pregnancy complications.

2. Materials and Methods

2.1 Materials

Table 2-1: List of Cells, in Alphabetical Order

Item	Catalog number	Company
Immortalized Human Endometrial Stromal Cells (EnSCs)	#T0533	Applied Biological Materials Inc., Richmond, Canada
Ishikawa Cell Line human (ISK)	#99040201	Merck, UK

Table 2-2: List of Reagents and Chemicals, in Alphabetical Order

Item	Catalog number	Company
2',7'-Dichlorfluorescein-Diacetat	D6883	Sigma-Aldrich, Germany
2-Mercaptoethanol	M6250	Sigma-Aldrich, Germany
8-Bromo-cAMP, sodium salt	#1140	Tocris, UK
Acrylamide/bis-solution	A124.2	Carl Roth, Germany
Amiloride -hydrochloride	BP008	Sigma-Aldrich, Germany
Antibiotic/antimycotic solution	#15240062	Invitrogen, Germany
Aprotinin	A6279	Sigma-Aldrich, Germany
Bovine Serum Albumin Fraction V	10735078001	Roche, Germany
Bradford Reagent	B6916	Sigma-Aldrich, Germany
Bromophenol Blue·Na-salt	15375.01	SERVA, Germany
CellTiter 96® AQueous One Solution Cell Proliferation Assay (MTS)	G3580	Promega, USA
Chicago Sky Blue 6B	C8679	Sigma-Aldrich, USA

cOmplete™-ULTRA-Mini-Tabletten, Protease-Inhibitor-Cocktail in EASYpacks	5892970001	Roche, Germany
D(+)-Saccharose	4621.1	Carl Roth, Germany
Deoxyribonuclease I, Alexa Fluor™ 488 Conjugate	D12371	Invitrogen, Germany
Dextran coated charcoal (DCC)	C6241	Sigma-Aldrich, USA
Dimethyl sulfoxide (DMSO)	D12345	Invitrogen, Germany
DMEM/F-12, HEPES, no phenol red	11039021	Thermofisher Scientific, Germany
Dulbecco's Phosphate Buffered Saline	D8537	Sigma-Aldrich, Germany
eBioscience Intracellular Fixation & Permeabilization Buffer Set	88-8824-00	Invitrogen, Germany
eBioscience™ Annexin V Apoptosis Detection Kits	88-8005-72	Invitrogen, Germany
Ethylene glycol-bis(2-aminoethylether) -N,N,N',N'-tetraacetic acid	E3889	Sigma-Aldrich, Germany
Fetal bovine serum (FBS)	10270106	Invitrogen, Germany
Glycerol	3783.1	Carl Roth, Germany
Ionomycin calcium salt	I3909	Sigma-Aldrich, Germany
Leupeptin	L8511	Sigma-Aldrich, Germany
L-glutamine	25030024	Invitrogen, Germany
Lipofectamine™ LTX Reagent with PLUS™ Reagent	15338100	Invitrogen, Germany
Lipofectamine™ RNAiMAX Transfection Reagent	13778075	Invitrogen, Germany

Maxima™ H Minus cDNA Synthesis Master Mix	M1681	Invitrogen, Germany
Medroxyprogesterone 17 acetate (MPA)	M1629	Sigma-Aldrich, Germany
Mowiol® 4-88	81381	Sigma-Aldrich, USA
Nifedipine	N7634	Sigma-Aldrich, Germany
Paraformaldehyde	158127	Sigma-Aldrich, Germany
Phalloidin	P2141	Sigma-Aldrich, Germany
Pierce 10X western blot transfer buffer, methanol-free	35045	Thermofisher Scientific, Germany
Phenylmethanesulfonyl fluoride	10837091001	Roche, Germany
PowerUp SYBR Green master mix	#A25742	Thermofisher Scientific, Germany
ProLong™ Gold Antifade Mountant with DNA Stain DAPI	P36931	Invitrogen, Germany
Propidium Iodide	P1304MP	Invitrogen, Germany
ProSieve QuadColor protein marker	193837	Lonza, USA
Recombinant Human Lefty-A Protein	746-LF-025/CF	R&D Systems, UK
RIPA Lysis and Extraction Buffer	89901	Thermofisher Scientific, Germany
SAGE 1-Step	67010010	Origio, Germany
Sodium chloride (NaCl)	#27810.295	VWR International, USA
Sodium dodecyl sulfate (SDS)	#L5750	Sigma-Aldrich, Germany
Sodium fluoride	S1504	Sigma-Aldrich, Germany
Sodium orthovanadate	S6508	Sigma-Aldrich, Germany
SuperSignal™ West Pico PLUS Chemiluminescent Substrate	34578	Thermofisher Scientific, Germany

TEMED	2367.3	Carl Roth, Germany
Thapsigargin	T7458	Invitrogen, Germany
Thymidine	T1895	Sigma-Aldrich, Germany
Tris-Hydrochloride	10812846001	Roche, Germany
Triton® X 100, 1 l	3051.2	Carl Roth, Germany
Trizma® Base	T1503	Sigma-Aldrich, Germany
TRIzol™ Reagent	15596026	Invitrogen, Germany
Trypan blue	T8154	Sigma-Aldrich, Germany
Trypsin Activity Assay Kit (Colorimetric)	ab102531	Abcam, UK
Trypsin-EDTA (0.25%), phenol red	25200056	Invitrogen, Germany
Tween 20	P1379	Sigma-Aldrich, Germany
UltraPure agarose	P1379	Sigma-Aldrich, Germany
Water for molecular biology, sterile filtered	95284	Sigma-Aldrich, Germany

Table 2-3: List of Consumable Supplies, in Alphabetical Order

Item	Catalog number	Company
50 mm x 9 mm Not TC-treated Tight-fit Lid Style Bacteriological Petri Dish, 20/Pack, 500/Case, Sterile	351006	Falcon, USA
6-well plate	353224	Corning, USA
96-well plate	353072	Corning, USA
Amersham™ Hybond® P Western blotting membranes, PVDF	GE10600023	Sigma-Aldrich, Germany

Bio-MLCT, cantilever C		Bruker AXS S.A.S., Champs-sur-Marne, France
Cell counting slides	1450015	Bio-Rad, Germany
Cell culture flask (T75)	658175	Greiner Bio-One, Germany
Cell lifter	3008	Corning, USA
Corning Falcon 15 ml conical centrifuge tubes	10773501	Thermofisher Scientific, Germany
Corning Falcon 50 ml conical centrifuge tubes	10788561	Thermofisher Scientific, Germany
Cover slips	474030-9000 000	Carl Zeiss, Germany
Gel cassettes, 1.5 mm	NC2015	Invitrogen, Germany
Glass slide	03-0004	R. Langenbrick GmbH, Germany
Microcentrifuge tubes	30125150	Eppendorf, Germany
Optical adhesive covers, PCR compatible	4360954	Thermofisher Scientific, Germany

Table 2-4: List of Antibodies, in Alphabetical Order

Item	Catalog number	Company
Anti-CACNA1C antibody [S57]	ab84814	Abcam, USA
Anti-COX2 / Cyclooxygenase 2 antibody	ab15191	Abcam, UK
Anti-rabbit IgG, HRP-linked Antibody	7074S	Cell Signaling Technology, Germany
DJ-1 (D29E5) XP® Rabbit mAb	5933T	Cell Signaling Technology, Germany
Donkey anti-Rabbit IgG (H+L) Highly Cross-Adsorbed	A-21207	Invitrogen, Germany

Secondary Antibody, Alexa Fluor™ 594		
eBioscience™ Phalloidin eFluor™ 660	50-6559-05	Invitrogen, Germany
GAPDH (14C10) Rabbit mAb	2118L	Cell Signaling Technology, Germany
Goat anti-Mouse IgG (H+L) Cross-Adsorbed Secondary Antibody, Alexa Fluor™ 568	A-11004	Invitrogen, Germany
Goat anti-Rabbit IgG (H+L) Cross-Adsorbed Secondary Antibody, Alexa Fluor™ 488	A-11008	Invitrogen, Germany
Horse Anti-Goat IgG Antibody (H+L), Biotinylated	BA-9500-1.5	Vector Laboratories, USA
Lefty Antibody (D-6)	sc-365845	Santa Cruz Biotechnology, Germany
Palladin (D9H2) Rabbit mAb	8518S	Cell Signaling Technology, Germany
Palladin Antibody (1E6)	NBP1-25959	NOVUS, USA
Pan-Actin (D18C11) Rabbit mAb (HRP Conjugate)	12748S	Cell Signaling Technology, Germany
Streptavidin, Alexa Fluor™ 488 Konjugat	S11223	Invitrogen, Germany

Table 2-5: List of Primers, in Alphabetical Order

Gene	Forward Primer	Reverse Primer
CACNA1C	5'-TGACTATTTTTGCCAATTGTGTG-3'	5'-GCGGAGGTAGGCATTGGG-3'
DJ-1	5'-AGTTCCACAACCTATTTCATGAG-3'	5'-CCATATGATGTGGTGGTTCTAC-3'
GLRX	5'-TTAAGAATTCGCTCAAGAGTTTG	5'-GAGCTCTAGATTACTGCAGAGCTC

	TGAACTGC-3'	CAATCTG-3'
GPX3	5'-GAAGTAACTGAAGGCCGTCTCATC-3'	5'-CACGGATTTCTTCCTGAACAAAG-3'
HSD11B1	5'-AGCAAGTTTGCTTTGGATGG-3'	5'-AGAGCTCCCCCTTTGATGAT-3'
IGFBP1	5'-CGAAGGCTCTCCATGTCACCA-3'	5'-TGTCTCCTGTGCCTTGGCTAAAC-3'
Ki-67	5'-CACACTCCACCTGTCCTGAA-3'	5'-GAGCAGGAGCTGGAGGGCTT-3'
L-19	5'-GCGGAAGGGTACAGCCAA-3'	5'-GCAGCCGGCGCAAA-3'
PALLD	5'-CAGGCTGTCAACCAAAGAGGTC-3'	5'-TCGTCTCCACTGTCCCTTGATC-3'
PRL	5'-AAGCTGTAGAGATTGAGGAGC AAAC-3'	5'-TCAGGATGAACCTGGCTGACTA-3'

Table 2-6: List of siRNAs and Plasmids, in Alphabetical Order

Item	ID	Catalog number	Company
pGW1-Myc-DJ1-WT	NP_009193.2.	29347	Addgene, USA
Silencer™ Pre-Designed siRNA	136368	AM16708	Thermofisher Scientific, Germany

Table 2-7: List of Machines, in Alphabetical Order

Item	Catalog number	Company
BD FACSCanto™ II Clinical Flow Cytometry System		BD Biosciences, Germany
DP71 digital microscope camera		Olympus, Japan
Electrophoresis power supply	E831	Consort, Belgium
EmbryoScope+ time-lapse system		Vitrolife, Germny
EVOS M7000	AMF7000	Invitrogen, Germany
iBright CL1000	A32749	Invitrogen, Germany

Incubator	9040-0012	Binder, Germany
Inverted phase-contrast microscope	Axiovert 100	Carl Zeiss, Germany
LSM 800 confocal laser scanning microscope		Carl Zeiss, Germany
MFP-3D-BIO AFM		Asylum Research, Santa Barbara, USA
Q Exactive HFX mass spectrometer		ThermoFisher Scientific, Germany
QuantStudio 3 PCR system		ThermoFisher Scientific, Germany
T100 thermal cycler	621BR57740	Bio-Rad, Germany
TC20 automated cell counter	1450102	Bio-Rad, Germany
Varioskan LUX multimode microplate reader	VLBL0TD2	ThermoFisher Scientific, Germany
Vortex mixer	K550GE	Bender & Hobein, Switzerland
Xcell SureLock Mini-Cell electrophoresis system	EI0001	Life Technologies, Germany
XCell SureLock™ Mini-Cell	EI0001	Invitrogen, Germany

Table 2-8: List of Software, in Alphabetical Order

Item	Version	Company
BioRender		BioRender, Canada
Excel	16.51	Microsoft Corporation, USA
FIJI	2.1.0	Open source
FlowJo	v10.8	Becton, Dickinson & Company, USA

Geneontology.org		Ashburner et al.; The Gene Ontology Consortium.
GraphPad Prism	9	GraphPad Software, USA
MaxQuant software package	1.6.7.0	Cox Lab, Germany
Metafluor		Universal Imaging, USA
Photoshop	CS6	Adobe, USA
Igor Pro		Wavemetrics, USA
Inkscape	v1.4	Open source
Endnote	v20	Clarivate, USA

2.2 Experimental Plan

2.2.1 Experimental Plan for Investigating the Role of PARK7 in Decidualization and Recurrent Pregnancy Loss

Based on the hypothesis that DJ-1 is important for controlling endometrial decidualization by modulating ROS levels and cell migration, contributing to impaired decidualization, as well as a higher risk of pregnancy loss, a comprehensive experimental plan was developed. After confirming the expression of DJ-1 in the endometrium through *in silico* data mining, the set of experiments focused on evaluating DJ-1 expression patterns during *in vitro* decidualization of EnSCs to establish its temporal and spatial dynamics (**Figure 2-1**).

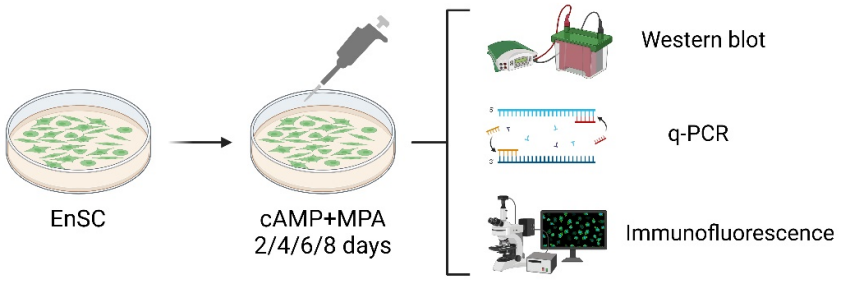

Figure 2-1: DJ-1 Expression during in vitro Decidualization of EnSCs.

Schematic depiction of the approach of in vitro experiment. EnSCs were subjected to treatment with cyclic adenosine monophosphate and medroxyprogesterone acetate (cAMP and MPA, C+M) every 48h for a total of 8 days. Western blot, qRT-PCR, and immunofluorescence analyses were subsequently performed. Created with BioRender.com.

Following this, DJ-1 expression was assessed in both human and mouse endometrial tissues to validate its relevance across species and reproductive conditions. Furthermore, the association between DJ-1 deficiency and adverse pregnancy outcomes was investigated in both human samples and mouse models to explore its potential role in pregnancy loss.

Subsequent experiments aimed to investigate the functional role of DJ-1 by knocking down its expression using siRNA transfection in EnSCs. The effects of DJ-1 knockdown on ROS production, and decidualization markers were analyzed to determine its regulatory mechanisms. Proteomic analyses were then performed to identify downstream proteins affected by DJ-1 deficiency, providing insights into the molecular pathways involved (**Figure 2-2A**). Based on the proteomic findings, targeted experiments were conducted to further validate the role of specific proteins in the DJ-1-mediated regulation of decidualization (**Figure 2-2B**).

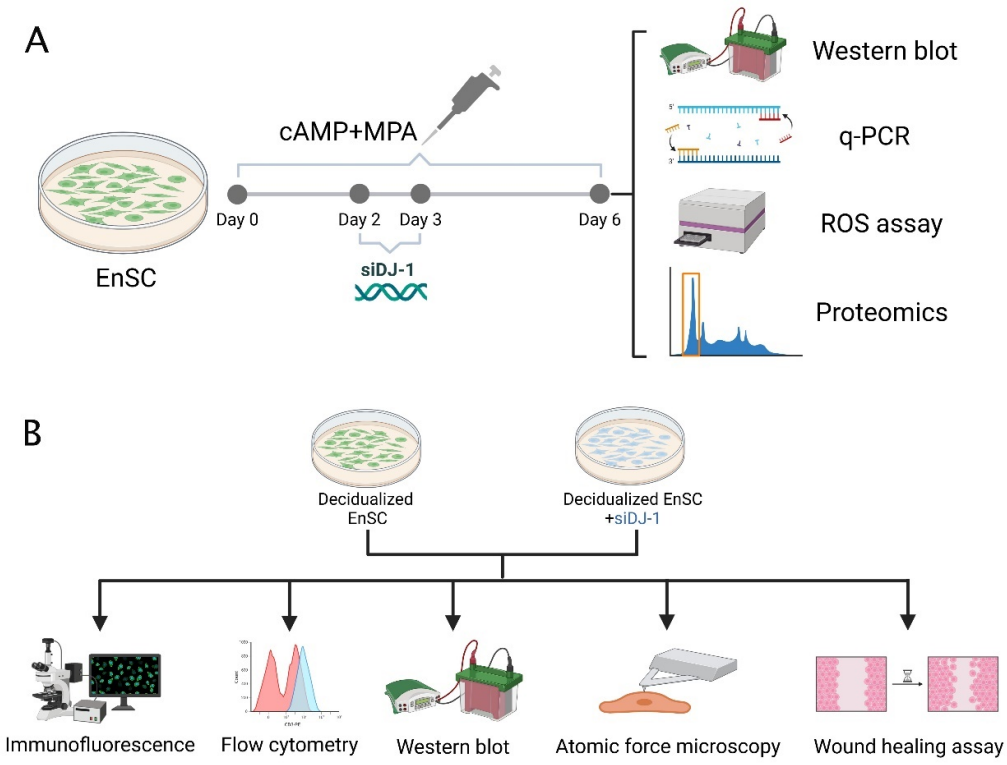

Figure 2-2: Overview of DJ-1 Silencing and Functional Analyses in Decidualized EnSCs.

Diagrammatic representation of the experimental approach. ***(A)*** *EnSCs were transfected by PARK7-targeting siRNA (siDJ-1) for 24 h, which was performed on the third day of a total of 6-day treatment with 0.5 µM 8-Br-cAMP and 1 µM MPA (C+M). Western blot, qRT-PCR, ROS assay and proteomics were subsequently performed.* ***(B)*** *Immunofluorescence staining, flow cytometry, western blot, atom force microscopy and wound healing assay were performed on decidualized EnSCs, as well as on decidualized EnSCs following transfection with siDJ-1. Created with BioRender.com.*

Finally, to explore potential therapeutic implications, DJ-1 overexpression experiments were carried out to investigate the possible effects of increasing DJ-1 levels on ROS regulation, decidualization, and downstream-related experiments, further exploring its role in recurrent pregnancy loss (**Figure 2-3**).

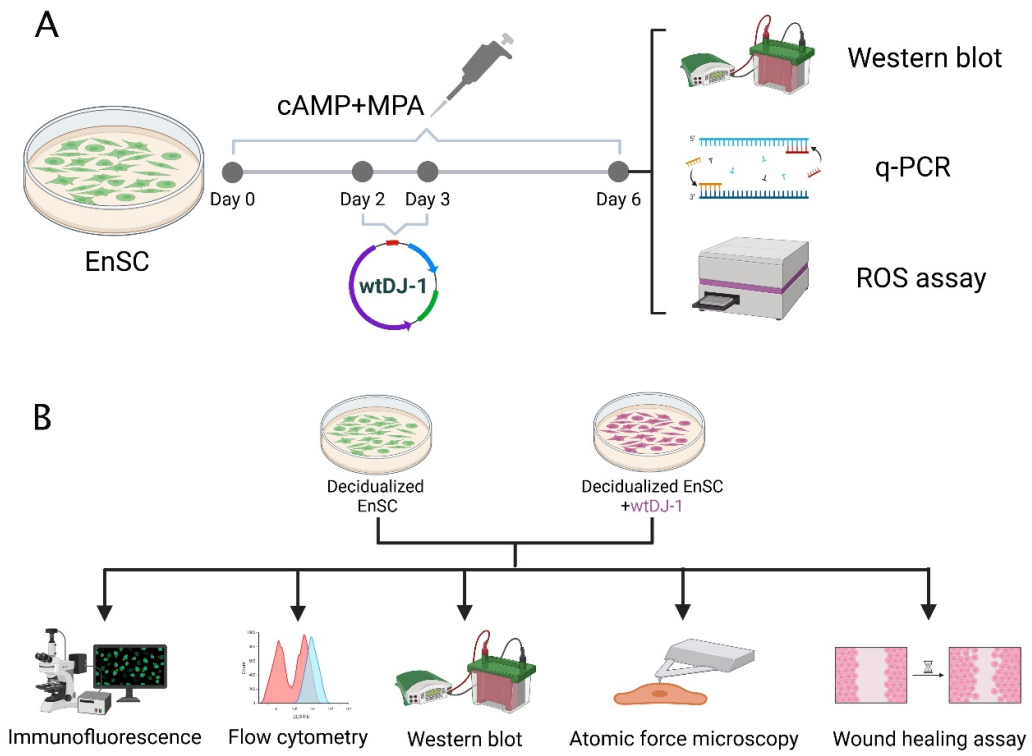

Figure 2-3: Schematic Representation of DJ-1 Overexpression and Functional Analyses in Decidualized EnSCs.

Schematic depiction of the experimental approach. ***(A)*** *EnSCs were transfected by pGW1-Myc-DJ-1-wt (wt-DJ-1) for 24 h, which was performed on the third day of a total of 6-day treatment with 0.5 µM 8-Br-cAMP and 1 µM MPA (C+M). Western blot, qRT-PCR, ROS assay and proteomics were subsequently performed.* ***(B)*** *Immunofluorescence, FACS, WB, AFM, and wound healing assays were performed on decidualized EnSCs, as well as on decidualized EnSCs transfected with wtDJ-1. Created with BioRender.com.*

2.2.2 Experimental Plan for Investigating the Role of LEFTY2 in Modulating Trypsin-Induced Calcium Entry

Based on the hypothesis that LEFTY2 impedes trypsin-induced calcium entry in endometrial cells by interfering with specific calcium channels and modulating $[Ca^{2+}]_i$, a series of experiments were designed to investigate the impact of LEFTY2 on trypsin-induced calcium signaling and the underlying mechanisms involved. The initial step involved *in silico* analysis to determine the expression profiles of genes associated with the classical trypsin pathway in human embryos at different developmental stages. Additionally, trypsin levels were measured using ELISA from single human embryo

conditioned medium to confirm the presence of embryo-derived trypsin activity (**Figure 2-4**).

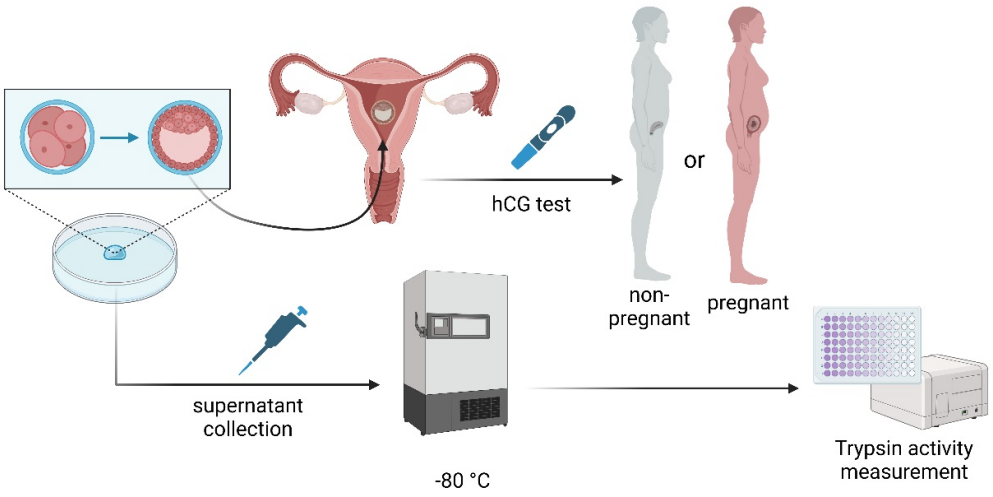

Figure 2-4: Schematic of Embryo Culture, Transfer, and Trypsin Activity Analysis Correlated with Pregnancy Outcome.

Individual embryos were cultured in 25 µl droplets of Sage 1-Step medium using the EmbryoScope. Embryos graded as 'A' were transferred back to the recipient. The embryo slides and corresponding culture media were collected immediately and stored at -80°C until needed for further use. Trypsin activity was measured by ELISA, and the samples were subsequently correlated with a positive pregnancy test. Created with BioRender.com.

In subsequent experiments, the effects of trypsin on intracellular calcium levels in Ishikawa cells were assessed using live-cell calcium imaging to determine how trypsin activates calcium entry. To evaluate the potential role of LEFTY2 in modulating this process, endometrial cells were treated with LEFTY2 prior to trypsin stimulation, and changes in $[Ca^{2+}]_i$ were recorded. To further investigate whether the inhibitory effect of LEFTY2 on calcium entry involves ENaC, the ENaC blocker amiloride was used. This experiment aimed to determine whether LEFTY2-mediated inhibition of calcium entry occurs through ENaC-dependent mechanisms. The next set of experiments focused on determining whether the inhibitory effect of LEFTY2 on calcium entry was associated with changes in L-type calcium channel expression (**Figure 2-5**).

Bioinformatic analysis of publicly available single-cell sequencing data was conducted to investigate the expression of the L-type calcium channel gene CACNA1C in endometrial

tissue. This was followed by experimental validation using qRT-PCR and immunofluorescence to quantify L-type calcium channel abundance in endometrial cells with and without LEFTY2 treatment (**Figure 2-5**).

Finally, to evaluate whether the inhibitory effect of LEFTY2 on trypsin-induced calcium entry was sensitive to nifedipine, a known L-type calcium channel blocker, intracellular calcium measurements were conducted with 10 µM nifedipine. The comparison of calcium responses with and without nifedipine helped establish whether LEFTY2's inhibition of trypsin-induced calcium entry occurs *via* L-type calcium channels (**Figure 2-5**).

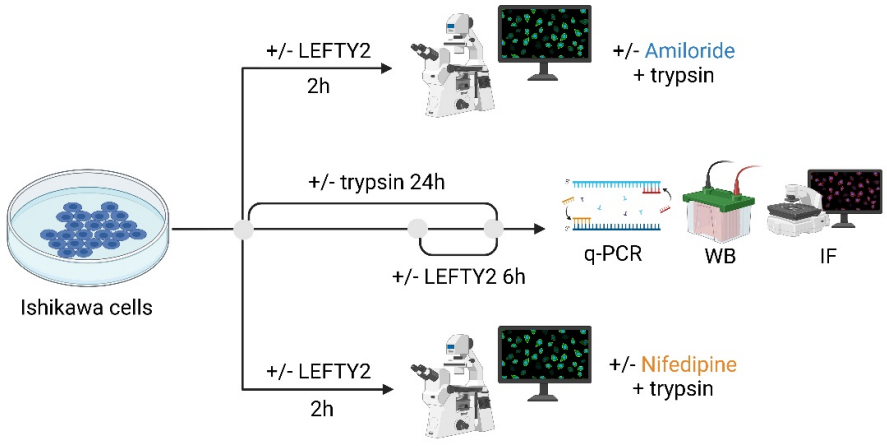

Figure 2-5: Schematic Overview of the Experimental Approach to Investigate the Role of LEFTY2 in Modulating Trypsin-induced Calcium Entry in Endometrial Cells.

The schematic illustrates the stepwise approach to assess the impact of LEFTY2 on $[Ca^{2+}]_i$ upon trypsin stimulation. Live-cell calcium imaging was used to measure trypsin-induced $[Ca^{2+}]_i$ changes, with or without the addition of the ENaC blocker amiloride, in the context of prior LEFTY2 treatment or not. L-type calcium channel abundance was evaluated using qRT-PCR, WB, and immunofluorescence. Subsequently, live-cell calcium imaging was conducted to measure trypsin-induced $[Ca^{2+}]_i$ changes in the presence or absence of the L-type calcium channel blocker nifedipine, with or without LEFTY2 pre-treatment. Created with BioRender.com.

2.3 Methods

2.3.1 Patient Selection and Sample Collection

The study received approval from the Anhui Medical University research ethic committee (No. PJ2018-07-20). The endometrial samples were obtained by Dr.

Huanhuan Jiang, at the Reproductive Medicine Center of the First Affiliated Hospital of Anhui Medical University. Patients did not receive hormone or steroidal treatment 3 months prior to samples collection. All participated patients provided written informed consent in line with The Declaration of Helsinki 2000 guidelines. Endometrial samples were collected at surgery and snap frozen immediately in LN2 before keeping at −80°C for later downstream analysis.

2.3.2 Cell Culture

EnSCs were incubated at 37°C in a humidified 5% CO_2 atmosphere in DMEM/F-12 medium containing 10% (v/v) dextran coated charcoal (DCC) striped fetal bovine serum, 1% (v/v) antibiotic-antimycotic solution, and 0.25% (v/v) L-glutamine. Cells were passaged when the confluency reached at 80%. Before treatment or transfection, the culture medium was changed to 2% (v/v) DCC striped FBS, 1% (v/v) antibiotic-antimycotic solution and 0.25% (v/v) L-glutamine. The cells were decidualized with 0.5 µM 8-Bromo-cAMP and 1 µM Medroxyprogesterone 17-acetate. All procedures were performed in a Class I laminar flow hood. Tests for mycoplasma contamination were regularly conducted and always gave a negative result.

The Ishikawa cells line (ISK), established from human endometrial adenocarcinoma (Brosens et al., 2014; Kumar et al., 2017; Salker, Hosseinzadeh, et al., 2016) were kept in Dulbecco's modified Eagle's medium/F12 containing 10% FBS, 1% (v/v) antibiotic-antimycotic solution, and 0.25% (v/v) L-glutamine. Cells were kept at 37°C in a humidified environment with 5% (v/v) CO_2. Cells were examined for mycoplasma contamination at regular intervals. Cells were normally seeded at 2 x 10^5 and allowed to recover for 24 h. To investigate CACNA1C expression, LEFTY2 treatment was conducted in ISK for 6 h (25 ng/ml) (Salker, Hosseinzadeh, et al., 2016; Salker, Schierbaum, et al., 2016; Salker et al., 2015) and/or trypsin for 24 h (20 µg/ml) (Ruan et al., 2012). For the Ca^{2+} measurement, cells were treated with LEFTY2 (25 ng/ml) for 6 h prior to measurement.

2.3.3 Transfection

EnSCs were seeded in 6-well plates at a concentration of 200,000 cells in each well in 2% DCC FBS media. For DJ-1 knockdown, EnSCs was transfected with small interference RNA (siPARK7) by using Lipofectamine RNAiMAX Transfection Reagent following the manufacturer's instructions. pGW1-Myc-DJ1-WT was a gift from Mark Cookson (Miller et al., 2003). Transfection was carried out by utilizing the Lipofectamine™ LTX Reagent with PLUS™ Reagent following the manufacturer's instructions. After 24 h the medium with transfection reagent was discarded and replaced with decidualization treatment medium. Cells were harvested for subsequent analysis.

2.3.4 Messenger RNA (mRNA) Extraction and Real-Time Quantitative Polymerase Chain Reaction (qRT-PCR)

Total mRNA was isolated from EnSCs or ISK using TRizol reagent. 1 µg of RNA was utilized to synthesize cDNA using the MaximaTM H Minus cDNA Synthesis Master Mix with dsDNase. mRNA concentration was determined by utilizing a Nanodrop. qRT-PCR was performed on the QuantStudio 3 Real-Time PCR System by using sets of gene-specific primers and the PowerUpTM SYBR® Green Master Mix. The relative differences in PCR product amounts were quantified by the $2^{-\Delta\Delta CT}$ method. Ribosomal L-19 as a housekeeping gene (Livak & Schmittgen, 2001).

The CT (Cycle Threshold) is the cycle number at which the fluorescence signal exceeds a threshold during qRT-PCR. Each target gene's CT value is normalized to a housekeeping gene, which is assumed to be expressed consistently across all samples:

$$\Delta CT = CT_{\,target\ gene} - CT_{\,reference\ gene}$$

The ΔΔCT was then determined by subtracting the ΔCT of the control samples from the ΔCT of the experimental samples:

$$\Delta\Delta CT = \Delta CT_{\,experimental} - \Delta CT_{\,control}$$

The gene expression fold change was determined using the formula:

$$Fold\ Change = 2^{-\Delta\Delta CT}$$

A fold change greater than 1 indicates upregulation, whereas a fold change less than 1 indicates downregulation. Each sample was tested in triplicate, and corresponding non-template controls were included in duplicate for every target gene. Melting curve analysis was processed on QuantStudio 3 PCR system. The subsequent agarose gel electrophoresis verified the amplification specificity. All the gene-specific primers used in this study was designed using primeblast (NCBI) and purchased from Sigma (Ye et al., 2012).

2.3.5 Protein Extraction and Western Blotting

G-actin protein extraction: To determine actin polymerization in EnSCs, EnSCs were kept in 80µL of Triton X-100 extraction buffer containing 0.3% Triton X-100, 5 mM Tris, 2 mM EGTA, 300 mM sucrose, 2 µM phalloidin, 1 mM PMSF, 10 µg/ml leupeptin, 20 µg/ml aprotinin, 1 mM sodium orthovanadate, and 50 mM NaF for 10 min on ice. The dissolvable proteins in the supernatant were collected through suction.

F-actin protein extraction: Cells were then incubated in 100 µl of RIPA buffer for 10 min on ice. The remaining Triton X - undissolved component was collected from the plate by scraping. All residual undissolved components were eliminated by centrifugation. An identical amount of each sample was mixed with Laemlli Buffer, and heated at 95 °C for 5 min.

Total cell protein samples were prepared by lysing the adherently cultured EnSCs in Laemmli buffer containing 0.5 M Tris hydrochloride pH 6.8, 20% Sodium dodecyl sulfate, 0.1% Bromophenol blue, 1% beta mercaptoethanol, and 20% glycerol. Whole cell extracts were heated at 95°C for 5 min.

Human tissues were washed in phosphate-buffered saline to remove any external contaminants. Subsequently, the tissues were homogenized in Radioimmunoprecipitation Assay (RIPA) buffer, supplemented with freshly added protease inhibitors, using the pestle method. Homogenization was carried out until a

uniform lysate was obtained. The homogenized samples were subsequently centrifuged at 13,000 g for 10 min at 4°C to pellet cellular debris and other insoluble components. The resulting supernatant containing solubilized proteins was carefully collected and transferred to fresh tubes for further analysis. To measure the protein concentration in the extracted samples, the Bradford protein assay method was employed. Briefly, Bradford reagent was loaded to the diluted protein samples following the manufacturer's guidelines. The absorbance of the resulting mixture was determined at the appropriate wavelength using a spectrophotometer, and protein concentrations were calculated using a standard curve generated with known concentrations of Bovine Serum Albumin (BSA).

20µg proteins were loaded on to a 12% sodium dodecyl sulfate poly-acrylamide gel (SDS-PAGE) using the XCell SureLock® Mini-Cell apparatus followed by electrophoresis. The protein from the gel was transferred onto poly-vinylidenefluoride membrane. After air-drying, the PVDF membranes were activated in 100% methanol and subsequently blocked with 5% skimmed milk or BSA for 1–2 h at room temperature (RT). Membranes were incubated overnight at 4°C with antibodies: human DJ-1 antibody (1:1000), human Palladin antibody (1:1000), human pan-actin antibody (1:1000), LEFTY antibody (1:500), human GAPDH (1:1000) was utilized as a loading control. After 3 times washing with TBS-T each for 10 min, the membranes were maintained with HRP-conjugated anti-rabbit secondary antibody (1:2000) at RT for 1 hour, followed by 3 times washing with TBS-T. A chemiluminescent detection kit was applied to the surface of the membranes, followed by visualization using the iBright Imaging System. Bands were quantified with FIJI Software (Schindelin et al., 2012).

2.3.6 Immunofluorescence

EnSCs were plated on 12 mm round coverslips at a density of 3000 cells per coverslip. Treatment for decidualization was conducted as mentioned earlier. Post treatment the cells were fixed for 15 min with 4% paraformaldehyde (PFA), washed 3 times with PBS, and permeabilized for 10 min in 0.1% Triton X-100/PBS. The coverslips were incubated

with 5% BSA in 0.1% TritonX-100/PBS for 1 h at RT and were probed overnight at 4°C with primary antibody: human DJ-1 antibody (1:100), Palladin antibody (1:80), anti-CACNA1C antibody (1:100). After 3 times washing, coverslips were maintained overnight at 4°C with secondary antibody: Alexa Fluor 488 (4 µg/ml), Alexa Fluor 568 (2 µg/ml). Cells were stained for F-actin with Phalloidin eFluor 660 (1:1000) for 30 min at RT. The coverslips were fixed with ProLong™ Gold Antifade Mountant with DNA Stain DAPI on slides. Immunofluorescence image acquisition was processed with the support of Dr. Nisha Mohd Rafiq and Ms. Birgit Fehrenbacher. Microscopy was carried out using LSM 800 confocal laser scanning microscope and EVOS M7000 cell imaging system with × 40 objective. Scale bar was 75 µm.

Protein expression levels in immunofluorescence images were quantified using Fiji. To measure the Integrated Density (the total fluorescence intensity within a cell), regions of interest (ROIs) were selected by manually outlining individual cells, and the Integrated Density was measured for each cell. Background regions without cells or fluorescence signal were selected. Several background regions were measured across the image to account for variability. The Mean Gray Value for each background ROI was recorded, and the average of these values was used as the Mean Background Intensity. The Corrected Total Cell Fluorescence (CTCF) for each cell was calculated using the formula:

$$CTCF = Integrated\ Density - (Area \times Mean\ Background\ Intensity)$$

Measurements were performed on at least five cells from multiple experiments to ensure reliable results. The data were then exported to Excel for further statistical analysis.

2.3.7 Flow Cytometry

EnSCs were fixed with 4% PFA for 10 min and then permeabilized with 1× permeabilization buffer and subsequently stained with 1 mg/ml of Deoxyribonuclease I, Alexa Fluor 488 (50 mg/ml) for the identification of G-actin, 1.0 µl of 1X fluorescent Phalloidin-eFluor 660 for the immunofluorescent observation of F-actin. Label

abundance was quantified by detecting signals in FITC (green) and APC (red) channel on FACSCanto II clinical flow cytometry system. The flow cytometry results were analyzed using FlowJo™ v10.8 Software. Geometric mean values for G- and F-actin fluorescence were obtained using FlowJo, and the G/F-actin ratio was calculated based on these values (Salker, Schierbaum, et al., 2016).

The treatment for EnSCs were conducted as mentioned above. The percentage of viable, apoptotic and necrotic cells was estimated by flow cytometry using the Annexin V apoptosis detection kit FITC in accordance with the manufacturer's instructions. Briefly, cells were harvested by trypsin and washed with PBS and 1× binding buffer, respectively, then cells were held in suspension in 1× binding buffer containing Annexin V-FITC solution (1:50). After that, cells were maintained at RT for 15 minutes in the dark, and washed with 1×binding buffer again. After adding Propidium Iodide (PI) solution (1:100), cells were kept at RT in the absence of light for 10 minutes prior to flow cytometry for cell apoptosis analysis. The flow cytometry results were analyzed using FlowJo™ v10.8 Software (Lakshmanan & Batra, 2013).

2.3.8 Mass Spectrometry (LC-MS/MS)

For proteome analyses, cell suspensions were prepared from decidualized EnSCs with and without siDJ-1 transfection as mentioned above. Cells were lysed by adding lysis buffer (5% 1M Tris/HCl pH 7,4, 2% 5M NaCl, 1% Triton X 100, 1% PMSF, 4% protease inhibitor cocktail) on ice. Ten micrograms of each sample were digested in solution with trypsin. After desalting using C18 stage tips, extracted peptides were separated on an Easy-nLC 1200 system coupled to a Q Exactive HFX mass spectrometer. The peptide mixtures were separated using a 90 minutes segmented gradient from to 10-33-50-90% of HPLC solvent B (80% acetonitrile in 0.1% formic acid) in HPLC solvent A (0.1% formic acid) at a flow rate of 200 nl/min. The 12 most intense precursor ions were sequentially fragmented in each scan cycle using higher energy collisional dissociation (HCD) fragmentation. Acquired MS spectra were processed with MaxQuant software package version 1.6.7.0 with integrated Andromeda search engine (Cox & Mann, 2008). Database

search was performed against a target-decoy Homo sapiens database obtained from Uniprot, containing 103.859 protein entries and 286 commonly observed contaminants. Peptide, protein and modification site identifications were reported at a false discovery rate (FDR) of 0.01, estimated by the target/decoy approach. The LFQ (Label-Free Quantification) algorithm was enabled, as well as match between runs and LFQ protein intensities were used for relative protein quantification. Data analysis was performed using Perseus and STRING v11 database (Tyanova et al., 2016). The mass spectrometry proteomics data have been deposited to the ProteomeXchange Consortium *via* the PRIDE (Perez-Riverol et al., 2022) partner repository with the dataset identifier PXD051694. Proteomics and the subsequent *in silico* analysis were performed by Anna Velic.

2.3.9 Wound Healing Assay

EnSCs were seeded in 6-well plate (100,000 cells per well). After 6 days of treatment until the cells were reaching 90-100% confluency, cells were synchronized by double thymidine (2 mm) blocking. The wells were then scratched with a 100 µL tip. Images were obtained immediately (0 h) using a 4× objective on the EVOS M7000 cell imaging system. Images were captured again after 6 h and 24 h. Wound healing quantification was performed using the FIJI software (Okumura et al., 2024).

2.3.10 AFM Force Mapping

AFM experiments were performed on live EnSCs with a commercial AFM setup. EnSCs were seeded on Petri dishes at a density of 3×10^4 cells/cm^2 and were treated as described above. Single EnSCs were imaged using the force mapping mode. Maps of 10×10 force-vs-indentation curves were recorded on a 10×10 µm^2 scan area on the central region of the cell using a pyramidal tip (spring constant 0.01 N/m, side angle 35 ± 2°), which was calibrated with the thermal noise method (S M Cook, 2006), and fitted with the pyramidal Sneddon model to determine the Young's modulus, E (Bilodeau,

1992). To calculate Young's modulus, stress (σ) is first determined as the applied force (F) divided by the original cross-sectional area (A) of the material:

$$\sigma = \frac{F}{A}$$

Strain (ϵ) is the relative deformation of the material, calculated as the change in length (ΔL) divided by the original length (L_0):

$$\epsilon = \frac{\Delta L}{L_0}$$

Then, plot the stress on the y-axis and the strain on the x-axis to create the stress-strain curve. The slope of the linear portion of this curve corresponds to Young's modulus. The slope of the linear portion of the stress-strain curve represents Young's modulus:

$$E = \frac{\sigma}{\epsilon}$$

Additionally, the whole cell body was imaged by performing maps of 50 × 50 force-vs-indentation curves on a 90 × 90 µm^2 scan area. The median of all Young´s modulus values in one map on a cell was considered representative of that cell. To minimize the influence of the underlying substrate, only stiffness values for cell regions with a height above 1 µm were considered and an indentation depth much smaller than the cell height was used. Data were analysed with the data analysis package Igor Pro. The measurements were carried out by Emily Hellwich and Prof. Tilman Schäffer.

2.3.11 Cell Viability Assay

EnSCs were seeded in a clear 96-well plate (3000 cells per well). After 6 days treatment, cells were maintained with 5 µL of CellTiter 96 Aqueous One Solution reagent for 3-4 h at 37 °C. Measurement of the absorbance at 490 nm for each sample was conducted using Varioskan™ LUX multimode microplate reader. The normalized OD values were calculated by dividing the treated group by the control. Data are illustrated as percentage.

2.3.12 Measurement of Cellular ROS

EnSCs were seeded in a black 96-well plate (3000 cells per well). To determine ROS production in decidualized EnSCs with or without DJ-1 knockdown, cells were co-incubated with 10 µM 2′,7′−dichlorofluorescin diacetate (DCFDA) for 30 min in the absence of light at RT. Cellular ROS production was measured at excitation and emission wavelengths of 499 and 522 nm, respectively, using the Varioskan™ LUX multimode microplate reader. The results were normalized to the cell count to estimate the amount of accumulated ROS per individual cell (Ng & Ooi, 2021).

2.3.13 Animal and Tissue Collection

Mating model: The generation and genotype of the DJ-1-deficient mice have previously been described in detail (Joselin et al., 2012). All animal procedures were approved by the University of Calgary Animal Care Committee (ACC Certification AC22-0072). Animals were maintained in strict accordance with the guidelines for the Use and Treatment of Animals set forth by the Animal Care Council of Canada and endorsed by the Canadian Institutes of Health Research. In brief, Wild-type (WT) females (10–12 weeks old) were placed with fertile males and vice versa, to ensure all the conceptuses were heterozygous, and the day a vaginal plug was observed was considered day 0.5 of pregnancy (dpc). The animals were euthanised by cervical dislocation at 7.5, dpc or until pups were delivered. This mouse mating model was conducted at Department of Clinical Neurosciences, Hotchkiss Brain Institute, Cumming School of Medicine, University of Calgary by Dr. Alvin Joselin, Dr. Doo Soon Im and Dr. Gaurav Kaushik.

Mouse implantation studies: Mice (BALB/c) were housed in animal facilities at the University of Rijeka, Faculty of Medicine and maintained in accordance with institutional and international guidelines. All experimental and surgical procedures involving mice complied with the Guide of Care and Use of Laboratory Animals and were approved by the University of Rijeka, Faculty of Medicine's ethical committee. Genetically modified

BALB/c, PRKO, and PRAKO mice were generously provided by John P. Lydon and Orla M. Conneely (Baylor College of Medicine Houston, Texas). WT females (10–12 weeks old) were placed with fertile males, and the day a vaginal plug was observed was considered day 0.5 of pregnancy (dpc). The animals were killed by cervical dislocation at 2.5, 4.5, 7.5, and 9.5 dpc. Intravenous injection of 1% (w/v) Chicago sky blue dye (0.1 mL/mouse) was utilized to make the implantation sites macroscopically visible. One uterine horn was fixed in 4% (w/v) PFA, and the other was frozen at −80°C for RNA or protein isolation. The mouse implantation study was performed at Department of Physiology and Pathophysiology, Medical School, University of Rijeka by Dr. Biserka Mulac-Jericevic, Tatjana Daka and Tihana Vujnović.

2.3.14 Immunofluorescence of Mouse Tissues

Tissue sections were deparaffinized and rehydrated through an ethanol gradient. Heat-induced antigen retrieval was performed in 10 mM sodium citrate, pH 6.0. To block nonspecific binding, tissue sections were kept with 1% BSA in PBS comprising 0.001% NaN_3 for 1 h at RT. Tissue sections were kept with primary antibodies diluted in 1% BSA in PBS with 0.001% NaN_3 overnight at 4 °C in a moist condition (Sucurovic et al., 2017).

For DJ-1 expression antibodies (D29E5) XP® Rabbit mAb (1:100), followed by Cell Signaling Fluor 594 donkey anti rabbit IgG (1:500) were used. For COX2 expression goat polyclonal COX2 antibodies (1:100), followed by biotinylated horse anti-goat IgG (1:300) were used. COX2 expression was visualizes by streptavidin (1:1000).

Nuclei were visualized with 4', 6-diamidino-2-phenylindole, dihydrochloride. The sections were mounted in Mowiol mounting media. Images were captured on Olympus imaging system BX51 equipped with DP71CCD camera and CellF imaging software was used. Images were edited using Photoshop CS6. This experiment was performed at Department of Physiology and Pathophysiology, Medical School, University of Rijeka by Dr. Biserka Mulac-Jericevic, Tatjana Daka and Tihana Vujnović.

2.3.15 Ca^{2+} Measurements

Fura-2 fluorescence was used to determine intracellular Ca^{2+} activity (Bhavsar et al., 2013). Cells were incubated with Fura-2/AM (2 µM) for 20 min at 37°C. Calcium measurements were conducted by alternately exciting the cells at 340 nm and 380 nm, using a Fluor 40×/1.30 oil objective on Axiovert 100 inverted phase-contrast microscope. Emitted fluorescence intensity was recorded at 505 nm. Data were obtained using Zeiss ZEN. Intracellular Ca^{2+} activity was calculated by dividing the fluorescence intensity at 340 nm by that at 380 nm. During the measurement, cells were kept either with or without the ENaC inhibitor, amiloride (1 µM), or the L type-Ca^{2+} channel inhibitor, nifedipine (10 µM) for the indicated duration. To quantify Ca^{2+} entry induced by trypsin, the slope (Δ ratio/s) and peak (Δ ratio) were calculated after the supplement of trypsin (Bhavsar et al., 2013; Yang et al., 2014). Intracellular calcium measurement was carried out with the support of Dr. Jing Yan, Dr. Md. Alauddin and Prof. Florian Lang.

2.3.16 Embryo Conditioned Media Collection and Trypsin Activity

Individual embryos were cultured in 25 µl droplets in Sage 1-step medium using the EmbryoScope. Embryos that were graded 'A' and were transferred back to the receipt. The embryo slide was obtained and the embryo media was collected immediately and stored at -80°C until further use. Trypsin activity kit was used and results calculated precisely following the manufacturer's guidelines. Samples were then correlated to a positive pregnancy test. This study was approved by the Ethics Commission at the Medical Faculty of Eberhard-Kars University of Tübingen (218/2023/B02). All participating patients/parents who were attending the IVF clinic at Universitätsklinikum Tübingen for unexplained female fertility provided informed consent in writing. Embryo culture media was collected by Dr. Steffen Kull and Dr. Melanie Henes.

2.3.17 In Silico Data Analysis

In silico analysis was carried out using these freely accessible gene expression datasets obtained from the Gene Expression Omnibus (GEO): Gene expression of embryos in pre-implantation development (Homo sapiens; ID:GDS3959); gene expression in peri-implantation phase and during implantation in the mouse uterus (ID: GSE44451); endometrium of patients with infertility and recurrent pregnancy loss (ID: GSE65102) (Lucas et al., 2016; Xie et al., 2010). Bioinformatic analysis was conducted on freely accessible single cell sequencing data obtained from the Single Cell Expression Atlas (Vento-Tormo et al., 2018).

For the results of proteomics, Gene Ontology (GO) analysis was performed to categorize the functional roles of differentially expressed genes. The analysis was conducted using PANTHER, which provides classification based on biological processes, molecular functions, and cellular components. Kyoto Encyclopedia of Genes and Genomes (KEGG) pathway enrichment analysis was conducted to identify significantly enriched biological pathways related to the differentially expressed genes. The analysis was performed using Metascape, which maps genes to KEGG pathways.

2.3.18 Statistical Analysis

The data are presented as arithmetic means ± standard error of the mean (SEM). the count of individual biological replicates in each experiment were denoted as n. Data were analyzed for significance using the student's t-test or one-way ANOVA in GraphPad Prism software. Statistical significance was considered when P value was less than <0.05. figures were made using GraphPad and Inkscape.

3. Results I: Loss of Parkinson's Disease Protein 7 Upregulates ROS and Cell Migration and is Associated with Recurrent Pregnancy Loss

This part of the dissertation hypothesizes that DJ-1 plays a critical role in regulating endometrial decidualization by modulating ROS levels and cell migration, thereby contributing to impaired decidualization and an increased risk of pregnancy loss. To explore this hypothesis, the expression patterns of DJ-1 in both human and mouse endometrial tissues were first examined. Proteomic analyses were then performed to identify downstream proteins involved in DJ-1-mediated regulation of decidualization, and the effects of DJ-1 deficiency were further investigated based on the proteomics results. Finally, the potential therapeutic implications of DJ-1 overexpression to reverse these effects were investigated.

3.1 Expression of DJ-1/PARK7 in Human Endometrial Tissue

DJ-1 has been implicated in various diseases, including cancer and neurodegeneration, but its role in the endometrium remains unclear (Cao et al., 2015; Kahle et al., 2009). To determine whether DJ-1 is expressed in normal human endometrial tissue, we first performed bioinformatic analysis on publicly available single cell sequencing data (Vento-Tormo et al., 2018). We observed a high expression of PARK7 in human decidua, particularly in endometrial decidual cells (**Figure 3-1A-C**) (Vento-Tormo et al., 2018). Additionally, to verify the expression of DJ-1 protein in the endometrium, we reviewed data from the Human Protein Atlas, which indicates that DJ-1 is expressed in both the endometrial glands and stroma. (**Figure 3-1D**) (Uhlen et al., 2005).

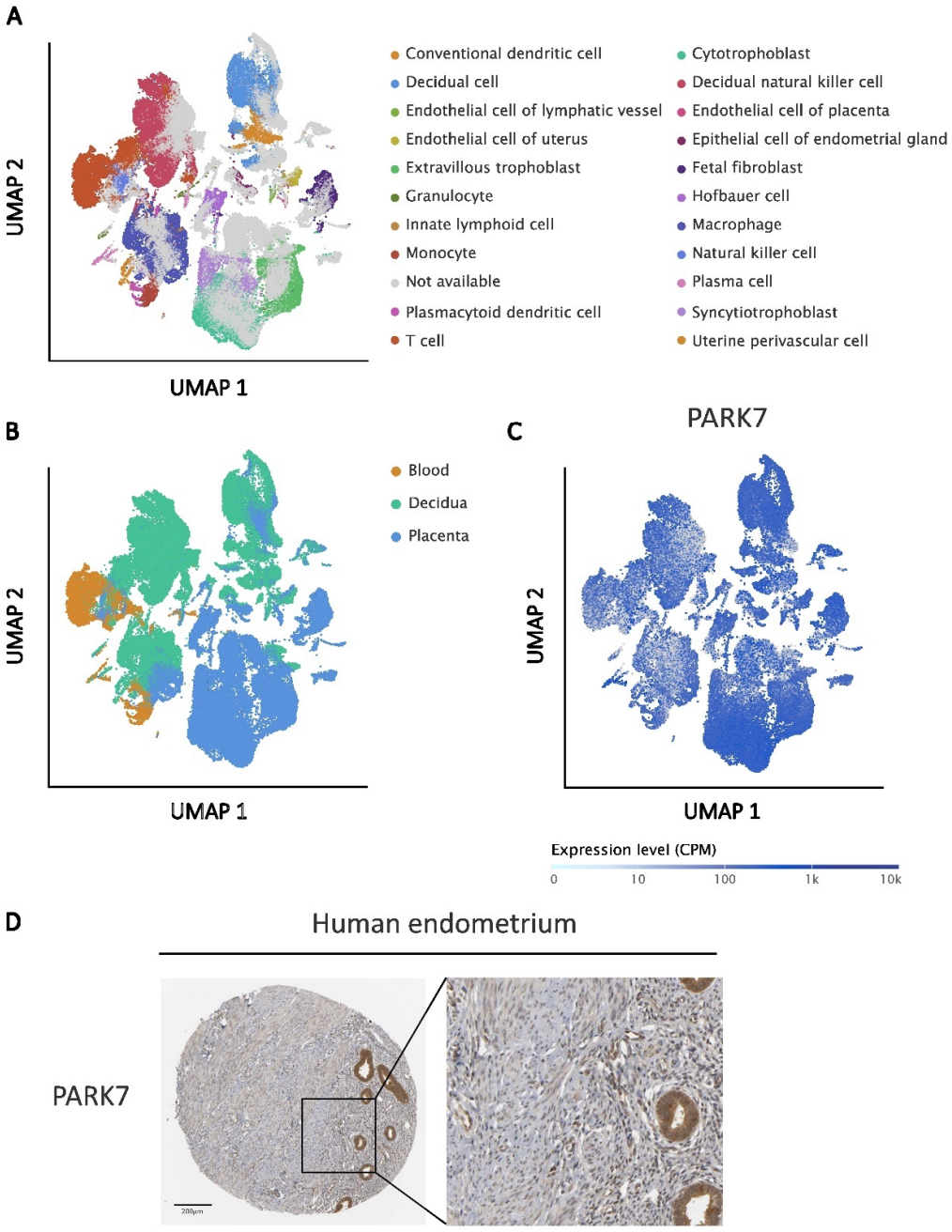

Figure 3-1: Expression of PARK7/DJ-1 in Human Endometrium.

(A) *Uniform manifold approximation and projection (UMAP) clustering of cell types; Cell types were annotated in the Single Cell Expression Atlas.* ***(B)*** *Uniform manifold approximation and projection (UMAP) clustering of tissues; Tissue compartments were annotated in the Single Cell Expression Atlas.* ***(C)*** *Expression of PARK7 in single cells, presented as counts per million (CPM), overlaid on the UMAP map.* ***(D)*** *Representative immunohistochemistry (IHC) images of DJ-1 protein expression in human endometrium tissues. Each right panel is an enlargement of the outlined area in the left panel in its respective column in the same sample. The IHC images were downloaded from The Human Protein Atlas.*

3.2 Enhanced DJ-1 Expression during EnSCs Decidualization

Since we confirmed the expression of DJ-1 in the endometrium and given that the process of decidualization in the endometrium is critical for the preparation and maintenance of a successful pregnancy (Gellersen & Brosens, 2014). To this end, EnSCs were subjected to treatment with 0.5 μM 8-Bromo-cyclic adenosine monophosphate and 1μM medroxyprogesterone acetate (cAMP and MPA, C+M) every 48 h for a total of 8 days. qRT-PCR analysis revealed a significant upregulation of DJ-1 mRNA level on the 6th day with a fold change of 3.16 following decidualization treatment (**Figure 3-2A**). The original gel image is provided in **Supplementary Figure 9-1**. Western blotting results demonstrated a significant increase in DJ-1 protein expression on the 6th day with a fold change of 1.75 (**Figure 3-2B**). The uncropped Western blot image is provided in **Supplementary Figure 9-2**. Given the importance of understanding the spatial distribution of DJ-1 in EnSCs, we further explored its protein localization. EnSCs were treated with C+M for 6 days, and immunofluorescence analysis was performed to confirm the expression and subcellular localization of DJ-1 in EnSCs. As depicted in **Figure 3-2C**, DJ-1 was dispersed in both the cytoplasm and nucleus of both untreated EnSCs. The intensity of DJ-1 was significantly elevated in decidualized cells, particularly within the nucleus.

Additionally, since cAMP and MPA were showed to increase DJ-1 expression, we aimed to determine whether the upregulation of DJ-1 is primarily induced by cAMP, MPA, or both. EnSCs were decidualized with cAMP or MPA for 6 days, and qRT-PCR analysis was subsequently performed. Our observations indicate that DJ-1 transcripts are upregulated with a fold change of 1.91 upon treatment solely with cAMP. (**Figure 3-2D**).

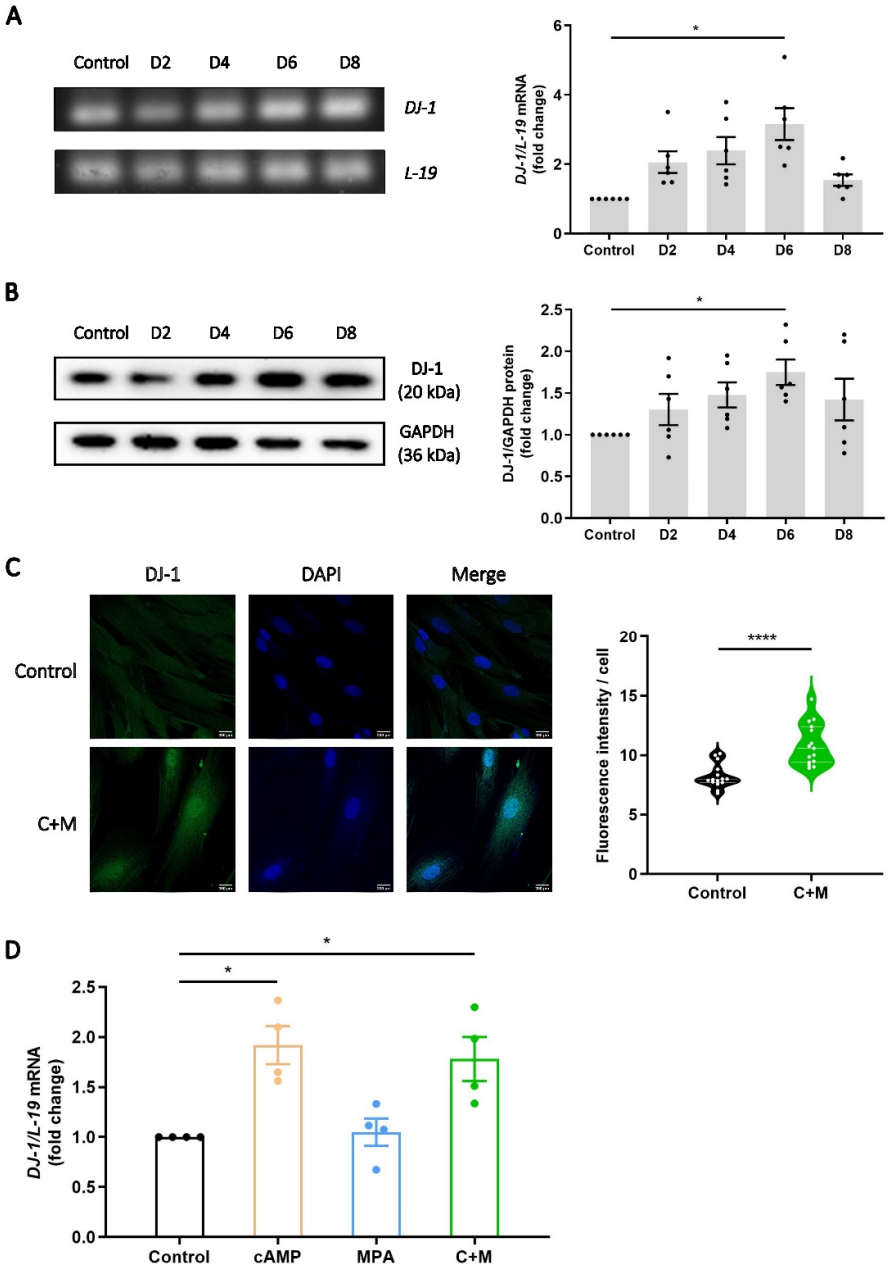

Figure 3-2: DJ-1 Expression in EnSCs during in vitro Decidualization.

(A) *DJ-1 mRNA level in EnSCs during decidualization were quantified by qRT-PCR (n = 6). Cycle threshold (Ct) values were adjusted relative to the housekeeping gene L-19.* ***(B)*** *Immunoblotting analysis of DJ-1 expression during the process of decidualization in EnSCs (n = 6). GAPDH served as a reference protein.* ***(C)*** *Immunofluorescence (IF) microscopy of untreated (Control, upper panel) and 6-day decidualized (C+M, lower panel) EnSCs showing DJ-1 subcellular localization. DJ-1 fluorescence intensity quantification results are shown (right). DJ-1: Alexa Fluor 488 (green); nucleus: DAPI (blue). Quantification performed from 3 experiments with >15 cells quantified for each condition. Scale bar = 200µm. Immunofluorescence image acquisition was carried out with the assistance of Ms. Birgit Fehrenbacher.* ***(D)*** *DJ-1 mRNA level in EnSCs treated with cAMP, MPA or C+M were detected by qRT-PCR (n = 4). Ct values were normalized to an average Ct value of housekeeping gene L-19. Data are shown as mean ± SEM. One way-ANOVA and Unpaired T-test was used to calculate statistical significance. *P < 0.05, **P < 0.01, ***P < 0.001, ****P < 0.0001.*

3.3 DJ-1 Expression in Mice and Human Endometrium during Early Pregnancy

In view of its multifunctional role, DJ-1 could also be a putative regulator of murine pregnancy. To investigate the expression of DJ-1 during mouse decidualization, we mined publicly available microarray data (GSE44451) that profiled gene expression during the peri-implantation phase (3.5 days post coitus; dpc) and during implantation (4.5 dpc) in the murine uterus. As depicted in **Figure 3-3A**, the expression of DJ-1 exhibited an increase once it entered the implantation stage in mice. Consistent with previous findings, at day 4.5 of pregnancy, strong COX2 staining was observed surrounding the murine implantation site, which was used to locate the site of implantation (Sucurovic et al., 2017, 2020). We employed double labelling and immunofluorescence techniques to compare DJ-1 and COX2 expression at day 4.5 of pregnancy. Our findings demonstrate the localization of DJ-1 surrounding the implantation site, as well as distally in the glandular epithelium, primarily within the nucleus (**Figure 3-3B**).

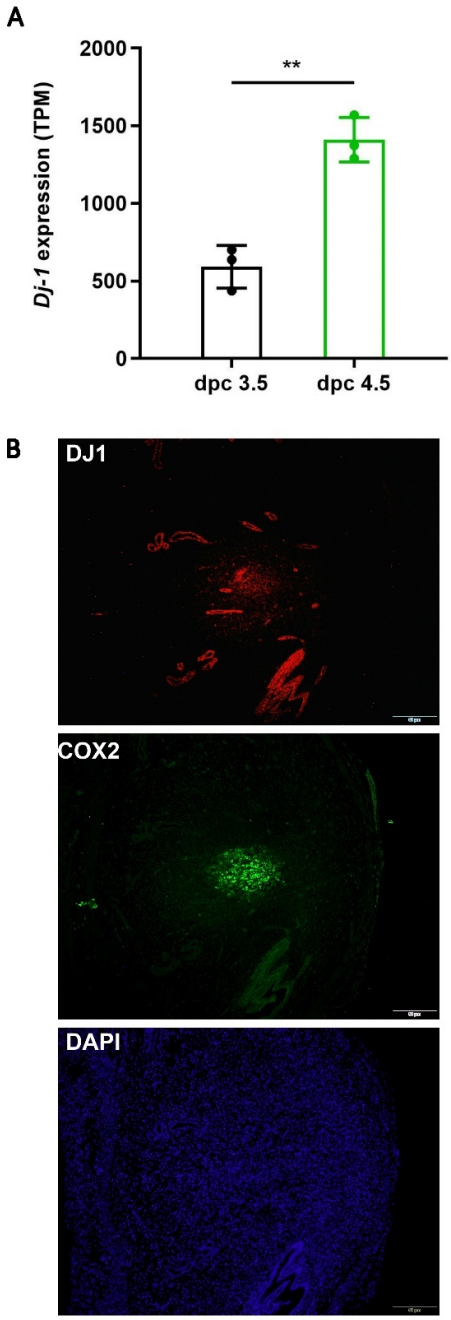

Figure 3-3: DJ-1 Expression during Early Pregnancy in Mouse Models.

(A) *Mouse Dj-1 gene expression before (dpc 3.5) and during (dpc 4.5) early pregnancy (n = 3) (GSE44451).* ***(B)*** *IF microscopy of mice uterus showing DJ-1 localization during implantation. DJ-1: Fluor 594 (red); COX2: Alexa Fluor 488 (green); nucleus: DAPI (blue). Scale bar = 50μm. The study was performed at Department of Physiology and Pathophysiology, Medical School, University of Rijeka by Dr. Biserka Mulac-Jericevic, Tatjana Daka and Tihana Vujnović. Data are presented as mean ± SEM. Unpaired T-test was used to calculate statistical significance. *P < 0.05, **P < 0.01, ***P < 0.001, ****P < 0.0001.*

Given previous indications implicating impaired decidualization and susceptibility to subsequent pregnancy failure (Salker et al., 2010), our observations indicate that DJ-1 is essential for ongoing decidualization and pregnancy, and thus, the loss of DJ-1 will have a determinantal effect on pregnancy outcomes. To verify this conjecture, we counted the sites of implantation and pups per litter in Dj-$1^{-/-}$ female mice crossed with WT males and WT females crossed with Dj-$1^{-/-}$ males, thereby negating the potential contribution of the offspring's genotype (**Figure 3-4A**). In Dj-$1^{-/-}$ females, the sites of implantation at 8.5 dpc was maintained, however the average litter size was significantly reduced, indicating an excess of 50% spontaneous fetal loss (**Figure 3-4B**).

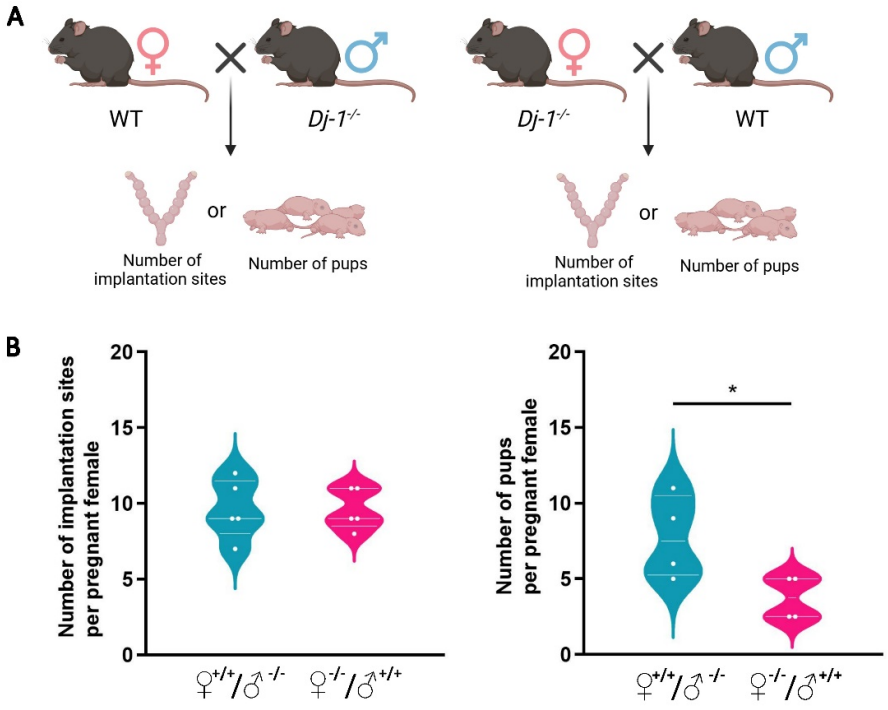

Figure 3-4: Impact of DJ-1 Deficiency on Pregnancy Outcomes in Mice.

(A) *Schematic depiction of mice mating model. The model was conducted at Department of Clinical Neurosciences, Hotchkiss Brain Institute, Cumming School of Medicine, University of Calgary by Dr. Alvin Joselin, Dr. Doo Soon Im and Dr. Gaurav Kaushik.* ***(B)*** *Number of implantation sites and pups per litter based on the breeding of Dj-$1^{-/-}$ female mice crossed with WT males, or WT females crossed with Dj-$1^{-/-}$ males (n = 4). Data are presented as mean ± SEM. Unpaired T-test was used to calculate statistical significance. *P < 0.05, **P < 0.01, ***P < 0.001, ****P < 0.0001.*

Given the abundant expression of DJ-1 in the human endometrium and the negative impact of DJ-1 deficiency on pregnancy outcomes in mice, we hypothesized that DJ-1 expression might be altered in women with RPL. To investigate this, we examined published transcriptome data from midluteal endometrial biopsies from 10 women with RPL and 10 subfertile women with no history of pregnancy losses. Age, body mass index (BMI), and the number of days after the luteinizing hormone peak when the samples were collected showed no significant differences between the two groups (**Supplementary Table 8-1**) (Lucas et al., 2016). As depicted in **Figure 3-5A**, the reduction in endometrial DJ-1 transcripts was observed. Moreover, protein samples of human endometrial tissue were collected from 9 women with RPL and 10 subfertile women with no history of losses (**Supplementary Table 8-2**). Western blotting was subsequently conducted. As illustrated in **Figure 3-5B**, the expression of DJ-1 protein in the RPL group was significantly diminished (52 % reduction) compared to the control.

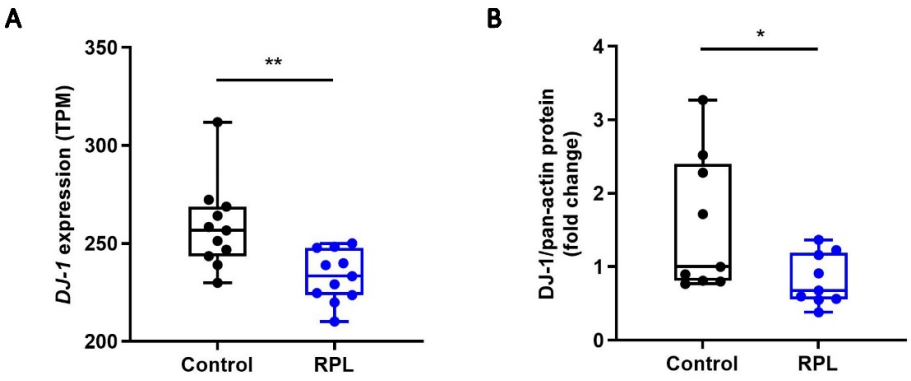

Figure 3-5: DJ-1 Expression during Early Pregnancy in Human

(A) *Human DJ-1 gene expression in endometrium of patients with Control (infertility) and recurrent pregnancy loss (n = 10) (GSE65102).* ***(B)*** *Immunoblotting analysis of DJ-1 protein level in endometrial tissue from patients with Control (infertility) (n = 10) and RPL (n = 9). Pan-actin served as a reference protein. Human endometrial samples were collected at Reproductive Medicine Center, the First Affiliated Hospital of Anhui Medical University by Huanhuan Jiang. Data are presented as mean ± SEM. Unpaired T-test was used to calculate statistical significance. *P < 0.05, **P < 0.01, ***P < 0.001, ****P < 0.0001.*

3.4 Expression of Decidualization Markers in EnSCs upon DJ-1 Knockdown

Decidualization serves as a crucial preparatory stage for pregnancy establishment (Gellersen & Brosens, 2014). To understand whether deficiency of DJ-1 impacts decidualization, the function of DJ-1 in EnSCs was assessed using siRNA-mediated gene silencing during this process. Firstly, DJ-1 knockdown was performed by treating EnSCs with C+M for 6 days, with transfection carried out on the third day for 24 h. Knockdown efficiency was further confirmed by qRT-PCR and WB. As depicted in **Figure 3-6A, B**, siRNA-mediated knockdown resulted in a significant reduction of DJ-1 expression at both the transcript (97% reduction) and protein level (65% reduction). The full blots of DJ-knockdown experiment are provided in **Supplementary Figure 9-3** and **9-4**. Notably, compared to decidualized EnSCs, the deficiency of DJ-1 caused a significant drop in the level of the key decidual marker *IGFBP1*. In contrast, no changes were observed in the expression levels of other decidual markers, such as *PRL* and *HSD11B1*. (**Figure 3-6C**).

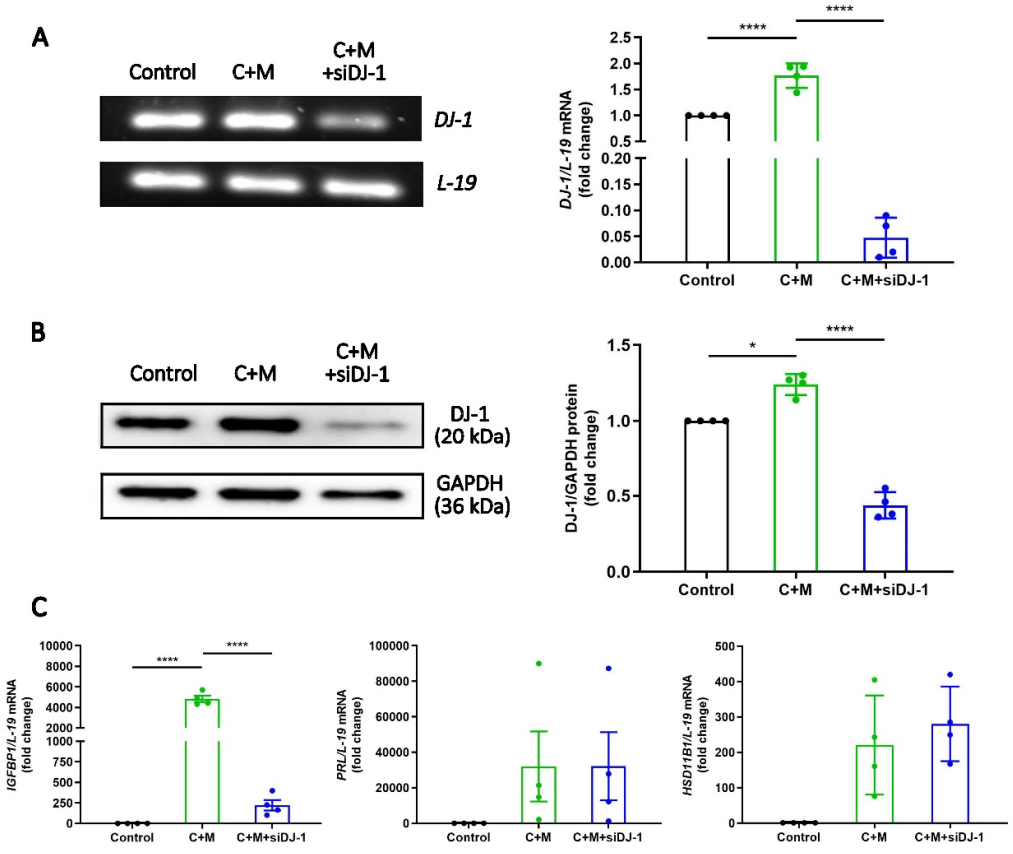

Figure 3-6: Decidualization Markers Expression in EnSCs Following DJ-1 Knockdown.

(A) *DJ-1 mRNA level and* ***(B)*** *DJ-1 protein level in EnSCs transfected by PARK7-targeting siRNA (siDJ-1) for 24 h, which was performed on the third day of a total of 6-day treatment with 0.5 µM 8-Br-cAMP and 1 µM MPA (C+M) (n = 4).* ***(C)*** *IGFBP, PRL and HSD11B1 mRNA expression level in decidualizing EnSCs with transfection of siDJ-1 (n = 4). The data are shown as mean ± SEM. One-way ANOVA was applied to determine statistical significance. *P < 0.05, **P < 0.01, ***P < 0.001, ****P < 0.0001.*

3.5 DJ-1 Loss Increases ROS Production, Leading to Reduced Cell Proliferation and Increased Cell Death

DJ-1 is an oxidative stress sensor that, participates in the onset of oxidative stress-related diseases (Joselin et al., 2012). It functions as an antioxidant through various mechanisms, including scavenging ROS (Zhang et al., 2020). We postulated that loss of DJ-1 will lead to increased ROS and impair the induction of antioxidants or ROS scavengers. To test this hypothesis, we assessed intracellular ROS production using the H_2-DCFDA assay, which relies on the oxidation of a non-fluorescent compound into a highly fluorescent product,

enabling the detection and quantification of intracellular ROS levels (Gomes et al., 2005). **Figure 3-7A** illustrates that, in comparison with decidualized EnSCs, DJ-1 knockdown resulted in a higher level of intracellular ROS production. We then tested whether loss of DJ-1 could impair the induction of antioxidant enzymes. As a result, GPX3, which reduces H_2O_2 and lipid peroxides using glutathione (GSH), and Glutaredoxin (GLRX), which regulates redox balance by reducing protein disulfide bonds with GSH, were both downregulated in EnSCs targeted with siDJ-1 (**Figure 3-7B**).

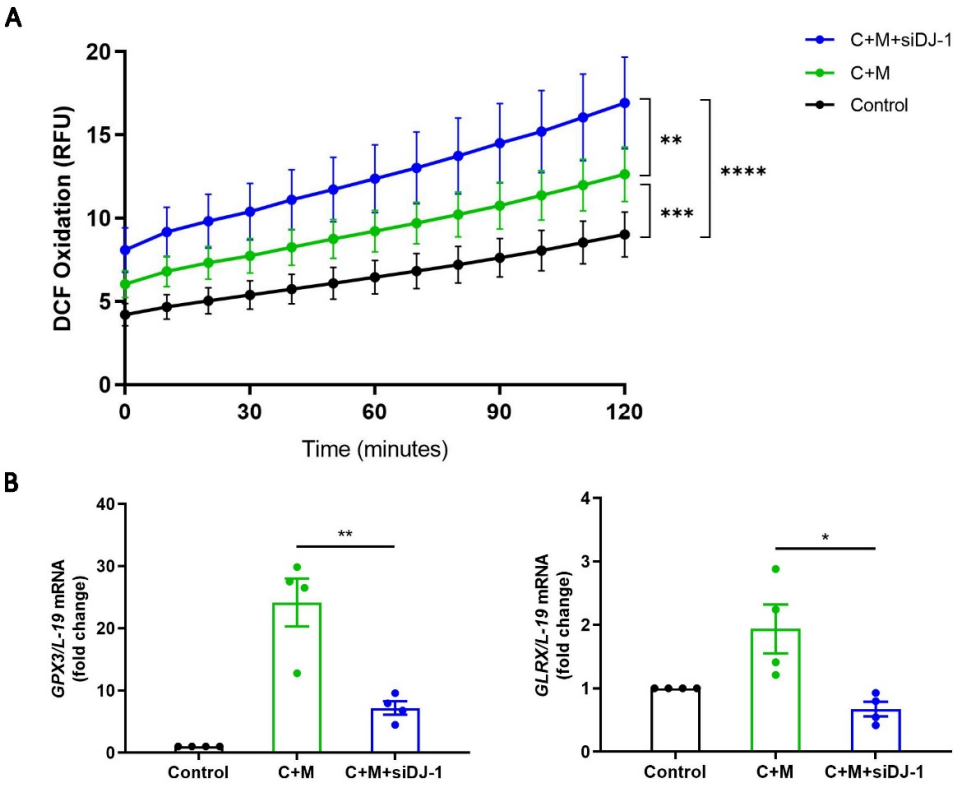

Figure 3-7: Effects of DJ-1 Loss on ROS Levels in EnSCs.

(A) *ROS DCF fluorescence intensity at the indicated time points.* ***(B)*** *GPX3 and GLRX mRNA expression level in decidualizing EnSCs with transfection of siDJ-1 (n = 4). The data are presented as mean ± SEM. One-way ANOVA and unpaired T-test was used to calculate statistical significance. *P < 0.05, **P < 0.01, ***P < 0.001, ****P < 0.0001.*

Since ROS are involved in cell signaling pathways that regulate cell growth and proliferation, we examined the expression of the cell proliferation marker Ki-67 (de Almeida et al., 2022). We observed a significant reduction in Ki-67 expression upon DJ-1 knockdown, indicating a decrease in cellular proliferation activity. This finding was further validated using a BrdU ELISA assay, as shown in **Figure 3-8A**. On the other hand, high ROS levels are a major trigger for various forms of programmed cell death. Therefore, we measured cell death by FACS, and the results showed an increase in cell death following DJ-1 knockdown, as depicted in **Figure 3-8B**.

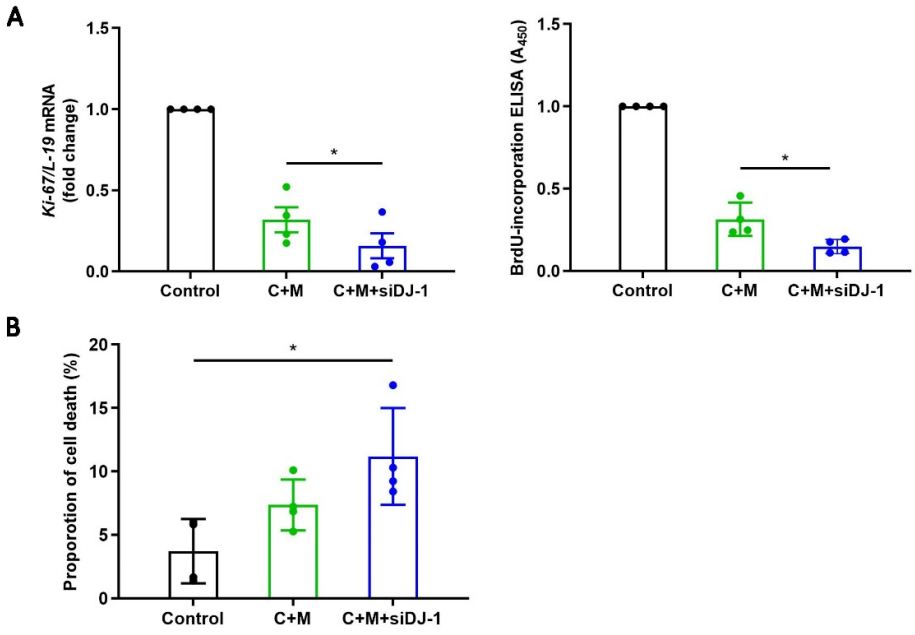

Figure 3-8: Effects of DJ-1 Loss on ROS Levels, Cell Proliferation and Death in EnSCs.

(A) *Ki-67 mRNA expression level in decidualizing EnSCs with transfection of siDJ-1 (n = 4); BrdU ELISA assay was carried out after treatment. Absorbance was recorded at 450 nm.* ***(B)*** *Cell death determined using Annexin V/PI staining after 6 days decidualization treatment with or without siDJ-1 transfection compared to untreated control (n = 4). The data are presented as mean ± SEM. One-way ANOVA was used to calculate statistical significance. *P < 0.05, **P < 0.01, ***P < 0.001, ****P < 0.0001.*

3.6 Proteomic Analysis of DJ-1 Knockdown in Decidual EnSCs

The known function of endometrial DJ-1 is sparse. In order to identify novel downstream targets of DJ-1, proteomics (mass spectrometry, LC-MS/MS) was employed to explore differentially expressed cellular proteins in decidual EnSCs induced by 6 days of treatment with C+M, with or without DJ-1 knockdown (**Figure 3-9A**). As a result, a total of 28 upregulated (orange) and 50 downregulated (green) proteins was observed (**Figure 3-9B, Supplementary Table 8-3, 8-4**).

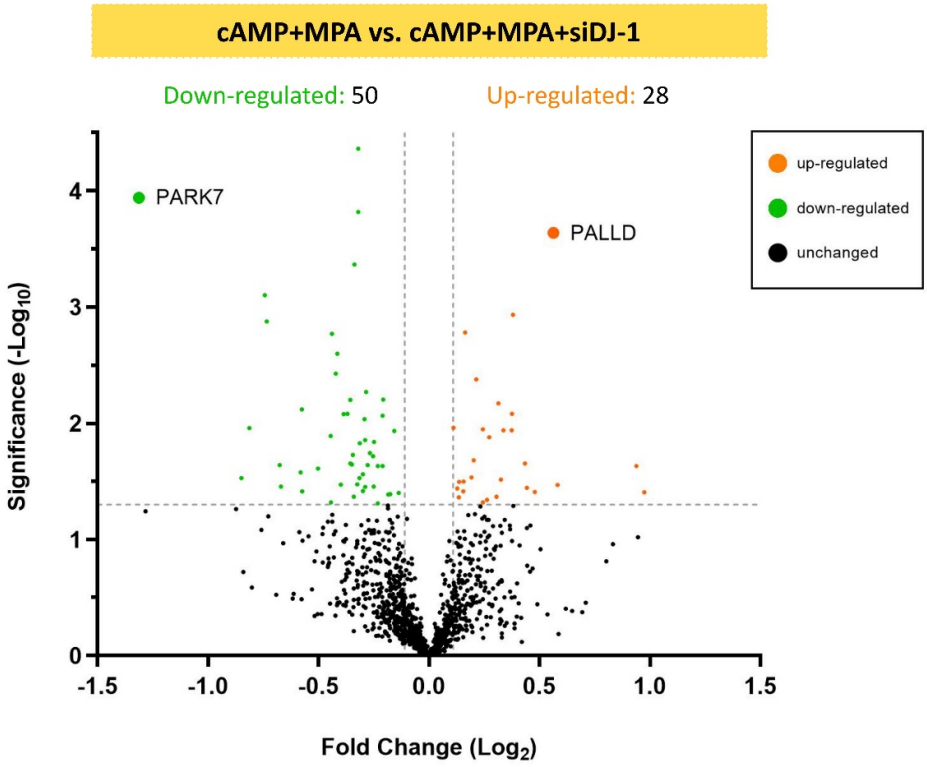

Figure 3-9: Identification of Novel Downstream Targets of DJ-1 via Proteomic Analysis in Decidual EnSCs.

Volcano plot of proteomic data. Results for decidualized EnSCs with or without siDJ-1 transfection are shown (n = 4). Orange circles show proteins which have significant increases. Green circles show proteins which have significant decreases. Black circles are proteins without any differences. Proteomics and the subsequent in silico analysis were performed by Anna Velic.

Upon loss of DJ-1, several proteins were significantly upregulated, including actin and cytoskeleton-associated proteins such as Integrin subunit alpha 5 (ITGA5), and Matrix

metallopeptidase 14 (MMP14) (**Figure 3-10A**). The significantly downregulated proteins included thioredoxin reductase 1 (TXNRD1), thioredoxin related transmembrane protein 3 (TMX3) and GLRX, which are involved in redox signaling (**Figure 3-10B**).

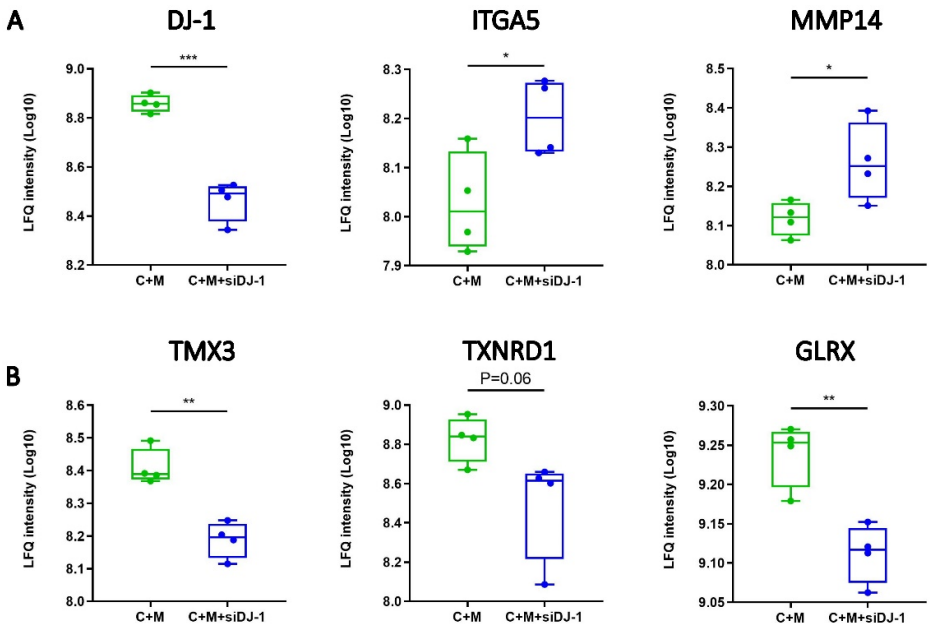

Figure 3-10: Differential Protein Expression in Decidual EnSCs upon DJ-1 Knockdown.

(A) *Expression of DJ-1 and cytoskeleton-associated proteins ITGA5 and MMP14 in decidualized EnSCs with or without siDJ-1 transfection. Presented as LFQ intensity.* ***(B)*** *Expression of redox signaling related proteins TMX3, TXNRD1 and GLRX in decidualized EnSCs with or without siDJ-1 transfection. The data are presented as mean ± SEM. Unpaired T-test was used to calculate statistical significance. *P < 0.05, **P < 0.01, ***P < 0.001, ****P < 0.0001.*

Gene Ontology (GO) analysis revealed molecular functions upregulated after DJ-1 knockdown are associated with cell adhesion molecule binding, GTP binding, the structural constituent of the cytoskeleton and NADPH:quinone reductase activity (**Figure 3-11A**). Additionally, Kyoto Encyclopedia of Genes and Genomes (KEGG) analysis indicated the contribution of signaling pathways related to tight junctions and gap junctions after DJ-1 knockdown (**Figure 3-11B**).

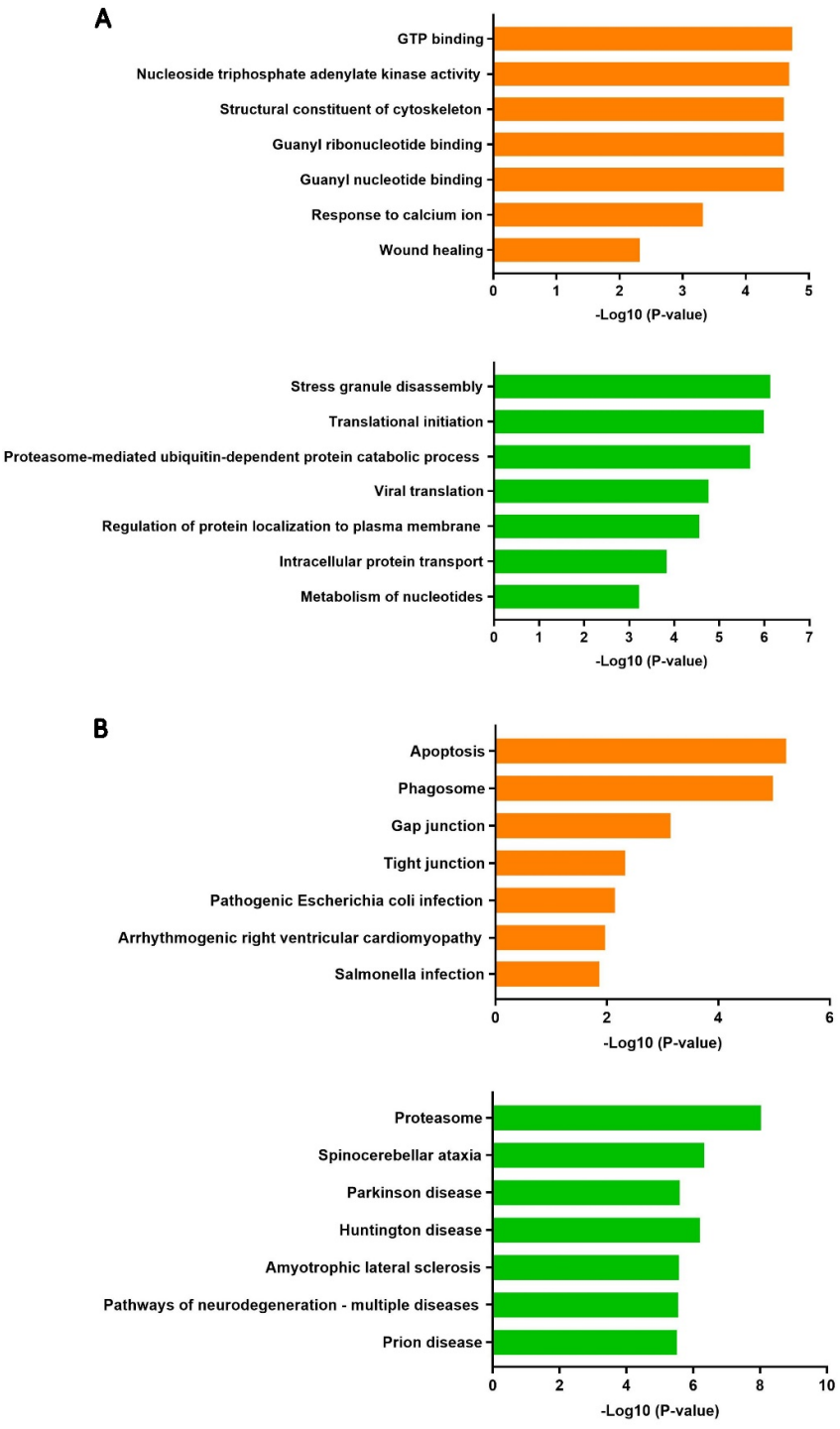

Figure 3-11: DJ-1 Downstream Pathways in Decidual EnSCs.

(A) *GO enrichment analysis of differentially expressed proteins. GO molecular function enrichment analyses of up-regulated (orange) and down-regulated (green) proteins were performed.* ***(B)*** *KEGG enrichment analysis up-regulated (orange) and down-regulated (green) proteins were performed.*

3.7 Palladin Levels and Its Potential Role in Early Pregnancy and Recurrent Pregnancy Loss

The cytoskeleton is crucial for the structural and functional changes during decidualization (Ihnatovych et al., 2009). By regulating cell shape, migration, adhesion, and signaling, cytoskeletal proteins facilitate the differentiation of EnSCs into decidual cells, which is crucial for embryo implantation and pregnancy establishment. Interestingly, our proteomics results showed that the level of Palladin, a cytoskeletal protein, significantly upregulated in the DJ-1 knockdown group in comparison to the control (**Figure 3-12A**). Western blotting was performed on decidual EnSCs with or without DJ-1 knockdown, and the results confirmed the upregulation (40%) of Palladin protein levels (**Figure 3-12B**). The full blot is shown in **Supplementary Figure 9-5**.

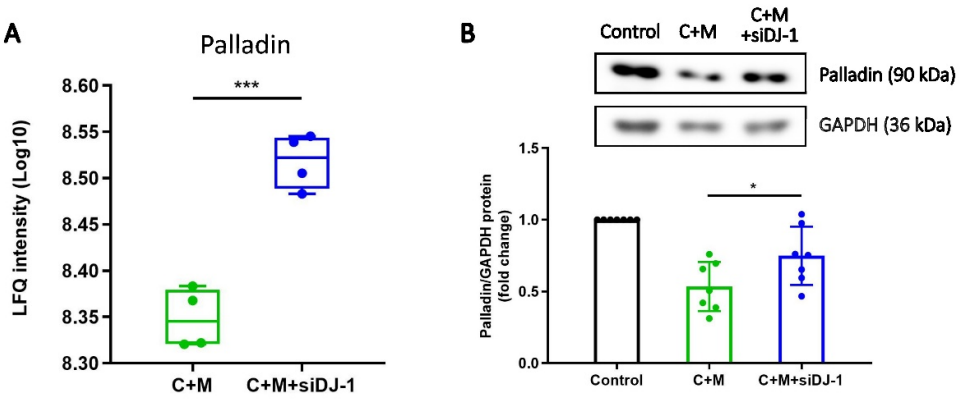

Figure 3-12: Expression of Palladin upon DJ-1 Knockdown in Decidual EnSCs.

(A) *Expression of Palladin in decidualized EnSCs with or without siDJ-1 transfection. Presented as LFQ intensity.* ***(B)*** *Immunoblotting analysis of Palladin expression in decidualizing EnSCs with or without transfection of siDJ-1 (n = 7). GAPDH was used as a loading control. The data are presented as mean ± SEM. One-way ANOVA and unpaired T-test were used to calculate statistical significance. *P < 0.05, **P < 0.01, ***P < 0.001, ****P < 0.0001.*

We further investigated whether Palladin also plays a role in early pregnancy. Firstly, we confirmed the presence of Palladin in the human endometrium. Single-cell sequencing

analysis revealed that the *PALLD* gene is actively expressed in human endometrial decidua cells, as shown in **Figure 3-13A-C** (Vento-Tormo et al., 2018). In addition, evidence from the Protein Atlas demonstrated Palladin protein expression in both stromal cells and glandular epithelial cells of the endometrium. (**Figure 3-13D**) (Uhlen et al., 2005).

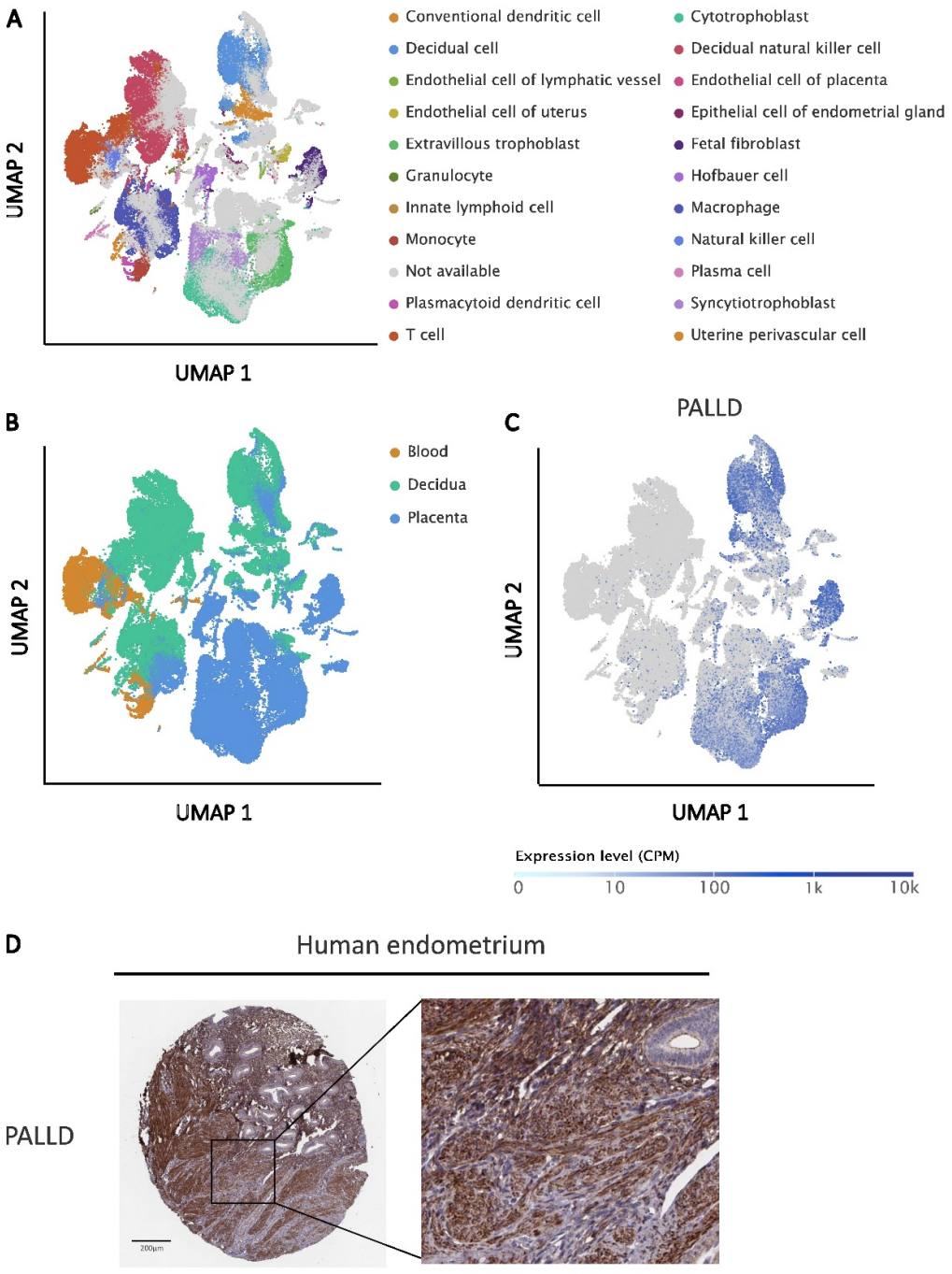

Figure 3-13: Expression of Palladin in vivo.

*Uniform manifold approximation and projection (UMAP) clustering of tissues and cell types; Cell types **(A)** and tissue compartments **(B)** were annotated in the Single Cell Expression Atlas. **(C)** Expression of PALLD in single cells, presented as counts per million (CPM), overlaid on the UMAP map. **(D)** Representative immunohistochemistry (IHC) images of Palladin protein expression in human endometrium tissues. Each right panel is an enlargement of the outlined area in the left panel in its respective column in the same sample. The IHC images were downloaded from The Human Protein Atlas.*

Since the data showed that Palladin can be found *in vivo*, and considering that decidualization is a critical process in establishing a receptive endometrium, we further treated EnSCs with C+M up to 8 days to investigate Palladin expression levels during decidualization. Notably, Palladin expression decreases during decidualization, reaching its lowest level during the window of implantation (**Figure 3-14A**). Furthermore, to investigate the expression of Palladin *in vivo*, we measured its mRNA levels during early pregnancy in mice. Consistent with our *in vitro* findings, mRNA levels of Palladin were reduced during early pregnancy (**Figure 3-14B**). To elucidate its potential role in pregnancy loss, we conducted western blot to investigate Palladin protein expression in human endometrial tissues. As depicted in **Figure 3-14C**, Palladin exhibited higher levels although not reaching significance in endometrial tissue obtained from patients experiencing RPL compared to the control.

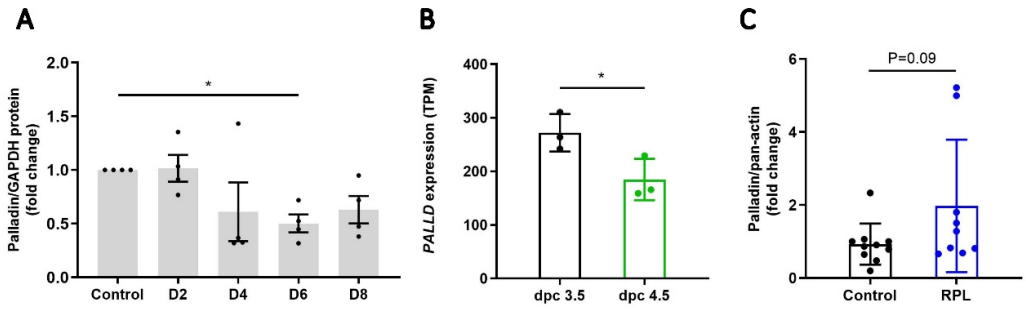

Figure 3-14: Expression of Palladin during Early Pregnancy.

(A) *Immunoblotting analysis of Palladin expression during decidualization in EnSCs (n = 6). GAPDH was used as a loading control.* ***(B)*** *Mouse PALLD gene expression before (dpc 3.5) and during (dpc 4.5) early pregnancy (n = 3) (GSE44451).* ***(C)*** *Immunoblotting analysis of Palladin protein expression in endometrial tissue from patients with infertility and RPL (n = 9). Pan-actin was used as a loading control. The data are presented as mean ± SEM. One-way ANOVA and unpaired T-test were used to calculate statistical significance. *P < 0.05, **P < 0.01, ***P < 0.001, ****P < 0.0001.*

3.8 Loss of DJ-1 Induces Cytoskeletal Dynamics Changes: Impact on Actin Polymerization, Cell Stiffness, and Cell Migration

Palladin functions as an actin-binding and actin-crosslinking protein with effects on cell morphology, mobility and force generation (Azatov et al., 2016; Jin et al., 2009). Here we sought to explore whether DJ-1 also plays a regulatory role in these cytoskeleton dynamics-related processes. To assess if there is a putative link between DJ-1 deficiency and the cytoskeleton, immunofluorescence staining was performed on decidualized EnSCs, as well as on decidualized EnSCs following transfection with siDJ-1. Palladin is an essential cytoskeleton scaffolding molecule by functioning as an F-actin-binding protein. As depicted in **Figure 3-15A, B**, compared to the rounded morphology observed in decidualized EnSCs, the depletion of DJ-1 led to a spindle-like deformation in EnSCs, concomitant with increased staining intensity for Palladin and F-actin. Notably, DJ-1 was found to partially co-localize with Palladin and F-actin, with Palladin predominantly exhibiting a punctate pattern along the stress fibers.

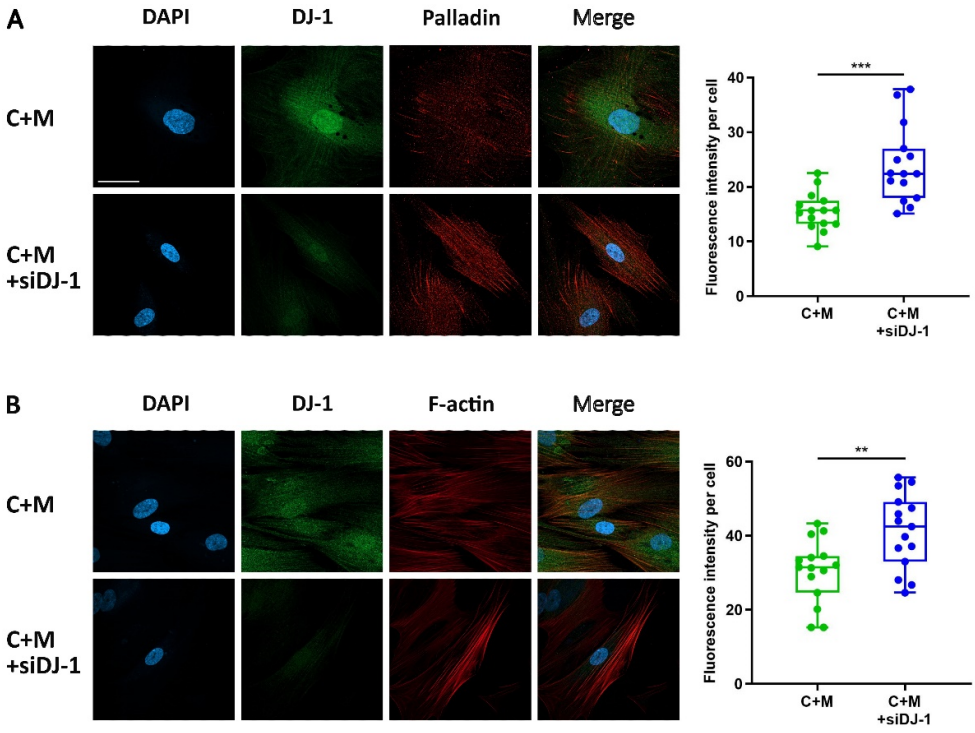

Figure 3-15: Expression and localization of Palladin and F-actin upon DJ-1 Knockdown.

(A) *Immunofluorescence staining of decidualized EnSCs (upper panel) with siDJ-1 transfection (lower panel) showed cell morphological changes. DJ-1: Alexa Fluor 488 (green); Palladin: Alexa Fluor 568 (red); nucleus: DAPI (blue), (n = 3), Scale bar (75 µm).* ***(B)*** *Immunofluorescence staining of decidualized EnSCs (upper panel) with siDJ-1 transfection (lower panel) showed cell morphological changes. DJ-1: Alexa Fluor 488 (green); nucleus: DAPI (blue); F-actin: Phalloidin (red), (n = 3), Scale bar (75 µm). quantification of immunofluorescence intensity performed from 3 experiments with >15 cells quantified for each condition. Immunofluorescence image acquisition was carried out with the assistance of Dr. Nisha Mohd Rafiq. The data are presented as mean ± SEM. Unpaired T-test was used to calculate statistical significance. *P < 0.05, **P < 0.01, ***P < 0.001, ****P < 0.0001.*

Previous studies have shown that Palladin overexpression results in profound changes in actin organization (Dixon et al., 2008). To determine the loss of DJ-1 influences G/F actin ratio, FACS and western blot analyses were employed. As depicted in **Figure 3-16A, B**, the deficiency of DJ-1 led to a significant decrease in the G/F actin ratio, indicating enhanced actin polymerization. The gating strategy is shown in **Supplementary Figure 9-6**. The full blot is shown in **Supplementary Figure 9-7**. Given a previous study indicating a potential relationship between actin polymerization and cell stiffness alteration (Salker,

Schierbaum, et al., 2016), we investigated the association of DJ-1 with cell stiffness using atomic force microscopy (AFM) on live EnSCs subjected to a 6-day decidualized treatment with or without DJ-1 knockdown. As illustrated in **Figure 3-16C**, the loss of DJ-1 in decidual EnSCs resulted in a significant increase in the Young's modulus. Taken together these results reveal that DJ-1 loss results in increased actin polymerization and cell stiffness.

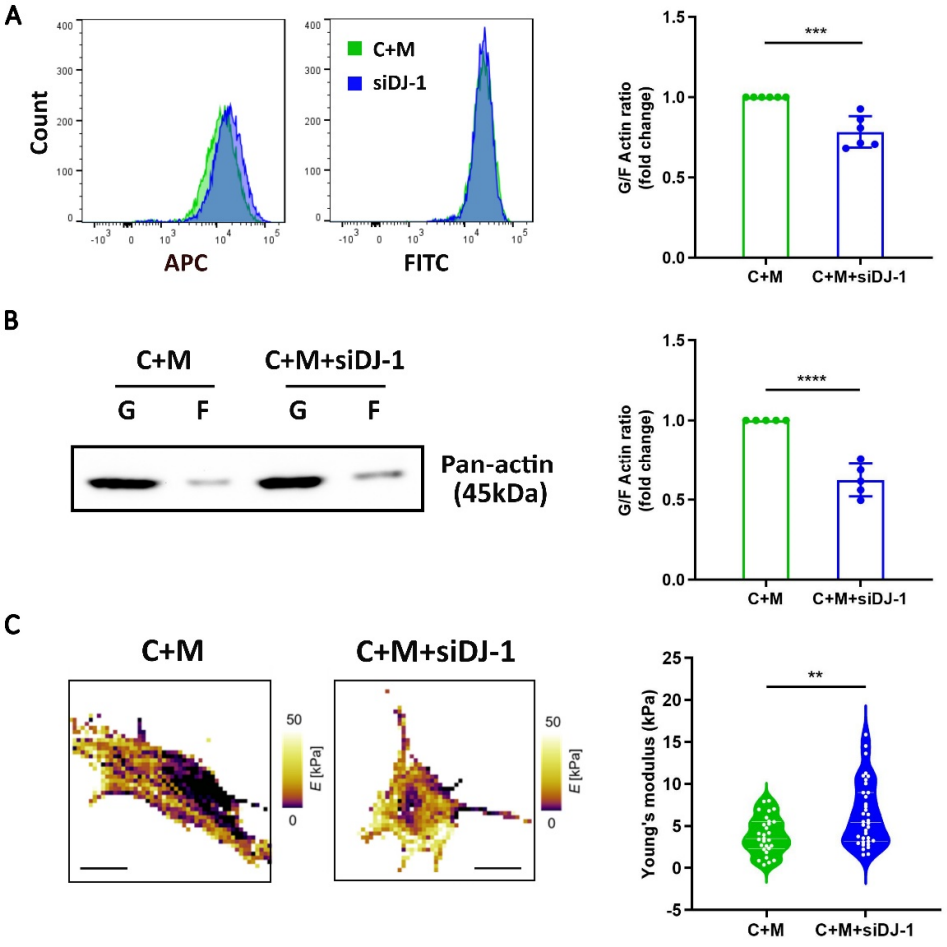

Figure 3-16: Loss of DJ-1 Cause Cell Cytoskeleton Change.

(A) *Fluorescence-activated cell sorting analysis (FACS) (n = 6),* ***(B)*** *Representative western blot and quantitative densitometric analysis (n = 5) of globular/fibrillar actin ratio (G/F-actin ratio) in decidualized EnSCs with or without siDJ-1 transfection.* ***(C)*** *AFM stiffness image of decidualized EnSCs with or without siDJ-1 transfection, and Young's modulus was measured. Scale bar (20 µm). AFM for cell stiffness measurements was carried out by Emily Hellwich and Prof. Tilman Schäffer. The data are presented as mean ± SEM. Unpaired T-test was used to calculate statistical significance. *P < 0.05, **P < 0.01, ***P < 0.001, ****P < 0.0001.*

Our proteomics analysis showed a reduction in the levels of antioxidant proteins following DJ-1 knockdown. A previous study showed that the generation of ROS can target F-actin and induce alterations in the actin cytoskeleton, and increase cell motility (Shannon et al., 2022). To test this, we first treated the cells with thymidine to negate the effect of proliferation, and then performed a cell motility (wound healing) assay. In keeping, we observed that 24 hours post-scratch, the migration of cells was significantly higher in DJ-1 knockdown EnSCs compared to the control (**Figure 3-17**).

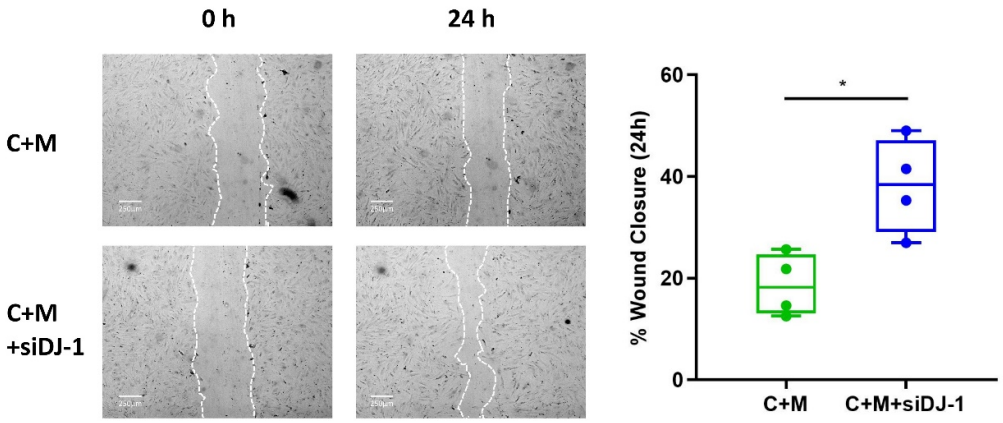

Figure 3-17: Loss of DJ-1 Cause Cell Dynamics Change.

*Representative images of scratched and recovering of wounded areas (marked by white lines) on confluence monolayers of EnSCs at different time points (n = 4). Percentage wound closure was determined by measuring the area of the wounds. The data are presented as mean ± SEM. Unpaired T-test was used to calculate statistical significance. *P < 0.05, **P < 0.01, ***P < 0.001, ****P < 0.0001.*

In summary, we found that DJ-1 expression increases during decidualization, and its loss is associated with poor pregnancy outcomes in mice and RPL in humans. Additionally, DJ-1 depletion caused a decrease in the decidual marker IGFBP1, as well as the upregulation of Palladin and downregulation of antioxidant enzyme proteins. These changes resulted in increased actin polymerization, enhanced cell stiffness and cell mobility.

3.9 Overexpression of DJ-1 Inhibited Expression of Palladin

Following the knockdown experiments that highlighted the functions of DJ-1 in decidualization, overexpression studies were performed to further investigate its functional significance. To achieve this, transfection with the pGW1-Myc-DJ-1-wt (wt-DJ-1) plasmid was performed in EnSCs, either with or without 6-day decidualization treatment. As illustrated in **Figure 3-18A, B**, wtDJ-1 exhibited successful upregulation at both the gene level (642.5-fold change) and the protein expression (4.0-fold change) of DJ-1 with decidualization treatment. Consequently, the expression of Palladin declined upon wtDJ-1 overexpression during decidualization, with a 34.2% reduction at the gene level and a 76.2% reduction at the protein level (**Figure 3-18C, D**). The full blot is shown in **Supplementary Figure 9-8**.

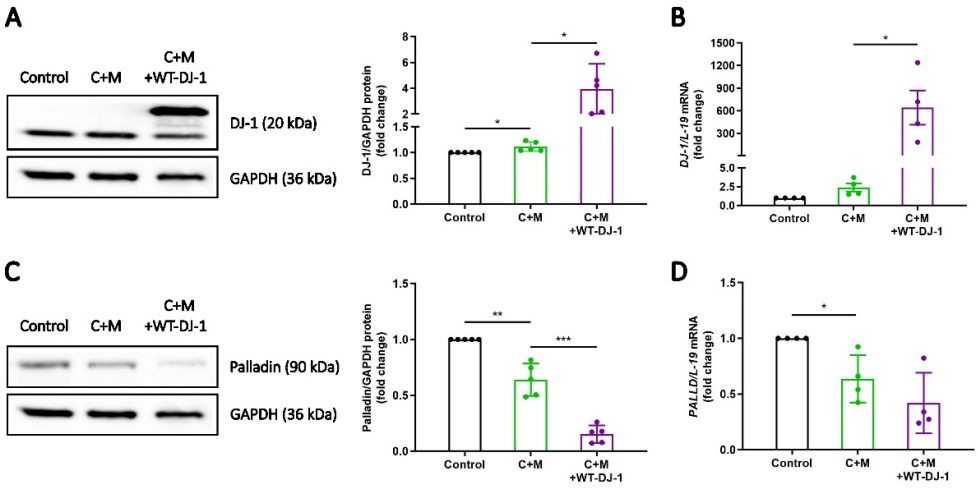

Figure 3-18: Downregulation of Palladin by DJ-1 Overexpression.

(A) *DJ-1 and* ***(C)*** *Palladin protein level in EnSCs transfected by pGW1-Myc-DJ-1-wt (wt-DJ-1) for 24 h, which was performed on the third day of a total of 6-day treatment with C+M (n = 4).* ***(B)*** *DJ-1 and* ***(D)*** *PALLD mRNA expression level in decidualizing EnSCs with transfection of wt-DJ-1 (n = 4). The data are presented as mean ± SEM. One-way ANOVA was used to calculate statistical significance. *P < 0.05, **P < 0.01, ***P < 0.001, ****P < 0.0001.*

Since DJ-1 is known to regulate cell survival and oxidative stress responses, we next explored its role in cell proliferation and ROS production during decidualization. To assess cell proliferation, we performed BrdU Assay on EnSCs using the same treatment as described above. We demonstrated that the overexpression of DJ-1 during decidualization increased cell proliferation (**Figure 3-19A**). Furthermore, the H_2-DCFDA assay demonstrated that in decidualized EnSCs, DJ-1 overexpression led to a decrease in ROS levels and an increase of antioxidants, including GPX3 and GLRX (**Figure 3-19B, C**).

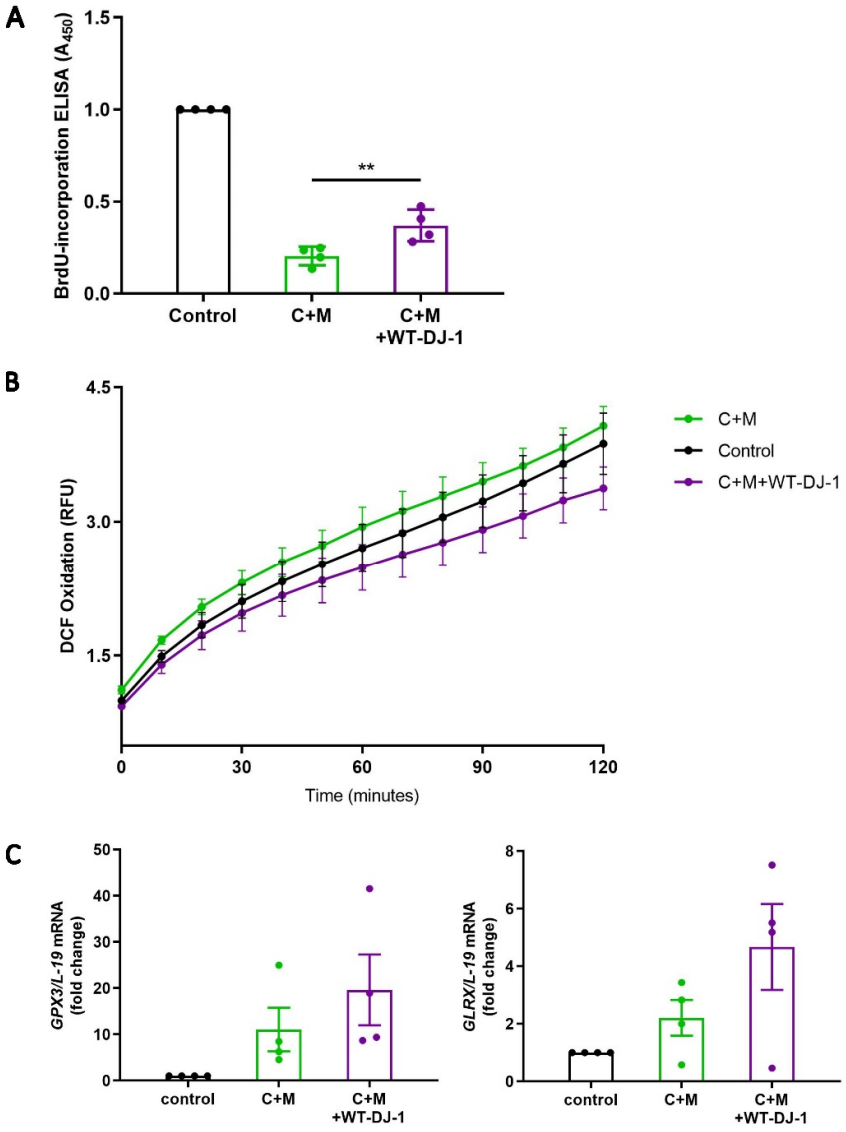

Figure 3-19: Downregulation of Palladin by DJ-1 Overexpression.

(A) *BrdU ELISA assay was carried out after treatment. Absorbance was measured at 450 nm.* ***(B)*** *ROS DCF fluorescence intensity was measured every 10 min over a total duration of 2 hours (n = 3).* ***(C)*** *GPX3 and GLRX mRNA expression level in decidualizing EnSCs with or without transfection of wtDJ-1 (n = 4). The data are presented as mean ± SEM. One-way ANOVA and unpaired T-test were used to calculate statistical significance. *P < 0.05, **P < 0.01, ***P < 0.001, ****P < 0.0001.*

3.10 Overexpression of DJ-1 Inhibits Actin Polymerization, Cell Stiffness, and Cell Migration

Since we observed the reduction of Palladin upon DJ-1 overexpression, we aimed to further investigate its subcellular localization and explore the association between DJ-1, Palladin, and F-actin. To achieve this, immunofluorescence staining was carried out on both decidualized EnSCs and decidualized EnSCs following transfection with wtDJ-1. As depicted in **Figure 3-20A, B**, overexpression of DJ-1 resulted in reduced Palladin and F-actin staining intensity. Notably, we observed that this reduction in F-actin was particularly pronounced in the perinuclear region.

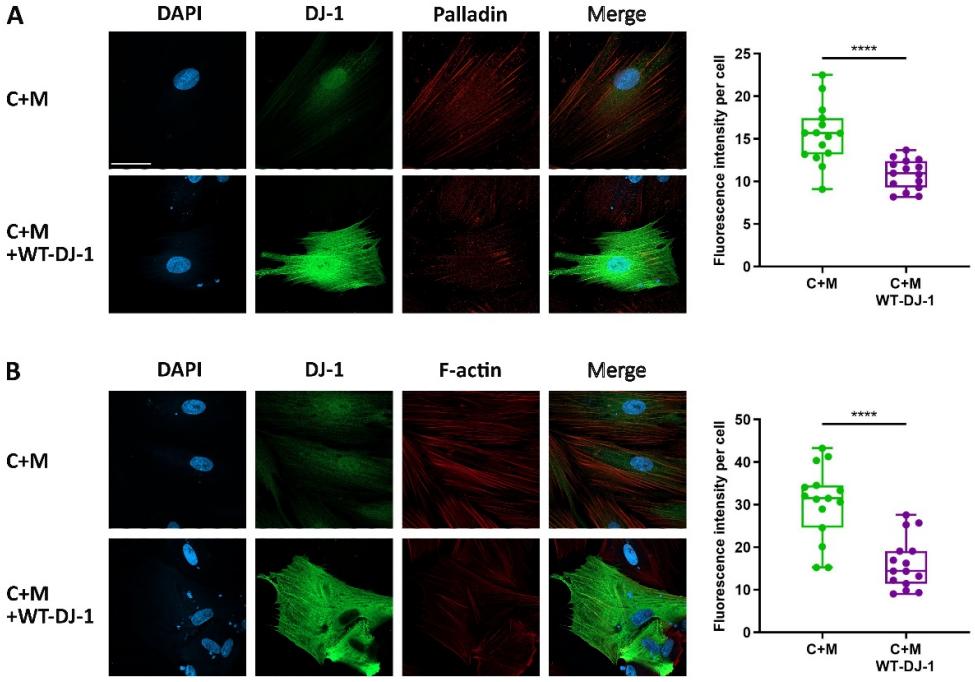

Figure 3-20: Expression and Localization of Palladin and F-actin upon DJ-1 Overexpression.

(A) *Immunofluorescence staining of decidualized EnSCs (upper panel) with WT-DJ-1 transfection (lower panel) showed cell morphological changes. DJ-1: Alexa Fluor 488 (green); Palladin: Alexa Fluor 568 (red); nucleus: DAPI (blue); (n = 3). Scale bar (75 µM).* ***(B)*** *Immunofluorescence staining of decidualized EnSCs (upper panel) with WT-DJ-1 transfection (lower panel) showed cell morphological changes. DJ-1: Alexa Fluor 488 (green); nucleus: DAPI (blue); F-actin: Phalloidin (orange); quantification of immunofluorescence intensity performed from 3 experiments with >15 cells quantified for each condition (n = 3). Scale bar (75 µM). Immunofluorescence image acquisition was carried out with the assistance of Dr. Nisha Mohd Rafiq. The data are presented as mean ± SEM. Unpaired T-test was used to calculate statistical significance. *P < 0.05, **P < 0.01, ***P < 0.001, ****P < 0.0001.*

Actin polymerization plays a critical role in various cellular processes, and understanding the balance between G and F actin is essential for assessing actin dynamics. To further investigate this, FACS and western blot analyses were employed to determine the G/F actin ratio. As exhibited in **Figure 3-21A, B**, the overexpression of DJ-1 caused an augmentation in the G/F actin ratio, indicating alleviated actin polymerization. The gating strategy is shown in **Supplementary Figure 9-9**. The full blot is shown in **Supplementary Figure 9-10**. Additionally, we investigated the association of DJ-1 with cell stiffness using AFM on live EnSCs subjected to a 6-day decidualized treatment with or without wtDJ-1 plasmid transfection. As illustrated in **Figure 3-21C**, the overexpression of DJ-1 in decidual EnSCs decreased the Young's modulus, reflecting a reduction in the cell stiffness.

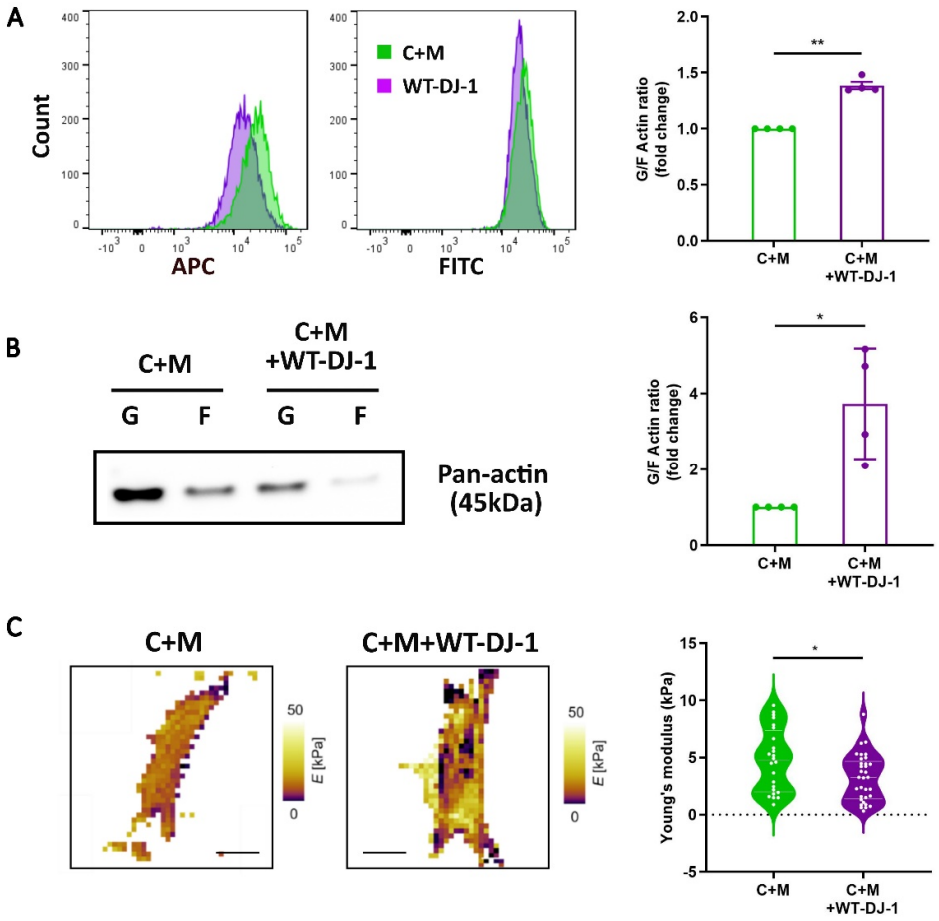

Figure 3-21: Overexpression of DJ-1 Causes Cell Cytoskeleton Changes.

(A) *Fluorescence-activated cell sorting analysis (FACS) (n = 6),* ***(B)*** *Representative Western blot and quantitative densitometric analysis (n = 5) of globular/fibrillar actin ratio (G/F-actin ratio) in EnSCs with or without WT-DJ-1.* ***(C)*** *AFM stiffness image and Young's modulus in decidualized EnSCs with or without WT-DJ-1. Scale bar (25 µM). AFM for cell stiffness measurements was carried out by Emily Hellwich and Prof. Tilman Schäffer. The data are presented as mean ± SEM. Unpaired T-test was used to calculate statistical significance. *P < 0.05, **P < 0.01, ***P < 0.001, ****P < 0.0001.*

Based on our findings that ROS levels decrease upon DJ-1 overexpression, we subsequently investigated whether lower ROS levels could, in turn, reduce cell motility. To explore this, a wound healing assay was conducted to assess cell motility and migration. As shown in **Figure 3-22**, 24 hours post-scratching, the extent of cell migration

into the cell-free region was markedly reduced in cells expressing wtDJ-1 compared to the decidualized EnSCs.

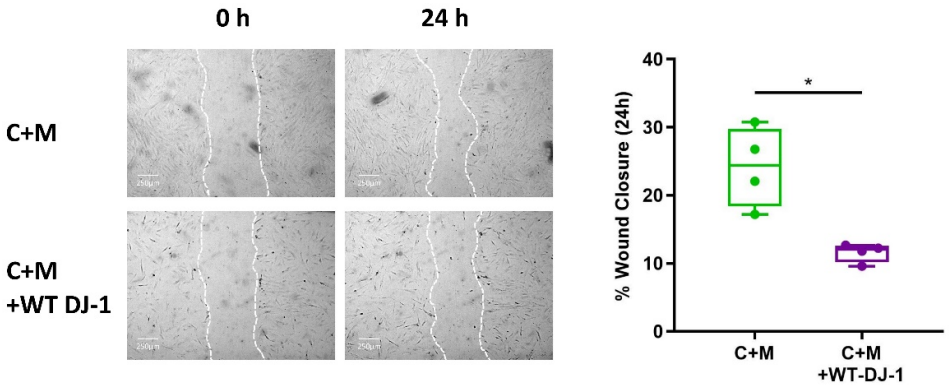

Figure 3-22: Overexpression of DJ-1 Cause Cell Dynamics Change.

*Representative images of scratched and recovering of wounded areas (marked by white lines) on confluence monolayers of EnSCs at different time points (n = 4). Percentage wound closure was determined by measuring the area of the wounds. The data are presented as mean ± SEM. Unpaired T-test was used to calculate statistical significance. *P < 0.05, **P < 0.01, ***P < 0.001, ****P < 0.0001.*

RPL is often associated with the implantation of embryos with chromosomal abnormalities or other developmental issues (Weimar et al., 2012). We hypothesize that the loss of DJ-1 could lead to increased cell mobility, which in turn might enhance the ability of the cells to interact with and potentially receive low-quality embryos. In the final set of experiments, we explored the possibility that the loss of DJ-1 could enhance cell migration when exposed to chemotactic factors secreted by aneuploidic cells. To model this, we used BeWo, a well-established trophoblastic cell line, as a model to simulate the aneuploidic cell environment. As seen in **Figure 3-23**, the absence of DJ-1 resulted in a pronounced increase in aberrant migratory capability compared to both the control group and cells expressing wtDJ-1.

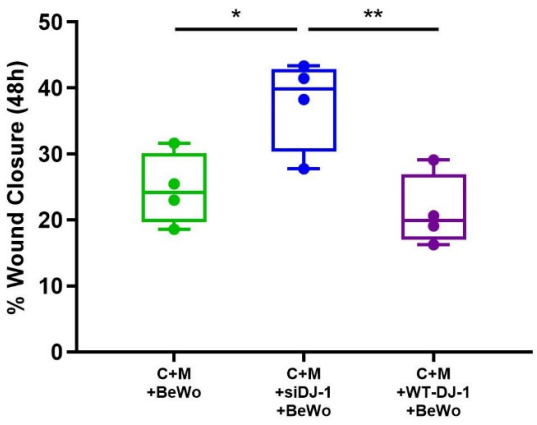

Figure 3-23: Migratory Capability of Decidual EnSCs upon DJ-1 Loss in Response to Chemotactic Factors from Aneuploidic Cells.

The percentage of wound closure in scratched decidualized EnSCs cultures treated with BeWo cell supernatant was determined by measuring the area of the wounds. The data are presented as mean ± SEM. One-way ANOVA was used to calculate statistical significance. *P < 0.05, **P < 0.01, ***P < 0.001, ****P < 0.0001.

To summarize, overexpression of DJ-1 resulted in a significant reduction in Palladin levels at both the gene and protein levels. Furthermore, DJ-1 overexpression enhanced cell proliferation and decreased ROS levels during decidualization. It also caused a decrease in cell polymerization, stiffness, and motility during this process. Notably, knockdown of DJ-1 was linked to an elevation in cell motility within an aneuploidic cell environment.

4. Results II: Embryo-Derived Trypsin-Induced Ca^{2+} Entry is Inhibited by Endometrial Infertility Factor, LEFTY2

In this part of the study, we began by performing *in silico* analyses to investigate the expression of key genes involved in the classical trypsin signaling pathway in human embryos. This was followed by detecting trypsin activity in human embryo conditioned medium using ELISA to confirm the presence of embryo-derived trypsin. Subsequent live-cell calcium imaging experiments evaluated trypsin-induced calcium entry in Ishikawa cells, both with and without LEFTY2 pre-treatment. To explore whether LEFTY2 modulates calcium entry through ENaC, the ENaC inhibitor amiloride was used. Further investigations focused on the involvement of L-type calcium channels, starting with bioinformatic analysis of CACNA1C expression in endometrial tissue, followed by experimental validation using qRT-PCR and immunofluorescence. Finally, functional studies using the L-type calcium channel blocker nifedipine were conducted to determine whether LEFTY2's inhibitory effect on trypsin-induced calcium entry is mediated through L-type calcium channels. These combined approaches aimed to clarify the mechanisms by which LEFTY2 regulates trypsin-induced calcium entry in Ishikawa cells.

4.1 Expression Patterns and Impact of Trypsin Pathway Genes in Human Preimplantation Embryos

Given the role of embryo-derived trypsin in implantation, we aimed to examine the expression of genes related to the trypsin pathway during early embryonic development (Brosens et al., 2014; Hennes et al., 2023). To achieve this, we mined publicly available transcriptomic data (GEO accession number: GDS3959) of human embryos at differing preimplantation developmental (1C; 1-cell embryo, 2C; 2-cell embryo, 4C; 4-cell embryo, 8C; 8-cell embryo, M; morula and B; blastocyst) (Xie et al., 2010). As depicted in **Figure 4-1**, transcriptomic analyses of key trypsin pathway genes were present in human embryos before implantation. Increased expression of the trypsinogen activators transmembrane serine protease 2 (TMPRSS2) and enteropeptidase (TMPRSS15), as well

as the serine proteases cationic trypsinogen (PRSS1) and prostasin (PRSS8), was observed (**Figure 4-1A-D**). As shown in **Figure 4-1E-I**, there is a reduced expression of the trypsin inhibitors, alpha-1-microglobulin/bikunin precursor (AMBP) and inter-alpha-trypsin inhibitor heavy chain H2, H3, and H4 (ITIH2 - 4). Altogether, these data infer that trypsin activity is established by the blastocyst stage during the embryonic development.

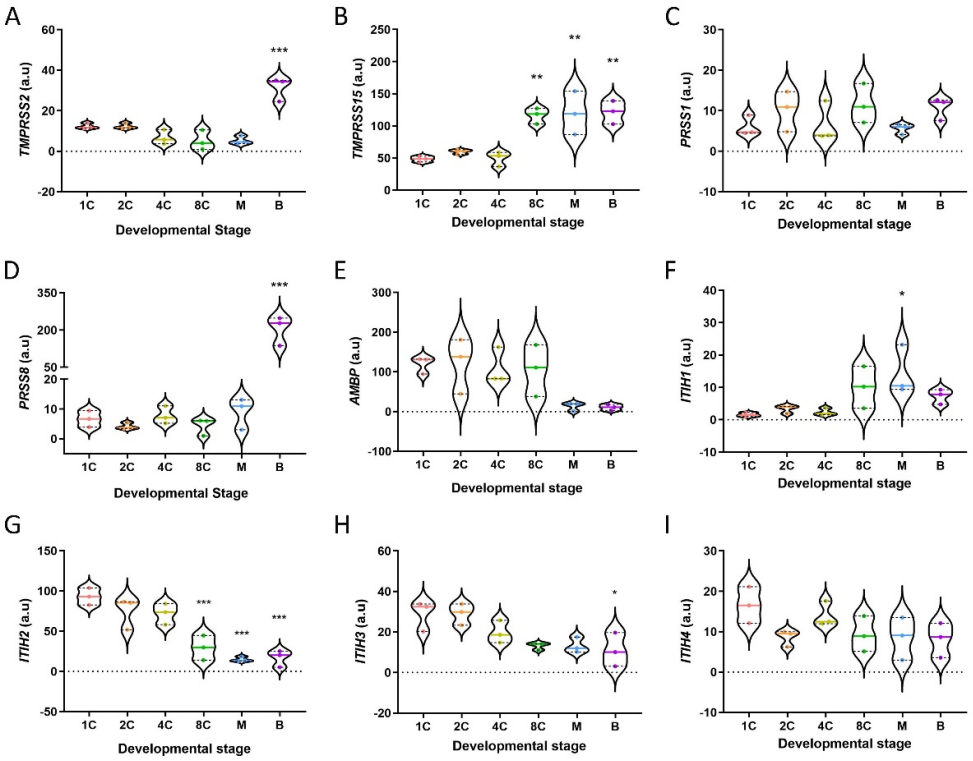

Figure 4-1: Stage-Specific Expression of Trypsin Pathway Genes in Human Preimplantation Embryos.

(A)-(I) *key classical trypsin pathway genes expression in human pre-implantation embryos (n = 3) (GEO accession number: GDS3959) (1C: 1-cell embryo, 2C: 2-cell embryo, 4C: 4-cell embryo, 8C: 8-cell embryo, M: morula, B: blastocyst). The data are presented as mean ± SEM. One-way ANOVA was used to calculate statistical significance. *P < 0.05, **P < 0.01, ***P < 0.001, ****P < 0.0001.*

Embryo-derived trypsin has been indicated to be crucial in the implantation process by modulating endometrial responses and facilitating the blastocyst invading into the endometrium (Hennes et al., 2023; Ruan et al., 2012). To explore the association between trypsin activity and human implantation, trypsin activity was determined in

embryo culture media (ECM), which was collected from individual single embryo transfer (SET) embryos on day 5. The requirements for SET include maternal age under 37 years, a minimum of one high-quality blastocyst (the embryo must have at least a "BB" grade for both embryonic cell cluster and the trophectoderm), and no prior unsuccessful IVF. By determining ECM from SETs, we controlled for variables, including patient age, prognosis, developmental stage and embryo quality, ensuring that the trypsin levels measured in the ECM were only associated with pregnancy outcomes. These ECM drops were then tested for trypsin levels using an ELISA, and the samples were categorized according to the results of the hCG test (pregnancy and non-pregnancy groups). Notably, trypsin activity was shown to be significantly elevated in ECM from embryos that successfully implanted (**Figure 4-2**). Our data shows that a successful pregnancy is associated with increasing amounts of trypsin levels in the ECM.

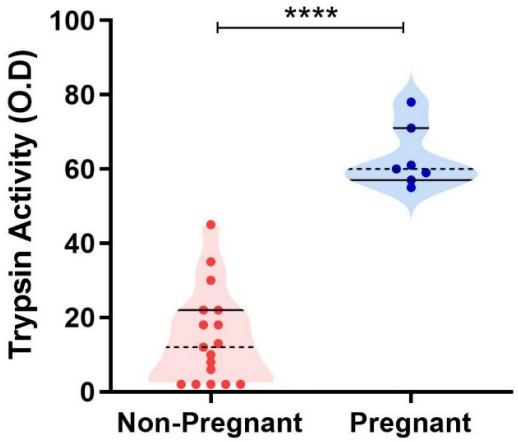

Figure 4-2: Trypsin Levels in Embryo Culture Media from Human IVF Blastocysts.

*Trypsin activity in single droplets collected (n = 26). All quantifications were carried out in duplicate, normalised to unconditioned medium and are shown as individual values. Pregnancy was confirmed using a hCG test. Embryo culture media was collected by Dr. Steffen Kull and Dr. Melanie Henes. The data are presented as mean ± SEM. Unpaired T-test was used to calculate statistical significance. *P < 0.05, **P < 0.01, ***P < 0.001, ****P < 0.0001.*

4.2 LEFTY2 Modulates Trypsin-Induced Calcium Influx in Endometrial Epithelial Cells

Given the important role of trypsin in modulating the endometrial environment during implantation, as well as its potential to influence intracellular calcium signaling in endometrial epithelial cells, we sought to investigate the impact of trypsin on $[Ca^{2+}]_i$ dynamics (Hennes et al., 2023; Ruan et al., 2012; Shmygol & Brosens, 2021). Trypsin, used as a model for embryo-derived protease activity (Brosens et al., 2014) has been shown to activate various signaling pathways essential for implantation. In the subsequent set of experiments, we examined how trypsin affects $[Ca^{2+}]_i$ activity and explored whether LEFTY2, a factor implicated in endometrial infertility, could interfere with this process. As illustrated in **Figure 4-3A-C**, the addition of trypsin (closed circles) led to a rapid increase in $[Ca^{2+}]_i$, characterized by a pronounced rise in both slope and peak. This trypsin-induced calcium influx was significantly attenuated by the ENaC blocker amiloride (10 µM), as shown in **Figure 4-3A, B and D**. Further analysis involved pre-treating endometrial epithelial cells with LEFTY2 (25 ng/ml, open circles) for 6 hours. This pre-treatment resulted in a notable reduction in trypsin-induced Ca^{2+} entry, as depicted in **Figure 4-3A, B and E**. Interestingly, the presence of amiloride in combination with LEFTY2 pre-treatment showed a trend towards an even greater reduction in $[Ca^{2+}]_i$, though this combined effect did not achieve statistical significance, as indicated in **Figure 4-3A, B and F**.

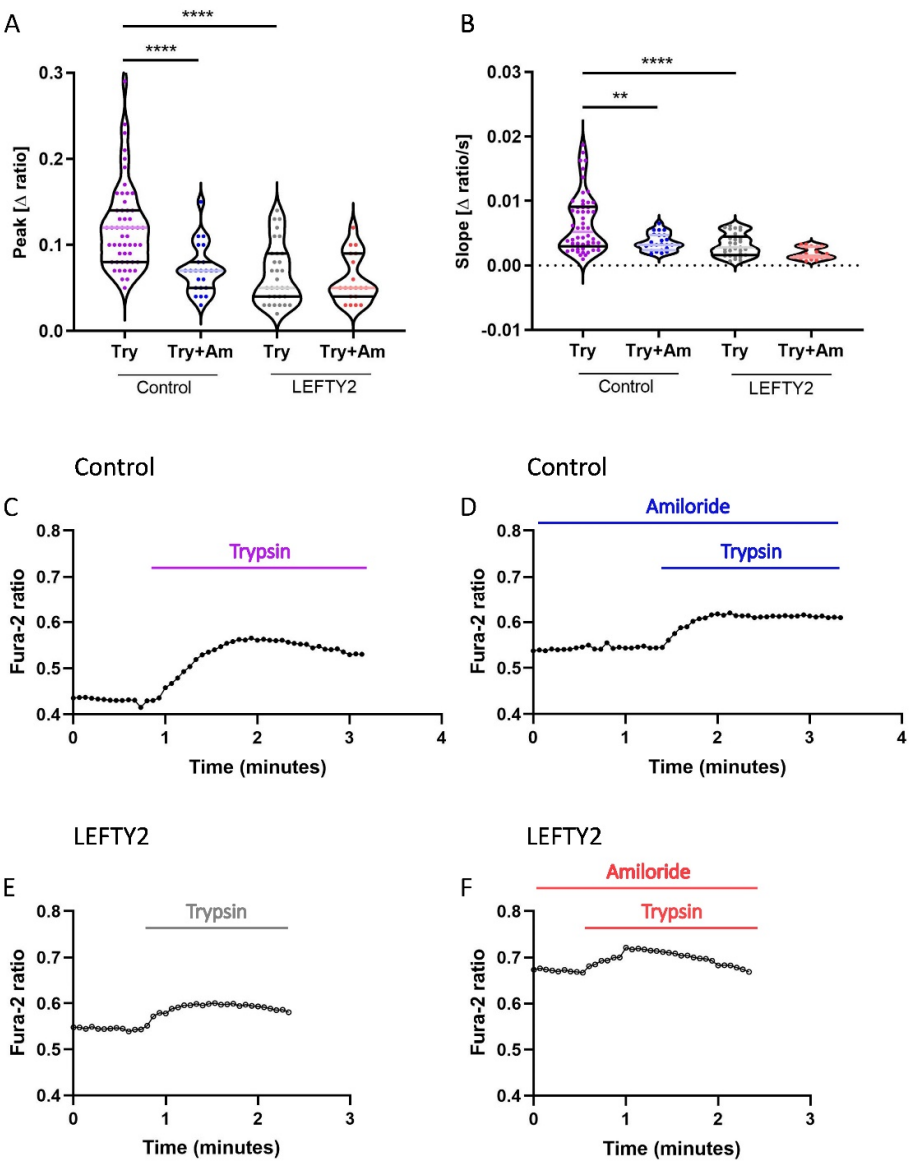

Figure 4-3: Trypsin Induced Ca^{2+} Entry in Human Endometrial Epithelial Cells without and with Amiloride and/or LEFTY2.

(A), (B) *Arithmetic means (± SEM, n = 19-54 cells) of the peak value a and slope b of the change in intracellular Ca^{2+} concentrations following trypsin treatment (purple) without and with the addition of amiloride (gray), without (left bars, Control) and with (right bars, LEFTY2) pretreatment with LEFTY2 (25 ng/ml, 6 h).* ***(C)-(F)*** *Original curves depicting showing intracellular Ca^{2+} concentrations in Fura-2/AM - stained human endometrial epithelial cells without (**C, D**; black circles) and with (**E, F**; open circles) pretreatment with LEFTY2 (25 ng/ml, 6 h) human endometrial epithelial cells prior to and following addition of trypsin (20 µg/ml) without **(C), (E)** and with **(D), (F)** the presence of amiloride (10 µM). The amplitude (peak) and the velocity (slope, calculated from the linear fit) of the Ca^{2+} entry were analysed. Intracellular Calcium measurement was performed with the assistance of Dr. Jing Yan, Dr. Md. Alauddin and Prof. Florian Lang. The data are presented as mean ± SEM. One-way ANOVA was used to calculate statistical significance. *P < 0.05, **P < 0.01, ***P < 0.001, ****P < 0.0001.*

4.3 LEFTY2 Attenuates Trypsin-Induced Upregulation of L-type Calcium Channels

Since we showed that the inhibition of LEFTY2 on trypsin-induced calcium entry does not act on ENaC, we next tested whether the inhibitory effect of LEFTY2 on Ca^{2+} entry was associated with changes in L-type calcium channel levels. Firstly, to determine whether L-type voltage gated Ca^{2+} channel (*CACNA1C*) is expressed in normal human endometrial tissue, we first performed bioinformatic analysis on publicly available single cell sequencing data (Vento-Tormo et al., 2018). We observed an expression of *CACNA1C* in human decidua, particularly in endometrial decidual cells (**Figure 4-4A-C**).

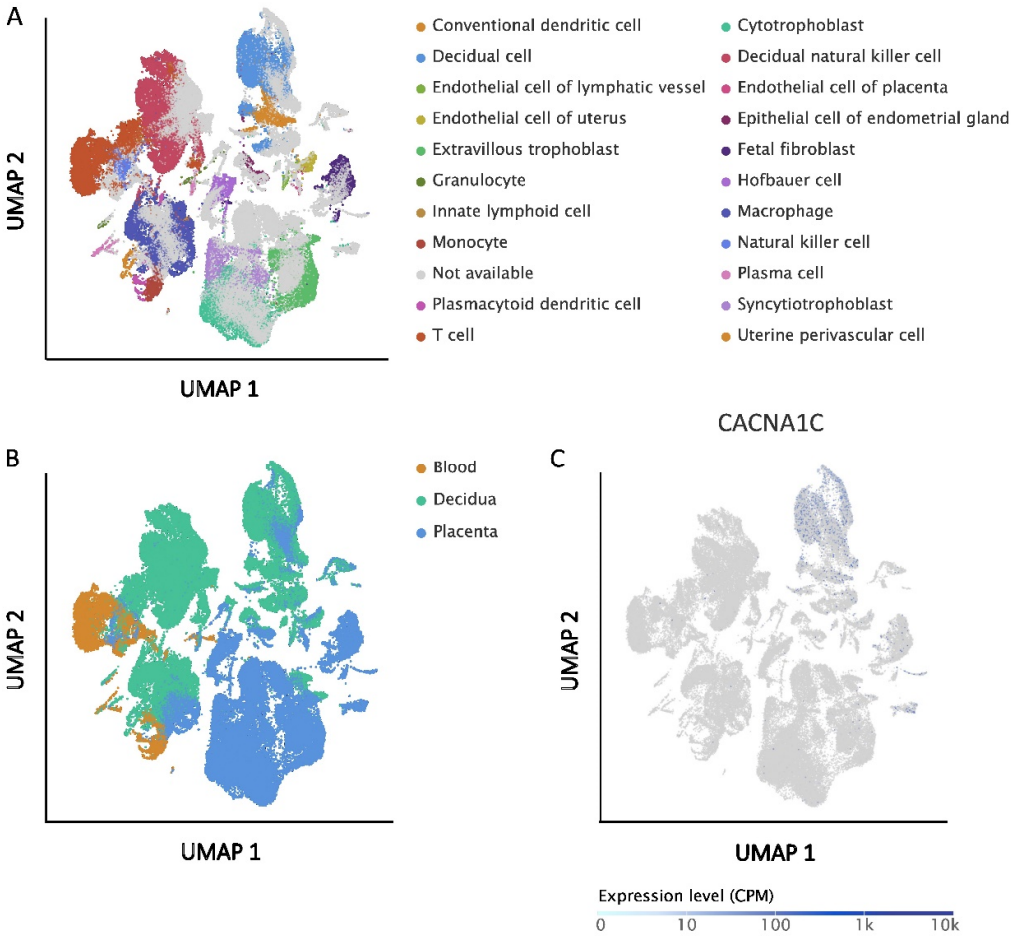

Figure 4-4: Expression of L-type Calcium Channel in Human Endometrium.

(A), (B) *Uniform manifold approximation and projection (UMAP) clustering of cell types* ***(A)*** *and tissues* ***(B)****; Tissue compartments and cell types were annotated in the Single Cell Expression Atlas.* ***(C)*** *Expression of CACNA1C in single cells, presented as counts per million (CPM), overlaid on the UMAP map.*

Following the confirmation of CACNA1C expression in human endometrial tissue, we next assessed the impact of LEFTY2 on L-type calcium channel expression. As shown in **Figure 4-5A**, treatment of trypsin alone increased *CACNA1C* transcript levels, in keeping with previous findings (Ruan et al., 2012). Transcript levels were reduced in the presence of LEFTY2 and following co-treatment with LEFTY2 and trypsin. To further investigate the protein expression level and localization of CACNA1C, we first confirmed the upregulation of LEFTY2 by western blot (**Figure 4-5B**). Subsequently,

immunofluorescence analysis demonstrated that the intensity of cytosolic CACNA1C increased upon trypsin treatment, while it decreased following treatment with LEFTY2 and co-treatment with LEFTY2 and trypsin (**Figure 4-5C**).

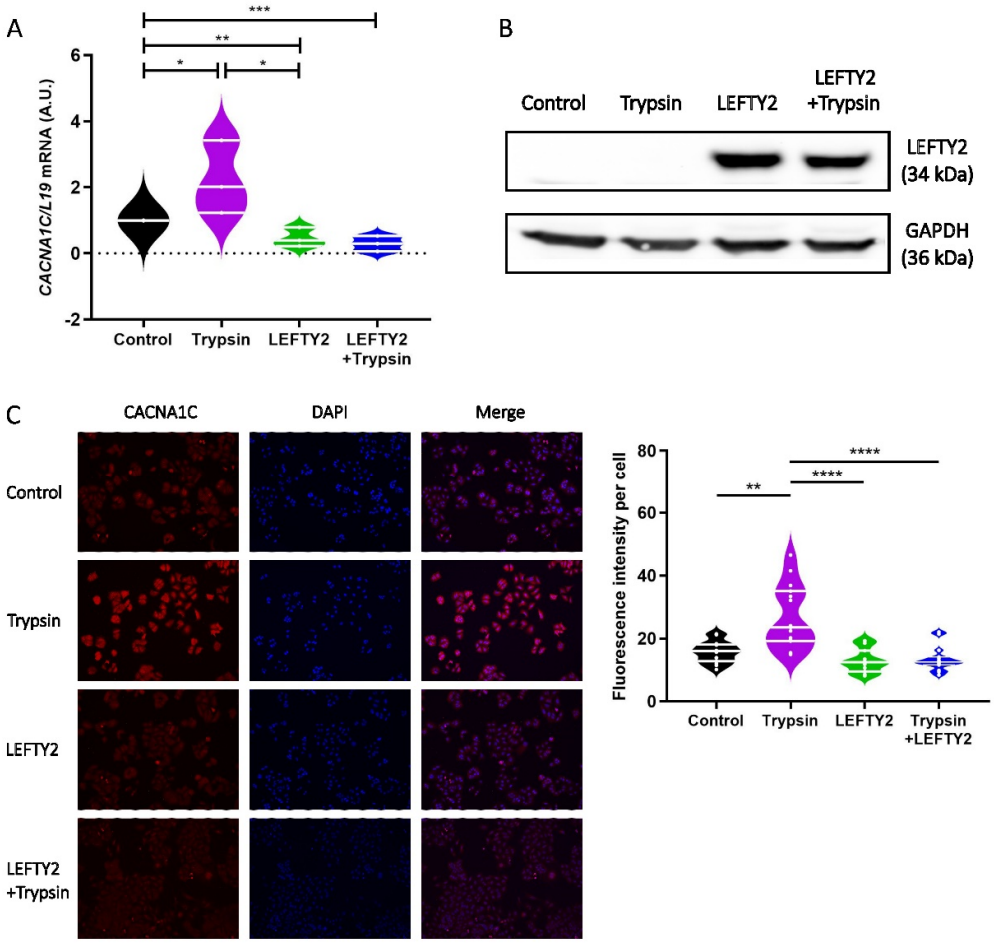

Figure 4-5: Effect of LEFTY2 on L-type Calcium Channel Abundance.

ISK were kept in the treatment with LEFTY2 (25 ng/ml) or without it for 6 h either with or without the treatment of Trypsin (20 µg/ml, 24h). ***(A)*** *Arithmetic means ± SEM (n = 6) of human L-type Calcium Channel (CACNA1C) transcript levels were measured by qRT-PCR, normalized to the levels of L19 mRNA and presented in arbitrary units (a.u.).* ***(B)*** *Western blot analysis of LEFTY2 expression during decidualization in ISK (n = 4). GAPDH was used as a loading control.* ***(C)*** *IF microscopy of ISK kept in the treatment with LEFTY2 (25 ng/ml) or without it for 6 h either with or without Trypsin (20 µg/ml, 24h) showing CACNA1C subcellular localization. CACNA1C fluorescence intensity quantification results were shown (right). CACNA1C: Alexa Fluor 568 (red); nucleus: DAPI (blue). Quantification performed from 3 experiments with >15 cells quantified for each condition. Scale bar = 25µm. The data are presented as mean ± SEM. One-way ANOVA was used to calculate statistical significance. *P < 0.05, **P < 0.01, ***P < 0.001, ****P < 0.0001.*

4.4 LEFTY2 and Nifedipine Interaction in Modulating Trypsin-Induced Calcium Entry

Given that we have shown LEFTY2 can reduce the expression of CACNA1C, we sought to evaluate whether the inhibitory effect of LEFTY2 on trypsin-induced Ca^{2+} entry is sensitive to nifedipine, a known L-type calcium channel blocker. To this end, we conducted experiments with trypsin both with or without the addition of nifedipine (10 μM) (Manohar et al., 2021). As depicted in **Figure 4-6A-D**, both the incline (slope) and the highest point (peak) of the $[Ca^{2+}]_i$ increase induced by trypsin (closed circles) were significantly attenuated when nifedipine was present. This indicates that nifedipine effectively blunts the trypsin-induced up-regulation of $[Ca^{2+}]_i$. Additionally, the pretreatment with LEFTY2 (25 ng/ml, open circles) led to a notable reduction in trypsin-induced Ca^{2+} entry, as depicted in **Figure 4-6A, B and E**. However, when LEFTY2 treatment was conducted upon the addition of nifedipine, it did not significantly alter the trypsin-induced Ca^{2+} increase, as depicted in **Figure 4-6A, B and F**. These findings indicated that the inhibitory action of LEFTY2 on Ca^{2+} entry is at least partially mediated through pathways sensitive to nifedipine.

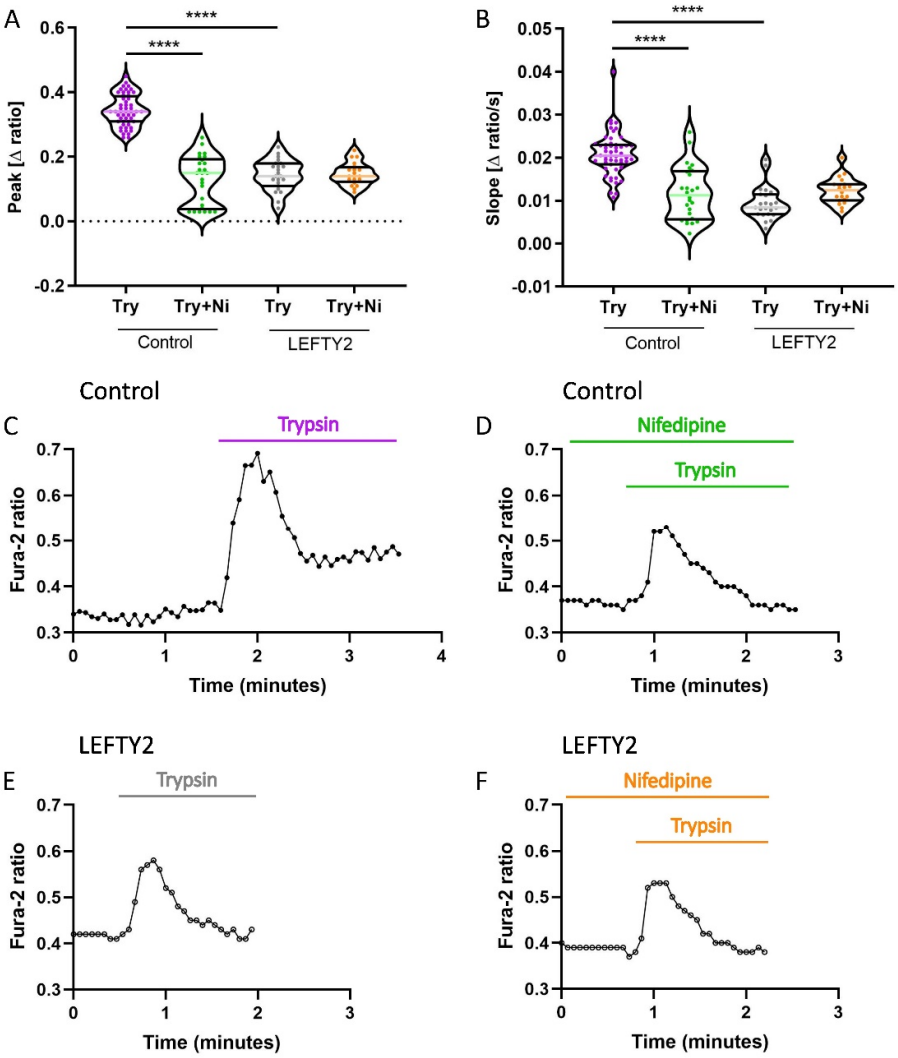

Figure 4-6: Trypsin-Induced Ca^{2+} entry in ISK without and with the addition of Nifedipine and/or LEFTY2

(A), (B) *Arithmetic means (± SEM, n = 19-54 cells) of the peak value* ***(A)*** *and slope* ***(B)*** *of the change in intracellular Ca^{2+} concentrations following trypsin treatment (purple) without and with the presence of nifedipine (green) without (left bars, Control) and with (right bars, LEFTY2) pretreatment with LEFTY2 (25 ng/ml, 6 h).* ***(C)-(F)*** *Representative original tracings showing intracellular Ca^{2+} concentrations in Fura-2/AM loaded human endometrial epithelial cells without (**C**, **D**; black circles) and with (**E**, **F**; black triangles) pretreatment with LEFTY2 (25 ng/ml, 6 h) human endometrial epithelial cells prior to and following addition of trypsin (20 µg/ml) without* ***(C), (E)*** *and with* ***(D), (F)*** *the presence of nifedipine (10 µM). The nifedipine (peak) and the velocity (slope, calculated from the linear fit) of the Ca^{2+} entry were analysed. Intracellular Calcium measurement was performed with the assistance of Dr. Jing Yan, Dr. Md. Alauddin and Prof. Florian Lang. The data are presented as mean ± SEM. One-way ANOVA was used to calculate statistical significance. *P < 0.05, **P < 0.01, ***P < 0.001, ****P < 0.0001.*

5. Discussion

5.1 The Function of DJ-1 in Early Pregnancy: Implications for RPL

RPL is a challenging reproductive condition associated with impaired endometrial decidualization. DJ-1 has been identified as a critical regulator of cellular processes, particularly in maintaining oxidative balance and facilitating cell migration. These functions are essential in terms of endometrial physiology, where precise regulation of ROS levels and cellular dynamics is crucial in successful decidualization—a process vital for creating an environment that facilitates implantation and supports pregnancy.

This study explored the hypothesis that DJ-1 significantly influences endometrial decidualization by modulating ROS levels, cell mobility, and stiffness, with its deficiency contributing to impaired decidualization and an increased risk of pregnancy loss. Initial findings demonstrated that DJ-1 expression is elevated in both human and mouse endometrial tissues during the decidualization process. Proteomic analyses further revealed that Palladin, a cytoskeletal regulatory protein, is involved in DJ-1-mediated pathways influencing cellular dynamics. Functional studies showed that DJ-1 deficiency exacerbates ROS levels, alters cell migration, and increases cell stiffness, collectively impairing the decidualization process, whilst DJ-1 overexpression has the ability to reverse adverse effects associated with DJ-1 loss. Together, these findings provide a comprehensive understanding of DJ-1's role in regulating endometrial function, offering insights into its therapeutic potential in mitigating pregnancy complications associated with impaired decidualization.

5.1.1 Oxidative Stress in Decidualization: Balancing ROS for Cellular Adaptation and Pregnancy Success

In humans decidualization is initiated around 6 days post ovulation of each menstrual period and is independent of an implanting blastocyst (Gellersen et al., 2007; Ochoa-Bernal & Fazleabas, 2020). This intricate process is orchestrated by postovulatory elevation in progesterone levels and escalating local cAMP production (Lavogina et al.,

2021). Decidualization initiates with a rising stress response in EnSCs, resulting in a burst of ROS, release of proinflammatory factors, arrest of cell cycle and silencing of stress pathways (Okada et al., 2018). EnSCs are then highly resistant to stress signals and are protected against oxidative and metabolic stress, but are also greatly resistant to adverse environmental factors (Okada et al., 2018). The decidua then forms a semblant-matrix and tolerogenic environment around the implanting embryo, which facilitates the invading extravillous trophoblast to form a hemochorial placenta (Ochoa-Bernal & Fazleabas, 2020). Approaching the end of the first trimester, the trophoblast plugs in the spiral arteries are removed. During this period, oxygen tension rises steeply (from ~20 mmHg to ~40 mmHg) (Brosens et al., 2022). The consequential wave of ROS stress-tests the resilience of the placental-decidual interface (Zhang et al., 2023).

Among the many factors interfering with decidualization, oxidative stress (OS) has been largely reported. It is characterized by the surge of ROS, O_2^-, H_2O_2 as well as OH^- (Agarwal et al., 2008; Ruder et al., 2008). ROS are side products of aerobic respiration and metabolism, which are physiologically essential for redox signaling pathways in different biological responses such as cell proliferation, differentiation, migration and gene expression (Finkel, 2011). cAMP may enhance endogenous ROS production, which occurs at the same time with a significant increase in PRL and IGFBP1 expression during decidualization (Al-Sabbagh et al., 2011; Sugawara et al., 2000). Moderate levels of ROS induce cellular adaptations to stress or resilience, a conserved (both in pro- & eukaryotes) response known as ‘hormesis’ (Nitti et al., 2022). Hormesis is a process that occurs in various biological responses such as aging, by which exposure to relatively low levels of stress protects the cells from higher stress (Nitti et al., 2022). Dröge reported that an oxidative burst is critical to ‘kick-start’ the redox defence mechanism and inducing the expression of genes encoding for antioxidants (Droge, 2002). Similarly, in our study, we observed that ROS levels and cell death slightly increase during decidualization. These findings underscore the importance of a robust antioxidant defence system, which is pivotal for maintaining a healthy pregnancy.

However excessive ROS impairs the decidualization process, with the induction of EnSCs apoptosis and reduces the number of implantation sites (Hussain et al., 2021; Shahin et

al., 2013). DJ-1, which has antioxidant functions, is found not only in the cytoplasm, but also in the nucleus, with a notable increase in nuclear localization. The nuclear translocation of DJ-1 may protect cells from oxidative stress-induced cell death (Kim et al., 2012). Conversely, DJ-1 knockdown significantly elevates ROS levels and leads to increased cell death. In 70% of first-trimester miscarriages, the cyto-trophoblastic part surrounding the embryo is delicate and fragmented across the placenta, in which damage from OS in immature villi is evident (Brosens et al., 2022). These pathological events unify miscarriages caused by both euploid and aneuploid, indicating regulation by an impaired decidual condition (Brosens et al., 2022). Similarly, in our study, we demonstrated that DJ-1 is expressed around the implantation site, and human recurrent pregnancy loss (RPL) is associated with lower levels of DJ-1. Furthermore, DJ-1 deficiency in female mice impairs pregnancy outcomes, as evidenced by smaller litter sizes. These findings highlight the importance of DJ-1 in maintaining a balanced redox state and ensuring healthy decidualization, as well as its critical role in protecting the implantation site from oxidative damage.

5.1.2 DJ-1 as a Key Antioxidant Regulator: Its Role in Decidualization and RPL

DJ-1, as an antioxidant protein, is extensively distributed throughout the human body, it has crucial functions in many physiological processes (Kahle et al., 2009) and has been extensively characterised in PD. Our study confirmed the presence of DJ-1 in the endometrium and revealed its dynamic expression pattern during decidualization, observed in both EnSCs and in a murine gene-knockout model. The increasing levels of DJ-1 correspond to rising levels of ROS, functioning to regulate ROS levels within physiological ranges conducive to normal decidualization. Conversely, loss of DJ-1 can elevate ROS levels, consequently disrupting the cAMP/ROS/IGFBP1 signaling pathway and impairing decidualization. Under basal conditions, DJ-1 is predominantly localized in the cytoplasm; however, upon exposure to OS, it can translocate from the cytoplasm to the mitochondria and subsequently to the nucleus (Junn et al., 2009). The distinct subcellular localization of DJ-1 fits well with the findings that the production of

endogenous ROS is spatially restricted within cellular compartment, and it is confined to a special subcellular location, at the site where free radicals impact physiological signaling (Kaludercic et al., 2014). The mitochondrial-localized DJ-1 appears to play a primary role in short-term protection against OS, after which it translocates to the nucleus (Zhou et al., 2020). Our findings further support this dynamic behaviour, as we observed heightened nuclear localization of DJ-1 following decidualization.

Several studies suggest that the endometrium in women with RPL exhibits a disordered and prolonged pro-inflammatory decidual response (Salker et al., 2012). This exaggerated early-stage inflammatory decidual response is thought to extend the window of implantation, promote endometrial receptivity and impede the selectivity of the endometrium (Salker et al., 2010). Furthermore, the absence of quality control at implantation is clinically manifested as a very short time-to-conception or 'superfertility,' a characteristic often observed in many RPL patients (Bhandari et al., 2016; Teklenburg et al., 2010). In our investigation, utilizing midluteal endometrial RNA-sequencing data from controls patients and those with RPL, we observed a significant reduction in DJ-1 gene expression in individuals with RPL. Given that the imbalance of ROS can lead to inflammation (Hussain et al., 2016), these results suggest a possible antioxidant role for DJ-1 in the pathogenesis of RPL. This finding was further supported by western blot analysis, which demonstrated a corresponding decrease in DJ-1 protein level in the endometrium collected from RPL patients, future studies are required in large cohorts to verify if DJ-1 can be a useful biomarker. Furthermore, in mice, within the implantation window, we observed the localization of DJ-1 surrounding the implantation site (crown like), suggesting a potential involvement of DJ-1 in early murine pregnancy by creating a self-governing, anti-inflammatory matrix surrounding the implanting embryo (Diniz-da-Costa et al., 2021). In a previous study, reduced expression of Foxp3 and regulatory T cells (Tregs) induction in DJ-1 knock out mice were reported, this may also further exacerbate and immune homeostasis during pregnancy resulting in pregnancy loss (Singh et al., 2015). Notwithstanding, in our *in vivo* murine model, we observed a notable reduction in litter size among female mice lacking DJ-1, indicating a potential role of maternal DJ-1 in maintaining normal pregnancy.

5.1.3 DJ-1 Regulates Actin Cytoskeleton Dynamics via Palladin

As previously reported, DJ-1 plays a role in controlling metastasis in cancer, which is associated with actin-regulating signaling pathways (Jin et al., 2020). In our present study, using LC-MS, we found that the actin-associated protein Palladin is upregulated upon DJ-1 knockdown during decidualization. Palladin, as well as myopalladin and myotilin, is part of a small protein family of immunoglobulin (Ig) domain-containing proteins, located in the Z-line and linked to the actin cytoskeleton (Otey et al., 2009). There are three main isoforms of Palladin have been characterized, including 200-kDa Palladin, which is the largest isoform and mainly expressed in the heart, testes and muscle; the 140-kDa isoform, which mainly appears in tissues with abundant smooth muscle; and the most common one, the 90-kDa isoform, is commonly expressed in different kinds of cells (Wang & Moser, 2008). The 140-kDa isoform was found increasing significantly during the phase of implantation in luminal EECs compared to the time of fertilization in a rat model (Nicholson et al., 2018) . In our study, we only observe the expression of 90-kDa isoform, which decreases during decidualization. Palladin is linked to different actin-based structures, such as stress fibers, focal adhesions, cell-cell junctions, and Z-lines. It is essential for the formation, structuring, and stabilization of the actin cytoskeleton (Jin, 2011; Otey et al., 2009). A previous study showed that Palladin$^{-/-}$ mouse embryo fibroblasts have increased globular actin and a decreased filament actin level (Liu et al., 2007). In keeping with our study, we demonstrated that Palladin has the capacity to augment actin polymerization, promote cell migration, and elevate cell stiffness, findings that align with and support these results.

In our study, we have shown that DJ-1 plays an unexpected but pivotal role in keeping the balance of Palladin expression and regulating cytoskeletal dynamics. These processes are essential for the progression of decidualization in early pregnancy. During decidualization, EnSCs undergoes morphological and cytoskeleton dynamics changes (Pan-Castillo et al., 2018), which are important for the endometrial receptivity and early pregnancy. In our study, we used immunofluorescence to show that aberrant DJ-1 levels

induce morphological changes in decidual EnSCs. Loss of DJ-1 can lead the round decidual EnSCs to adopt an epithelial-like shape, while overexpression of DJ-1 decreases the cell area. Consistent with previous results, DJ-1 deficiency causes higher intensity of Palladin, which colocalizes with DJ-1 on stress fibers. Additionally, the higher intensity of F-actin upon DJ-1 knockdown indicates a potential enhancement of actin polymerization. Stabilization of the actin cytoskeleton by the stabilization of F-actin can prevent the differentiation of EnSCs into decidual cells (Ihnatovych et al., 2009). Furthermore, a significant reduction in cell stiffness and surface roughness was observed in EnSCs following decidualization (Pan-Castillo et al., 2018), while there is no significant change in cell migration during decidualization (Lavogina et al., 2021). Our study found that DJ-1 deficiency during decidualization enhances actin polymerization and cell stiffness, whereas DJ-1 overexpression has the opposite effect. Therefore, the aberrant actin dynamics and cell stiffness caused by DJ-1 alteration may impair decidualization.

5.1.4 DJ-1 Modulates ROS Levels, Leading to Cytoskeleton Dynamics Changes and Impacting Early Pregnancy

ROS is known for its ability to induce cell mobility (Shannon et al., 2022). It can modify proteins like cofilin, promoting actin filament reorganization essential for cell movement (Kim et al., 2009). Additionally, ROS enhance integrin activation and focal adhesion kinase (FAK) signaling, which regulates cell-matrix interactions and adhesion (Ben Mahdi et al., 2000). This ROS-mediated regulation of cytoskeletal rearrangement and adhesion dynamics enables cells to adapt their movement in response to external cues, supporting efficient migration (Shannon et al., 2022). GPX3, acting as a ROS scavenger and has pivotal functions in keeping cellular homeostasis (Nirgude & Choudhary, 2021). Deficiency of GPX3 has been associated with increasing level of epithelial-mesenchymal transition (EMT) markers, including Vimentin, and reduced expression of the epithelial marker E-Cadherin (Cai et al., 2019). Additionally, GPX3 downregulates MMP9 by inhibiting the FAK/AKT signaling pathway, thereby inhibiting metastasis (Zhu et al., 2018). Consistent with these findings, our study demonstrates that absence of DJ-1 leads to

reduced transcription of GPX3, leading to aberrant accumulation of ROS. This dysregulation further enhances cell mobility, as observed. Interestingly, the migration of EnSCs of RPL women can be elicited by embryos under the normal standard, which indicate the super-fertility state of the endometrium in RPL women (Weimar et al., 2012). This was further reinforced with our own experimental data, showing that loss of DJ-1 resulting in more migration to aneuploidic chemotactic signals. How decidualization converts the characterization of EnSCs to fit the embryonic signals is unexplored, despite selective migration of EnSCs to embryos with high quality has been shown to be associated with the hsa-miR-320a (MIR320A) secreted by embryo (Berkhout et al., 2020), which is an evolutionarily conserved microRNA important for embryo development during pre-implantation phase. Using miRDB database (https://mirdb.org/) reveals a tentative binding sequence of miR-320 on the 3'UTR on Palladin as well as other actin-related genes. Furthermore, miR-320 has a known role on actin dynamics (Nguyen & Lee, 2022). Therefore, taken together, this increased cell mobility through the reduction of miR-320a may additionally drive the endometrium into a hyper-receptive state, making it more susceptible to implantation of low-quality embryos and ultimately contributing to RPL. However, additional research is needed to verify this hypothesis.

5.2 The Impact of LEFTY2 on Calcium Entry Induced by Embryo-Derived Trypsin: Implications for Implantation Success and Unexplained Infertility

Infertility is a complex condition that often involves various molecular and cellular mechanisms. Enhanced LEFTY2 expression has been associated with unexplained infertility and implantation failure, suggesting its significant role in reproductive health. In my thesis, we assessed the impact of LEFTY2 on embryo-derived trypsin-induced calcium entry and explored the fundamental pathways involved. Initially, *in silico* analyses confirmed the presence of key genes associated with the classical trypsin signaling pathway in human embryos. This was followed by the detection of lower levels of embryo-derived trypsin in the conditioned medium from women with infertility, as

measured by ELISA. Live-cell calcium imaging experiments revealed that LEFTY2 can inhibit trypsin-induced calcium influx in Ishikawa cells, although this effect is not mediated by the epithelial sodium channel (ENaC). Further investigation into the mechanisms behind this inhibition revealed the involvement of L-type calcium channels, with bioinformatic analyses confirming the expression of CACNA1C in endometrial tissue. Experimental validation through qRT-PCR and immunofluorescence further supported these findings. Functional studies using the L-type calcium channel blocker nifedipine demonstrated that LEFTY2's inhibitory effect on trypsin-induced calcium entry is mediated through these channels. Our findings suggest that LEFTY2 plays a critical role in modulating calcium influx induced by trypsin, and we provide evidence for the involvement of L-type calcium channels in this process. Furthermore, our study provides a foundation for further exploration of LEFTY2 as a possible biomolecule that can be targeted in terms of fertility treatments and the restoration of proper calcium signaling in ISK.

5.2.1 Role of Embryo-Derived Trypsin in Implantation Success and Unexplained Infertility

Unexplained infertility presents a major challenge for reproductive medicine professionals. Reduced endometrial receptivity during the implantation window for embryos may be a key factor contributing to unexplained infertility and failed IVF cycles (Stevens Brentjens et al., 2022). Previous studies showed that the endometrium can act as a ‘bio-sensor’ of embryo quality, which prevents the maternal contribution for non-viable embryos (Brosens & Gellersen, 2010; Macklon & Brosens, 2014; Teklenburg et al., 2010). The ‘selection hypothesis’ suggests that an excessive or pronounced decidual response can shorten the window of receptivity and enhance the elimination of embryos, thereby lowering the risk of miscarriage but potentially preventing conception (Brosens et al., 2014). Therefore, the human uterus has an intrinsic ability to adapt and can adjust its receptivity and selectivity traits (Gellersen & Brosens, 2014).

It is posited that embryos communicate *via* trypsin, which is produced through the enzymatic breakdown of trypsinogen (Hegyi & Sahin-Toth, 2017; Whitcomb et al., 1996; Zheng et al., 2009). Enteropeptidase is considered the 'principal regulator' of trypsin activity because of its involvement in trypsinogen cleavage and activation (Szabo et al., 2003; Whitcomb et al., 1996; Zheng et al., 2009). This activation triggers the release of trypsin, resulting in an enhanced production of trypsin (Szabo et al., 2003). PRSS1, the gene encoding trypsinogen, is not modulated during pre-implantation development (Brosens et al., 2014) and the gene encoding PRSS8, located on chromosome 16 is a serine protease expressed highly by healthy embryos. Interestingly, chromosomes 16 and 22 are the most common trisomy in human embryos (Munne et al., 2004). The elevated gene copy number in trisomic embryos may lead to embryo-derived trypsin overproduction, which can facilitate enhanced invasion of the embryo (Ma et al., 2009; Quenby et al., 2002). It is notable to point out that PRSS8 knockout mice display embryo lethality due to the impairment of placenta (Hummler et al., 2013) and a polymorphism in PRSS8 has been linked to severe pre-eclampsia (Luo et al., 2014). The present study demonstrates that trypsin level can be detected in ECM from SET and was associated with successful pregnancies. These findings establish that embryo-derived trypsin could be used as an indicator for successful embryo implantation.

During the peri-implantation period in mice, ENaC expression on the epithelial surface has been shown to be upregulated (Liu et al., 2014). It controls water and electrolyte resorption and is known to contribute to uterine closure in mice (Li et al., 2023). Furthermore, ENaC are activated by a variety of mechanical stimuli, such as changes in shear stress or stretching of the epithelial tissue (Kleyman et al., 2018), and by serine proteases, which cleave specific segments of the channel to facilitate its activation (Shi et al., 2013). Serine proteases, including trypsin, are present at the embryo-endometrial interface, where they are released by the embryo and are essential for successful implantation (Brosens et al., 2014; Salamonsen & Nie, 2002). As previously proposed, trypsin likely facilitates its effects through the activation of ENaC, resulting in Na^+ influx and subsequent membrane depolarization. This depolarization activated the L-type voltage gated Ca^{2+} channel, resulting in a sustained cytosolic Ca^{2+} activity ($[Ca^{2+}]_i$) rise.

The increase in $[Ca^{2+}]_i$ resulted in a COX2 dependent rise in PGE_2 release, thereby augmenting the process of implantation and decidualization (Ruan et al., 2012).

5.2.2 LEFTY2 Modulates Trypsin-Induced Ca^{2+} Entry and Its Role in Endometrial Infertility

Further, our present observations reveal that endometrial infertility factor LEFTY2 downregulates trypsin-induced Ca^{2+} entry. Treatment of ISK with trypsin was followed by $[Ca^{2+}]_i$ going up rapidly, which was significantly blunted by ENaC inhibitor amiloride. As suggested earlier (Ruan et al., 2012), trypsin is presumably effective by activation of ENaC with subsequent Na^+ entry and the cell membrane depolarization (Ruan et al., 2012). We discuss the limitations of employing an *in vitro* model using human carcinoma-derived EECs, as the responses and underlying molecular mechanisms may not accurately reflect the *in vivo* conditions. However, this cell line has been used in numerous studies to investigate receptivity and implantation (Ruane et al., 2024; X. Wang et al., 2024). Notwithstanding, our data reveal that the inhibitory effect of LEFTY2 on trypsin induced Ca^{2+} entry could not have been due to inhibition of ENaC, which is actually upregulated by LEFTY2 (Salker, Hosseinzadeh, et al., 2016). The trypsin induced $[Ca^{2+}]_i$ increase was strongly and significantly blunted by nifedipine. In the presence of nifedipine, LEFTY2 did not further modify trypsin induced increase of $[Ca^{2+}]_i$. Thus, LEFTY2 downregulated trypsin induced $[Ca^{2+}]_i$ increase is largely due to interference with nifedipine sensitive Ca^{2+} entry. Interestingly, there have been two clinical trials with the use of nifedipine prior to embryo transfers with the conjecture that a relaxed myometrium and vasodilation may serve to improve implantation rates. However, both studies showed a decrease in pregnancy rates compared to the placebo group, this negative effect seen maybe due to blocking the required rise in calcium necessary for implantation (Nataj Majd et al., 2022; Ng et al., 2019). Furthermore, we also cannot rule the contribution of other calcium channels in the process of implantation and infertility. A study by Bahar N. et al showed that there was a change in the methylation status and transcriptomic levels of several T-type calcium channels and was correlated with

recurrent implantation failure (Davoodi Nik et al., 2024). Further work is required validate whether LEFTY2 can alter additional transporters and ion channels.

Endometrial LEFTY2 seems to have a dual function in the modulating of Ca^{2+} entry. Firstly, the decrease of Orai1 prevents the conversion of the endometrium into a receptive phenotype by attenuating the level of Ca^{2+} sensitive receptivity genes (Salker et al., 2018). Secondly, LEFTY2 downregulates the effect of trypsin induced Ca^{2+} entry and could prevent embryo-induced Ca^{2+} entry. It might be plausible to suggest that both Orai1 and SOCE are required for fine-tuning endometrial receptivity prior to embryo implantation and that trypsin-induced Ca^{2+} entry takes the leading role during embryo implantation (Ruan et al., 2012), suggesting that LEFTY2 is a strong inhibitor of both, SOCE and trypsin-induced Ca^{2+} entry.

5.3 Limitations

While these findings provide significant insights, several limitations should be acknowledged. First, the specific signaling pathways and mechanisms connecting DJ-1 to cytoskeletal rearrangements and ROS regulation remain to be fully elucidated. Additionally, investigating the role of Palladin in an *in vivo* model could provide further clarity. Furthermore, the human samples used for DJ-1 expression analysis were obtained only from women with infertility and recurrent pregnancy loss. Including healthy controls would have strengthened the study. Moreover, exploring interactions with other cell types during decidualization would provide important insights for future research.

The mechanisms by which LEFTY2 modulates trypsin-induced calcium entry *in vivo* are also not yet fully characterized. Another limitation of our study is that the ECM samples were sourced from patients with infertility. Consequently, the generalizability of these findings to a broader population, including individuals without known fertility issues, remains uncertain and warrants further investigation. Future research involving a more diverse patient cohort is necessary to confirm the observed association between ECM-

derived trypsin activity and successful pregnancy outcomes, while also accounting for variables, including genetic background and ancestry.

It is also crucial to translate these findings from murine models to human pregnancy, as species-specific biological differences could influence the observed effects. Future studies should explore the therapeutic potential of modulating DJ-1 expression or trypsin activity to prevent pregnancy loss and examine their roles in various genetic and environmental contexts. Integrating these molecular insights into broader frameworks of decidualization and implantation will be essential. Such efforts could lead to the development of novel diagnostic markers and targeted therapies aimed at improving pregnancy outcomes in patients experiencing recurrent pregnancy loss or implantation failure.

5.4 Conclusion and Outlook

In conclusion, our study advances the understanding of the molecular mechanisms underlying early pregnancy, particularly focusing on the roles of DJ-1 in oxidative stress and cytoskeletal dynamics, and LEFTY2 in regulating trypsin-induced calcium entry. Decidualization is accompanied by a burst of ROS, triggering the induction of antioxidant defenses. By the end of the first trimester, the removal of trophoblastic plugs from the spiral arteries results in a steep rise in oxygen tension, generating a wave of ROS that tests the resilience of the placental-decidual interface. In this context, we uncovered an unexpected yet pivotal role for DJ-1 in the human endometrium during initial pregnancy phase. DJ-1 deficiency was demonstrated to be involved with both murine and human pregnancy loss, characterized by reduced expression of key decidual markers, elevated ROS levels, and elevated cell death. Moreover, loss of DJ-1 disrupted cytoskeletal dynamics, particularly actin polymerization, leading to altered cell morphology and migration patterns *via* Palladin. This dysregulation enhanced the migration of cells toward chemotactic signals from aneuploid trophoblasts. Importantly, DJ-1 overexpression reversed these effects, further underscoring its central role in ROS regulation, cytoskeletal rearrangements, and cell migration during early pregnancy.

Additionally, our findings reveal that embryo-derived trypsin is produced by human embryos, with increasing amounts correlating with successful pregnancy outcomes. We also demonstrated a negative regulatory effect of LEFTY2 on trypsin-induced nifedipine-sensitive Ca^{2+} entry, a mechanism contributing to the adverse impact of LEFTY2 on embryo implantation. Together, these results illuminate the intricate molecular and cellular interactions at the maternal-fetal interface and highlight the importance of DJ-1 and trypsin in supporting a successful pregnancy while identifying potential pathways implicated in pregnancy loss.

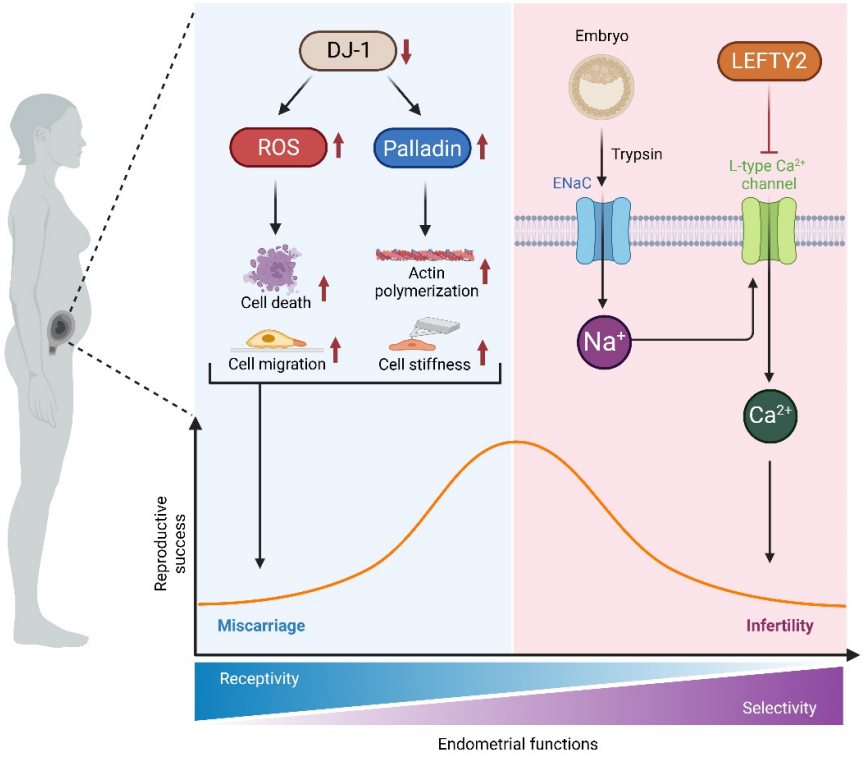

Figure 5-1: Balancing Endometrial Receptivity versus Selectivity during Early Pregnancy.

DJ-1 regulates oxidative stress responses, cytoskeletal dynamics, and cell migration through ROS modulation and actin polymerization, supporting successful implantation and mitigating pregnancy loss. LEFTY2 modulates trypsin-induced Ca^{2+} entry by blocking nifedipine sensitive L-type calcium channel, highlighting its role in regulating embryo implantation and selectivity at the maternal-fetal interface. Created with BioRender.com.

6. Abstract

Successful pregnancy is critically dependent on the remodelling of the EnSCs into specialized decidual EnSCs and the establishment of endometrial receptivity. Disruptions in these processes are associated with complications such as RPL and unexplained infertility. While DJ-1 is implicated in neurodegeneration, its role in pregnancy remains unknown. Ca^{2+} signaling and the endometrial expression of infertility factor LEFTY2 also play key roles in embryo implantation, with LEFTY2 negatively regulating receptivity. However, the molecular mechanisms linking these pathways remain to be elucidated.

In the first study, we used systems biology, functional studies, and bioinformatics to investigate the role of DJ-1 during early pregnancy. DJ-1 expression in both human and murine endometrium was examined during the window of implantation, and its functional role was further analyzed through knockdown and overexpression experiments. The results revealed that DJ-1 expression increased during early pregnancy, with its loss associated with pregnancy failure. Furthermore, DJ-1 knockdown led to increased ROS production, increased Palladin expression, and enhanced cell stiffness and cell motility, with these effects being reversed upon DJ-1 overexpression.

In the second study, human embryo conditioned medium was used to assess trypsin levels and their association with infertility. The effect of LEFTY2 on trypsin-induced Ca^{2+} entry was investigated in human endometrial epithelial cells through qRT-PCR, immunofluorescence, and Fura2 fluorescence for quantifying intracellular Ca^{2+} ($[Ca^{2+}]_i$) levels. The results demonstrated that trypsin released by the blastocyst facilitated successful pregnancy by promoting $[Ca^{2+}]_i$ entry through L-type Ca^{2+} channels in endometrial cells. Furthermore, LEFTY2 inhibited trypsin-induced Ca^{2+} entry by blocking the expression of nifedipine-sensitive L-type Ca^{2+} channel.

These findings highlight the indispensable roles of DJ-1 in maintaining decidual cytoskeletal integrity and LEFTY2's interference with trypsin-induced Ca^{2+} signaling in modulating endometrial functions. These results provide insight into recurrent pregnancy loss and unexplained infertility, offering potential therapeutic targets to improve pregnancy outcomes and IVF success rates.

7. Zusammenfassung

Eine erfolgreiche Schwangerschaft hängt maßgeblich von der Umwandlung der EnSCs in spezialisierte dezidуale EnSCs und der Etablierung der endometrialen Empfänglichkeit während des kurzen Zeitfenster für die Implantation ab. Störungen in diesen Prozessen sind mit Komplikationen wie wiederholten Fehlgeburten und ungeklärter Unfruchtbarkeit verbunden. Während DJ-1 mit neurodegenerativen Erkrankungen in Verbindung gebracht wird, bleibt seine Rolle in der Schwangerschaft unbekannt. Calcium-Signalgebung und die endometriale Expression des Infertilitätsfaktors LEFTY2 spielen eine Schlüsselrolle bei der Embryoimplantation, wobei LEFTY2 die Empfänglichkeit negativ reguliert. Die molekularen Mechanismen, die diese Signalwege verbinden, sind jedoch noch nicht verstanden.

In der ersten Studie verwendeten wir Systembiologie, funktionelle Studien und Bioinformatik, um die Rolle von DJ-1 während der frühen Schwangerschaft zu untersuchen. Die DJ-1-Expression im Endometrium von Mensch und Maus wurde während des Implantationsfensters untersucht, und seine funktionelle Rolle weiter durch Knockdown- und Überexpressionsexperimente analysiert. Die Ergebnisse zeigten, dass die DJ-1-Expression während der frühen Schwangerschaft anstieg, wobei der Verlust von DJ-1 mit einem Schwangerschaftsversagen assoziiert war. Darüber hinaus führte der DJ-1-Knockdown zu einer erhöhten ROS-Produktion, einer erhöhten Palladin-Expression, sowie einer erhöhten Zellsteifigkeit und Zellbeweglichkeit, wobei diese Effekte durch DJ-1-Überexpression reversibel waren.

In der zweiten Studie wurde ein humanes Embryo-konditioniertes Medium verwendet, um den Trypsinspiegel und dessen Zusammenhang mit Unfruchtbarkeit zu bewerten. Der Effekt von LEFTY2 auf die durch Trypsin induzierten Ca^{2+}-Aufnahme wurde in menschlichen endometrialen Epithelzellen mittels qRT-PCR, Immunfluoreszenz und Fura2-Fluoreszenz zur Quantifizierung der intrazellulären Ca^{2+}-Konzentration ($[Ca^{2+}]_i$) untersucht. Die Ergebnisse zeigten, dass Trypsin, welches von der Blastozyste freigesetzt wurde, eine erfolgreiche Schwangerschaft förderte, indem es den $[Ca^{2+}]_i$-Eintritt durch L-Typ Ca^{2+}-Kanäle in Endometriumzellen erleichterte. Darüber hinaus inhibierte LEFTY2

den durch Trypsin induzierten Ca^{2+}-Einstrom, indem es die Expression von Nifedipin-empfindlichen L-Tpy Ca^{2+}-Kanälen blockierte.

Diese Ergebnisse unterstreichen die unverzichtbare Rolle von DJ-1 bei der Aufrechterhaltung der Integrität des dezidualen Zytoskeletts und die hemmende Wirkung von LEFTY2 auf die Trypsin-induzierte Ca^{2+}-Signalgebung bei der Modulation endometrialer Funktionen. Die Ergebnisse liefern Einblicke in wiederholte Fehlgeburten sowie ungeklärte Unfruchtbarkeit und geben Hinweise auf potenzielle therapeutische Ansätze zur Verbesserung von Schwangerschaftsergebnissen und der Erfolgsraten von IVF.

8. Bibliography

Agarwal, A., Gupta, S., Sekhon, L., & Shah, R. (2008). Redox considerations in female reproductive function and assisted reproduction: from molecular mechanisms to health implications. *Antioxid Redox Signal*, *10*(8), 1375-1403. https://doi.org/10.1089/ars.2007.1964

Aghajanova, L. (2004). Leukemia inhibitory factor and human embryo implantation. *Ann N Y Acad Sci*, *1034*, 176-183. https://doi.org/10.1196/annals.1335.020

Al-Sabbagh, M., Fusi, L., Higham, J., Lee, Y., Lei, K., Hanyaloglu, A. C., Lam, E. W., Christian, M., & Brosens, J. J. (2011). NADPH oxidase-derived reactive oxygen species mediate decidualization of human endometrial stromal cells in response to cyclic AMP signaling. *Endocrinology*, *152*(2), 730-740. https://doi.org/10.1210/en.2010-0899

Aleyasin, H., Rousseaux, M. W., Phillips, M., Kim, R. H., Bland, R. J., Callaghan, S., Slack, R. S., During, M. J., Mak, T. W., & Park, D. S. (2007). The Parkinson's disease gene DJ-1 is also a key regulator of stroke-induced damage. *Proc Natl Acad Sci U S A*, *104*(47), 18748-18753. https://doi.org/10.1073/pnas.0709379104

Amatullah, H., Maron-Gutierrez, T., Shan, Y., Gupta, S., Tsoporis, J. N., Varkouhi, A. K., Teixeira Monteiro, A. P., He, X., Yin, J., Marshall, J. C., Rocco, P. R. M., Zhang, H., Kuebler, W. M., & Dos Santos, C. C. (2021). Protective function of DJ-1/PARK7 in lipopolysaccharide and ventilator-induced acute lung injury. *Redox Biol*, *38*, 101796. https://doi.org/10.1016/j.redox.2020.101796

Arango, N. A., Szotek, P. P., Manganaro, T. F., Oliva, E., Donahoe, P. K., & Teixeira, J. (2005). Conditional deletion of beta-catenin in the mesenchyme of the developing mouse uterus results in a switch to adipogenesis in the myometrium. *Dev Biol*, *288*(1), 276-283. https://doi.org/10.1016/j.ydbio.2005.09.045

Ashary, N., Tiwari, A., & Modi, D. (2018). Embryo Implantation: War in Times of Love. *Endocrinology*, *159*(2), 1188-1198. https://doi.org/10.1210/en.2017-03082

Azatov, M., Goicoechea, S. M., Otey, C. A., & Upadhyaya, A. (2016). The actin crosslinking protein palladin modulates force generation and mechanosensitivity of tumor associated fibroblasts. *Sci Rep*, *6*, 28805. https://doi.org/10.1038/srep28805

Bahmed, K., Boukhenouna, S., Karim, L., Andrews, T., Lin, J., Powers, R., Wilson, M. A., Lin, C. R., Messier, E., Reisdorph, N., Powell, R. L., Tang, H. Y., Mason, R. J., Criner, G. J., & Kosmider, B. (2019). The effect of cysteine oxidation on DJ-1 cytoprotective function in human alveolar type II cells. *Cell Death Dis*, *10*(9), 638. https://doi.org/10.1038/s41419-019-1833-5

Bala, R., Singh, V., Rajender, S., & Singh, K. (2021). Environment, Lifestyle, and Female Infertility. *Reprod Sci*, *28*(3), 617-638. https://doi.org/10.1007/s43032-020-00279-3

Bamberger, C. M., Else, T., Bamberger, A. M., Beil, F. U., & Schulte, H. M. (1999). Dissociative glucocorticoid activity of medroxyprogesterone acetate in normal human lymphocytes. *J Clin Endocrinol Metab*, *84*(11), 4055-4061. https://doi.org/10.1210/jcem.84.11.6091

Ben Mahdi, M. H., Andrieu, V., & Pasquier, C. (2000). Focal adhesion kinase regulation by oxidative stress in different cell types. *IUBMB Life*, *50*(4-5), 291-299. https://doi.org/10.1080/713803721

Bensellam, M., Laybutt, D. R., & Jonas, J. C. (2012). The molecular mechanisms of pancreatic beta-cell glucotoxicity: recent findings and future research directions. *Mol Cell Endocrinol*, *364*(1-2), 1-27. https://doi.org/10.1016/j.mce.2012.08.003

Bereshchenko, O., Bruscoli, S., & Riccardi, C. (2018). Glucocorticoids, Sex Hormones, and Immunity. *Front Immunol*, *9*, 1332. https://doi.org/10.3389/fimmu.2018.01332

Berkhout, R. P., Keijser, R., Repping, S., Lambalk, C. B., Afink, G. B., Mastenbroek, S., & Hamer, G. (2020). High-quality human preimplantation embryos stimulate endometrial stromal cell migration via secretion of microRNA hsa-miR-320a. *Hum Reprod*, *35*(8), 1797-1807. https://doi.org/10.1093/humrep/deaa149

Bhandari, H. M., Tan, B. K., & Quenby, S. (2016). Superfertility is more prevalent in obese women with recurrent early pregnancy miscarriage. *BJOG*, *123*(2), 217-222. https://doi.org/10.1111/1471-0528.13806

Bhavsar, S. K., Schmidt, S., Bobbala, D., Nurbaeva, M. K., Hosseinzadeh, Z., Merches, K., Fajol, A., Wilmes, J., & Lang, F. (2013). AMPKalpha1-sensitivity of Orai1 and Ca(2+) entry in T - lymphocytes. *Cell Physiol Biochem*, *32*(3), 687-698. https://doi.org/10.1159/000354472

Bilodeau, G. G. (1992). Regular pyramid punch problem. *J. Appl. Mech*, *59*, 519-523.

Bonifati, V., Rizzu, P., van Baren, M. J., Schaap, O., Breedveld, G. J., Krieger, E., Dekker, M. C., Squitieri, F., Ibanez, P., Joosse, M., van Dongen, J. W., Vanacore, N., van Swieten, J. C., Brice, A., Meco, G., van Duijn, C. M., Oostra, B. A., & Heutink, P. (2003). Mutations in the DJ-1 gene associated with autosomal recessive early-onset parkinsonism. *Science*, *299*(5604), 256-259. https://doi.org/10.1126/science.1077209

Brosens, J. J., Bennett, P. R., Abrahams, V. M., Ramhorst, R., Coomarasamy, A., Quenby, S., Lucas, E. S., & McCoy, R. C. (2022). Maternal selection of human embryos in early gestation: Insights from recurrent miscarriage. *Semin Cell Dev Biol*, *131*, 14-24. https://doi.org/10.1016/j.semcdb.2022.01.007

Brosens, J. J., & Gellersen, B. (2010). Something new about early pregnancy: decidual biosensoring and natural embryo selection. *Ultrasound Obstet Gynecol*, *36*(1), 1-5. https://doi.org/10.1002/uog.7714

Brosens, J. J., Salker, M. S., Teklenburg, G., Nautiyal, J., Salter, S., Lucas, E. S., Steel, J. H., Christian, M., Chan, Y. W., Boomsma, C. M., Moore, J. D., Hartshorne, G. M., Sucurovic, S., Mulac-Jericevic, B., Heijnen, C. J., Quenby, S., Koerkamp, M. J., Holstege, F. C., Shmygol, A., & Macklon, N. S. (2014). Uterine selection of human embryos at implantation. *Sci Rep*, *4*, 3894. https://doi.org/10.1038/srep03894

Buneeva, O. A., & Medvedev, A. E. (2021). DJ-1 Protein and Its Role in the Development of Parkinson's Disease: Studies on Experimental Models. *Biochemistry (Mosc)*, *86*(6), 627-640. https://doi.org/10.1134/S000629792106002X

Busnelli, A., Garolla, A., Di Credico, E., D'Ippolito, S., Merola, A. M., Milardi, D., Pontecorvi, A., Scambia, G., & Di Simone, N. (2023). Sperm DNA fragmentation and idiopathic recurrent pregnancy loss: Results from a multicenter case-control study. *Andrology*, *11*(8), 1673-1681. https://doi.org/10.1111/andr.13395

Cai, M., Sikong, Y., Wang, Q., Zhu, S., Pang, F., & Cui, X. (2019). Gpx3 prevents migration and invasion in gastric cancer by targeting NFsmall ka, CyrillicB/Wnt5a/JNK signaling. *Int J Clin Exp Pathol*, *12*(4), 1194-1203. https://www.ncbi.nlm.nih.gov/pubmed/31933934

Cao, J., Lou, S., Ying, M., & Yang, B. (2015). DJ-1 as a human oncogene and potential therapeutic target. *Biochem Pharmacol*, *93*(3), 241-250. https://doi.org/10.1016/j.bcp.2014.11.012

Carson, D. D., Lagow, E., Thathiah, A., Al-Shami, R., Farach-Carson, M. C., Vernon, M., Yuan, L., Fritz, M. A., & Lessey, B. (2002). Changes in gene expression during the early to mid-luteal (receptive phase) transition in human endometrium detected by high-density microarray screening. *Mol Hum Reprod*, *8*(9), 871-879. https://doi.org/10.1093/molehr/8.9.871

Cha, J., Sun, X., & Dey, S. K. (2012). Mechanisms of implantation: strategies for successful pregnancy. *Nat Med*, *18*(12), 1754-1767. https://doi.org/10.1038/nm.3012

Chen, W. T., Yang, H. B., Ke, T. W., Liao, W. L., & Hung, S. Y. (2021). Serum DJ-1 Is a Biomarker of Colorectal Cancer and DJ-1 Activates Mitophagy to Promote Colorectal Cancer Progression. *Cancers (Basel)*, *13*(16). https://doi.org/10.3390/cancers13164151

Chunna, A., & Pu, X. P. (2017). Role of DJ-1 in Fertilization. *Adv Exp Med Biol*, *1037*, 61-66. https://doi.org/10.1007/978-981-10-6583-5_5

Cloke, B., Huhtinen, K., Fusi, L., Kajihara, T., Yliheikkila, M., Ho, K. K., Teklenburg, G., Lavery, S., Jones, M. C., Trew, G., Kim, J. J., Lam, E. W., Cartwright, J. E., Poutanen, M., & Brosens, J. J. (2008). The androgen and progesterone receptors regulate distinct gene networks and cellular functions in decidualizing endometrium. *Endocrinology*, *149*(9), 4462-4474. https://doi.org/10.1210/en.2008-0356

Coast, E., Lattof, S. R., & Strong, J. (2019). Puberty and menstruation knowledge among young adolescents in low- and middle-income countries: a scoping review. *Int J Public Health*, *64*(2), 293-304. https://doi.org/10.1007/s00038-019-01209-0

Colvin, C. W., & Abdullatif, H. (2013). Anatomy of female puberty: The clinical relevance of developmental changes in the reproductive system. *Clin Anat*, *26*(1), 115-129. https://doi.org/10.1002/ca.22164

Cope, D. I., & Monsivais, D. (2022). Progesterone Receptor Signaling in the Uterus Is Essential for Pregnancy Success. *Cells*, *11*(9). https://doi.org/10.3390/cells11091474

Cornet, P. B., Picquet, C., Lemoine, P., Osteen, K. G., Bruner-Tran, K. L., Tabibzadeh, S., Courtoy, P. J., Eeckhout, Y., Marbaix, E., & Henriet, P. (2002). Regulation and function of LEFTY-A/EBAF in the human endometrium. mRNA expression during the menstrual cycle, control by progesterone, and effect on matrix metalloprotineases. *J Biol Chem*, *277*(45), 42496-42504. https://doi.org/10.1074/jbc.M201793200

Cox, J., & Mann, M. (2008). MaxQuant enables high peptide identification rates, individualized p.p.b.-range mass accuracies and proteome-wide protein quantification. *Nat Biotechnol*, *26*(12), 1367-1372. https://doi.org/10.1038/nbt.1511

Critchley, H. O. D., Maybin, J. A., Armstrong, G. M., & Williams, A. R. W. (2020). Physiology of the Endometrium and Regulation of Menstruation. *Physiol Rev*, *100*(3), 1149-1179. https://doi.org/10.1152/physrev.00031.2019

D'Ippolito, S., Ticconi, C., Tersigni, C., Garofalo, S., Martino, C., Lanzone, A., Scambia, G., & Di Simone, N. (2020). The pathogenic role of autoantibodies in recurrent pregnancy loss. *Am J Reprod Immunol*, *83*(1), e13200. https://doi.org/10.1111/aji.13200

Davoodi Nik, B., Hashemi Karoii, D., Favaedi, R., Ramazanali, F., Jahangiri, M., Movaghar, B., & Shahhoseini, M. (2024). Differential expression of ion channel coding genes in the endometrium of women experiencing recurrent implantation failures. *Sci Rep*, *14*(1), 19822. https://doi.org/10.1038/s41598-024-70778-9

de Almeida, A., de Oliveira, J., da Silva Pontes, L. V., de Souza Junior, J. F., Goncalves, T. A. F., Dantas, S. H., de Almeida Feitosa, M. S., Silva, A. O., & de Medeiros, I. A. (2022). ROS: Basic Concepts, Sources, Cellular Signaling, and its Implications in Aging Pathways. *Oxid Med Cell Longev*, *2022*, 1225578. https://doi.org/10.1155/2022/1225578

de Ziegler, D., Fanchin, R., de Moustier, B., & Bulletti, C. (1998). The hormonal control of endometrial receptivity: estrogen (E2) and progesterone. *J Reprod Immunol*, *39*(1-2), 149-166. https://doi.org/10.1016/s0165-0378(98)00019-9

Deligdisch-Schor, L., & Mares Miceli, A. (2020). Hormonal Biophysiology of the Uterus. *Adv Exp Med Biol*, *1242*, 1-12. https://doi.org/10.1007/978-3-030-38474-6_1

Diaz-Vivancos, P., de Simone, A., Kiddle, G., & Foyer, C. H. (2015). Glutathione--linking cell proliferation to oxidative stress. *Free Radic Biol Med*, *89*, 1154-1164. https://doi.org/10.1016/j.freeradbiomed.2015.09.023

Dimitriadis, E., Menkhorst, E., Saito, S., Kutteh, W. H., & Brosens, J. J. (2020). Recurrent pregnancy loss. *Nat Rev Dis Primers*, *6*(1), 98. https://doi.org/10.1038/s41572-020-00228-z

Diniz-da-Costa, M., Kong, C. S., Fishwick, K. J., Rawlings, T., Brighton, P. J., Hawkes, A., Odendaal, J., Quenby, S., Ott, S., Lucas, E. S., Vrljicak, P., & Brosens, J. J. (2021). Characterization of highly proliferative decidual precursor cells during the window of implantation in human endometrium. *Stem Cells*, *39*(8), 1067-1080. https://doi.org/10.1002/stem.3367

Dixon, R. D., Arneman, D. K., Rachlin, A. S., Sundaresan, N. R., Costello, M. J., Campbell, S. L., & Otey, C. A. (2008). Palladin is an actin cross-linking protein that uses immunoglobulin-like domains to bind filamentous actin. *J Biol Chem*, *283*(10), 6222-6231. https://doi.org/10.1074/jbc.M707694200

Dolgacheva, L. P., Berezhnov, A. V., Fedotova, E. I., Zinchenko, V. P., & Abramov, A. Y. (2019). Role of DJ-1 in the mechanism of pathogenesis of Parkinson's disease. *J Bioenerg Biomembr*, *51*(3), 175-188. https://doi.org/10.1007/s10863-019-09798-4

Dougherty, M. P., Poch, A. M., Chorich, L. P., Hawkins, Z. A., Xu, H., Roman, R. A., Liu, H., Brakta, S., Taylor, H. S., Knight, J., Kim, H. G., Diamond, M. P., & Layman, L. C. (2023). Unexplained Female Infertility Associated with Genetic Disease Variants. *N Engl J Med*, *388*(11), 1055-1056. https://doi.org/10.1056/NEJMc2211539

Droge, W. (2002). Free radicals in the physiological control of cell function. *Physiol Rev*, *82*(1), 47-95. https://doi.org/10.1152/physrev.00018.2001

Dunn, C. L., Kelly, R. W., & Critchley, H. O. (2003). Decidualization of the human endometrial stromal cell: an enigmatic transformation. *Reprod Biomed Online*, *7*(2), 151-161. https://doi.org/10.1016/s1472-6483(10)61745-2

Eberhard, D., & Lammert, E. (2017). The Role of the Antioxidant Protein DJ-1 in Type 2 Diabetes Mellitus. *Adv Exp Med Biol*, *1037*, 173-186. https://doi.org/10.1007/978-981-10-6583-5_11

Ehsani, M., Mohammadnia-Afrouzi, M., Mirzakhani, M., Esmaeilzadeh, S., & Shahbazi, M. (2019). Female Unexplained Infertility: A Disease with Imbalanced Adaptive Immunity. *J Hum Reprod Sci*, *12*(4), 274-282. https://doi.org/10.4103/jhrs.JHRS_30_19

Emokpae, M. A., & Brown, S. I. (2021). Effects of lifestyle factors on fertility: practical recommendations for modification. *Reprod Fertil*, *2*(1), R13-R26. https://doi.org/10.1530/RAF-20-0046

Eshre Guideline Group on RPL, Bender Atik, R., Christiansen, O. B., Elson, J., Kolte, A. M., Lewis, S., Middeldorp, S., McHeik, S., Peramo, B., Quenby, S., Nielsen, H. S., van der Hoorn, M. L., Vermeulen, N., & Goddijn, M. (2023). ESHRE guideline: recurrent pregnancy loss: an update in 2022. *Hum Reprod Open*, *2023*(1), hoad002. https://doi.org/10.1093/hropen/hoad002

Finkel, T. (2011). Signal transduction by reactive oxygen species. *J Cell Biol*, *194*(1), 7-15. https://doi.org/10.1083/jcb.201102095

Gao, W., Feng, F., Ma, X., Zhang, R., Li, L., Yue, F., Lv, M., & Liu, L. (2022). Progress of oxidative stress in endometrium decidualization. *J Obstet Gynaecol*, *42*(8), 3429-3434. https://doi.org/10.1080/01443615.2022.2144171

Garrisi, J. G., Colls, P., Ferry, K. M., Zheng, X., Garrisi, M. G., & Munne, S. (2009). Effect of infertility, maternal age, and number of previous miscarriages on the outcome of preimplantation genetic diagnosis for idiopathic recurrent pregnancy loss. *Fertil Steril*, *92*(1), 288-295. https://doi.org/10.1016/j.fertnstert.2008.05.056

Gellersen, B., Brosens, I. A., & Brosens, J. J. (2007). Decidualization of the human endometrium: mechanisms, functions, and clinical perspectives. *Semin Reprod Med*, *25*(6), 445-453. https://doi.org/10.1055/s-2007-991042

Gellersen, B., & Brosens, J. J. (2014). Cyclic decidualization of the human endometrium in reproductive health and failure. *Endocr Rev*, *35*(6), 851-905. https://doi.org/10.1210/er.2014-1045

Genovese, H. G., & McQueen, D. B. (2023). The prevalence of sporadic and recurrent pregnancy loss. *Fertil Steril*, *120*(5), 934-936. https://doi.org/10.1016/j.fertnstert.2023.08.954

Gomes, A., Fernandes, E., & Lima, J. L. (2005). Fluorescence probes used for detection of reactive oxygen species. *J Biochem Biophys Methods*, *65*(2-3), 45-80. https://doi.org/10.1016/j.jbbm.2005.10.003

Gomez-Chavez, F., Correa, D., Navarrete-Meneses, P., Cancino-Diaz, J. C., Cancino-Diaz, M. E., & Rodriguez-Martinez, S. (2021). NF-kappaB and Its Regulators During Pregnancy. *Front Immunol*, *12*, 679106. https://doi.org/10.3389/fimmu.2021.679106

Governini, L., Luongo, F. P., Haxhiu, A., Piomboni, P., & Luddi, A. (2021). Main actors behind the endometrial receptivity and successful implantation. *Tissue Cell*, *73*, 101656. https://doi.org/10.1016/j.tice.2021.101656

Guerin, L. R., Prins, J. R., & Robertson, S. A. (2009). Regulatory T-cells and immune tolerance in pregnancy: a new target for infertility treatment? *Hum Reprod Update*, *15*(5), 517-535. https://doi.org/10.1093/humupd/dmp004

Guo, J., Gao, J., Yu, X., Luo, H., Xiong, X., & Huang, O. (2015). Expression of DJ-1 and mTOR in eutopic and ectopic endometria of patients with endometriosis and adenomyosis. *Gynecol Obstet Invest*, *79*(3), 195-200. https://doi.org/10.1159/000365569

Guzeloglu-Kayisli, O., Kayisli, U. A., & Taylor, H. S. (2009). The role of growth factors and cytokines during implantation: endocrine and paracrine interactions. *Semin Reprod Med*, *27*(1), 62-79. https://doi.org/10.1055/s-0028-1108011

Hantak, A. M., Bagchi, I. C., & Bagchi, M. K. (2014). Role of uterine stromal-epithelial crosstalk in embryo implantation. *Int J Dev Biol*, *58*(2-4), 139-146. https://doi.org/10.1387/ijdb.130348mb

Hegyi, E., & Sahin-Toth, M. (2017). Genetic Risk in Chronic Pancreatitis: The Trypsin-Dependent Pathway. *Dig Dis Sci*, *62*(7), 1692-1701. https://doi.org/10.1007/s10620-017-4601-3

Hennes, A., Devroe, J., De Clercq, K., Ciprietti, M., Held, K., Luyten, K., Van Ranst, N., Maenhoudt, N., Peeraer, K., Vankelecom, H., Voets, T., & Vriens, J. (2023). Protease secretions by the invading blastocyst induce calcium oscillations in endometrial epithelial cells via the protease-activated receptor 2. *Reprod Biol Endocrinol*, *21*(1), 37. https://doi.org/10.1186/s12958-023-01085-7

Hijioka, M., Inden, M., Yanagisawa, D., & Kitamura, Y. (2017). DJ-1/PARK7: A New Therapeutic Target for Neurodegenerative Disorders. *Biol Pharm Bull*, *40*(5), 548-552. https://doi.org/10.1248/bpb.b16-01006

Holdsworth-Carson, S. J., Menkhorst, E., Maybin, J. A., King, A., & Girling, J. E. (2023). Cyclic processes in the uterine tubes, endometrium, myometrium, and cervix: pathways and perturbations. *Mol Hum Reprod*, *29*(5). https://doi.org/10.1093/molehr/gaad012

Honbou, K., Suzuki, N. N., Horiuchi, M., Niki, T., Taira, T., Ariga, H., & Inagaki, F. (2003). The crystal structure of DJ-1, a protein related to male fertility and Parkinson's disease. *J Biol Chem*, *278*(33), 31380-31384. https://doi.org/10.1074/jbc.M305878200

Hummler, E., Dousse, A., Rieder, A., Stehle, J. C., Rubera, I., Osterheld, M. C., Beermann, F., Frateschi, S., & Charles, R. P. (2013). The channel-activating protease CAP1/Prss8 is required for placental labyrinth maturation. *PLoS One*, *8*(2), e55796. https://doi.org/10.1371/journal.pone.0055796

Hussain, T., Murtaza, G., Metwally, E., Kalhoro, D. H., Kalhoro, M. S., Rahu, B. A., Sahito, R. G. A., Yin, Y., Yang, H., Chughtai, M. I., & Tan, B. (2021). The Role of Oxidative Stress and

Antioxidant Balance in Pregnancy. *Mediators Inflamm*, *2021*, 9962860. https://doi.org/10.1155/2021/9962860

Hussain, T., Tan, B., Yin, Y., Blachier, F., Tossou, M. C., & Rahu, N. (2016). Oxidative Stress and Inflammation: What Polyphenols Can Do for Us? *Oxid Med Cell Longev*, *2016*, 7432797. https://doi.org/10.1155/2016/7432797

Ihnatovych, I., Livak, M., Reed, J., de Lanerolle, P., & Strakova, Z. (2009). Manipulating actin dynamics affects human in vitro decidualization. *Biol Reprod*, *81*(1), 222-230. https://doi.org/10.1095/biolreprod.108.074666

Jarrell, J. (2018). The significance and evolution of menstruation. *Best Pract Res Clin Obstet Gynaecol*, *50*, 18-26. https://doi.org/10.1016/j.bpobgyn.2018.01.007

Jiang, Y. H., Shi, Y., He, Y. P., Du, J., Li, R. S., Shi, H. J., Sun, Z. G., & Wang, J. (2011). Serine protease inhibitor 4-(2-aminoethyl)benzenesulfonyl fluoride hydrochloride (AEBSF) inhibits the rat embryo implantation in vivo and interferes with cell adhesion in vitro. *Contraception*, *84*(6), 642-648. https://doi.org/10.1016/j.contraception.2011.03.017

Jin, F., Wang, H., Li, D., Fang, C., Li, W., Shi, Q., Diao, Y., Ding, Z., Dai, X., Tao, L., Sunagawa, M., Wu, F., Qian, Y., & Liu, Y. (2020). DJ-1 promotes cell proliferation and tumor metastasis in esophageal squamous cell carcinoma via the Wnt/beta-catenin signaling pathway. *Int J Oncol*, *56*(5), 1115-1128. https://doi.org/10.3892/ijo.2020.5005

Jin, L. (2011). The actin associated protein palladin in smooth muscle and in the development of diseases of the cardiovasculature and in cancer. *J Muscle Res Cell Motil*, *32*(1), 7-17. https://doi.org/10.1007/s10974-011-9246-9

Jin, L., Yoshida, T., Ho, R., Owens, G. K., & Somlyo, A. V. (2009). The actin-associated protein Palladin is required for development of normal contractile properties of smooth muscle cells derived from embryoid bodies. *J Biol Chem*, *284*(4), 2121-2130. https://doi.org/10.1074/jbc.M806095200

Joselin, A. P., Hewitt, S. J., Callaghan, S. M., Kim, R. H., Chung, Y. H., Mak, T. W., Shen, J., Slack, R. S., & Park, D. S. (2012). ROS-dependent regulation of Parkin and DJ-1 localization during oxidative stress in neurons. *Hum Mol Genet*, *21*(22), 4888-4903. https://doi.org/10.1093/hmg/dds325

Junn, E., Jang, W. H., Zhao, X., Jeong, B. S., & Mouradian, M. M. (2009). Mitochondrial localization of DJ-1 leads to enhanced neuroprotection. *J Neurosci Res*, *87*(1), 123-129. https://doi.org/10.1002/jnr.21831

Kahle, P. J., Waak, J., & Gasser, T. (2009). DJ-1 and prevention of oxidative stress in Parkinson's disease and other age-related disorders. *Free Radic Biol Med*, *47*(10), 1354-1361. https://doi.org/10.1016/j.freeradbiomed.2009.08.003

Kaludercic, N., Deshwal, S., & Di Lisa, F. (2014). Reactive oxygen species and redox compartmentalization. *Front Physiol*, *5*, 285. https://doi.org/10.3389/fphys.2014.00285

Karpovich, N., Klemmt, P., Hwang, J. H., McVeigh, J. E., Heath, J. K., Barlow, D. H., & Mardon, H. J. (2005). The production of interleukin-11 and decidualization are compromised in endometrial stromal cells derived from patients with infertility. *J Clin Endocrinol Metab*, *90*(3), 1607-1612. https://doi.org/10.1210/jc.2004-0868

Kasahara, K., Takakura, K., Takebayashi, K., Kimura, F., Nakanishi, K., & Noda, Y. (2001). The role of human chorionic gonadotropin on decidualization of endometrial stromal cells in vitro. *J Clin Endocrinol Metab*, *86*(3), 1281-1286. https://doi.org/10.1210/jcem.86.3.7281

Kawate, T., Tsuchiya, B., & Iwaya, K. (2017). Expression of DJ-1 in Cancer Cells: Its Correlation with Clinical Significance. *Adv Exp Med Biol*, *1037*, 45-59. https://doi.org/10.1007/978-981-10-6583-5_4

Kim, J. A., Bang, C. H., Song, G. G., Kim, J. H., Choi, S. J., & Jung, J. H. (2020). Tumour necrosis factor alpha gene polymorphisms in women with recurrent pregnancy loss: a meta-analysis. *Hum Fertil (Camb)*, *23*(3), 159-169. https://doi.org/10.1080/14647273.2018.1543899

Kim, J. S., Huang, T. Y., & Bokoch, G. M. (2009). Reactive oxygen species regulate a slingshot-cofilin activation pathway. *Mol Biol Cell*, *20*(11), 2650-2660. https://doi.org/10.1091/mbc.e09-02-0131

Kim, S. J., Park, Y. J., Hwang, I. Y., Youdim, M. B., Park, K. S., & Oh, Y. J. (2012). Nuclear translocation of DJ-1 during oxidative stress-induced neuronal cell death. *Free Radic Biol Med*, *53*(4), 936-950. https://doi.org/10.1016/j.freeradbiomed.2012.05.035

Kim, Y. S., Yuan, J., Dewar, A., Borg, J. P., Threadgill, D. W., Sun, X., & Dey, S. K. (2023). An unanticipated discourse of HB-EGF with VANGL2 signaling during embryo implantation. *Proc Natl Acad Sci U S A*, *120*(20), e2302937120. https://doi.org/10.1073/pnas.2302937120

Kiss, R., Zhu, M., Jojart, B., Czajlik, A., Solti, K., Forizs, B., Nagy, E., Zsila, F., Beke-Somfai, T., & Toth, G. (2017). Structural features of human DJ-1 in distinct Cys106 oxidative states and their relevance to its loss of function in disease. *Biochim Biophys Acta Gen Subj*, *1861*(11 Pt A), 2619-2629. https://doi.org/10.1016/j.bbagen.2017.08.017

Kleyman, T. R., Kashlan, O. B., & Hughey, R. P. (2018). Epithelial Na(+) Channel Regulation by Extracellular and Intracellular Factors. *Annu Rev Physiol*, *80*, 263-281. https://doi.org/10.1146/annurev-physiol-021317-121143

Kothapalli, R., Buyuksal, I., Wu, S. Q., Chegini, N., & Tabibzadeh, S. (1997). Detection of ebaf, a novel human gene of the transforming growth factor beta superfamily association of gene expression with endometrial bleeding. *J Clin Invest*, *99*(10), 2342-2350. https://doi.org/10.1172/JCI119415

Kumar, V., Soni, U. K., Maurya, V. K., Singh, K., & Jha, R. K. (2017). Integrin beta8 (ITGB8) activates VAV-RAC1 signaling via FAK in the acquisition of endometrial epithelial cell receptivity for blastocyst implantation. *Sci Rep*, *7*(1), 1885. https://doi.org/10.1038/s41598-017-01764-7

Kwon, H. S., Hwang, H. S., Sohn, I. S., & Park, S. H. (2013). Expression of DJ-1 proteins in placentas from women with severe preeclampsia. *Eur J Obstet Gynecol Reprod Biol*, *168*(1), 40-44. https://doi.org/10.1016/j.ejogrb.2012.12.024

Lakshmanan, I., & Batra, S. K. (2013). Protocol for Apoptosis Assay by Flow Cytometry Using Annexin V Staining Method. *Bio Protoc*, *3*(6). https://doi.org/10.21769/bioprotoc.374

Lass, A., Weiser, W., Munafo, A., & Loumaye, E. (2001). Leukemia inhibitory factor in human reproduction. *Fertil Steril*, *76*(6), 1091-1096. https://doi.org/10.1016/s0015-0282(01)02878-3

Lavogina, D., Stepanjuk, A., Peters, M., Samuel, K., Kasvandik, S., Khatun, M., Arffman, R. K., Enkvist, E., Viht, K., Kopanchuk, S., Lattekivi, F., Velthut-Meikas, A., Uri, A., Piltonen, T. T., Rinken, A., & Salumets, A. (2021). Progesterone triggers Rho kinase-cofilin axis during in vitro and in vivo endometrial decidualization. *Hum Reprod*, *36*(8), 2230-2248. https://doi.org/10.1093/humrep/deab161

Lessey, B. A., & Young, S. L. (2019). What exactly is endometrial receptivity? *Fertil Steril*, *111*(4), 611-617. https://doi.org/10.1016/j.fertnstert.2019.02.009

Li, X., & O'Malley, B. W. (2003). Unfolding the action of progesterone receptors. *J Biol Chem*, *278*(41), 39261-39264. https://doi.org/10.1074/jbc.R300024200

Li, Y., Martin, T. E., Hancock, J. M., Li, R., Viswanathan, S., Lydon, J. P., Zheng, Y., & Ye, X. (2023). Visualization of preimplantation uterine fluid absorption in mice using Alexa Fluor 488 Hydrazidedagger. *Biol Reprod*, *108*(2), 204-217. https://doi.org/10.1093/biolre/ioac198

Liang, Y., Shuai, Q., Wang, Y., Jin, S., Feng, Z., Chen, B., Liang, T., Liu, Z., Zhao, H., Chen, Z., Wang, C., & Xie, J. (2021). 1-Nitropyrene exposure impairs embryo implantation through disrupting endometrial receptivity genes expression and producing excessive ROS. *Ecotoxicol Environ Saf*, *227*, 112939. https://doi.org/10.1016/j.ecoenv.2021.112939

Lin, H. Y., Zhang, H., Yang, Q., Wang, H. X., Wang, H. M., Chai, K. X., Chen, L. M., & Zhu, C. (2006). Expression of prostasin and protease nexin-1 in rhesus monkey (Macaca mulatta) endometrium and placenta during early pregnancy. *J Histochem Cytochem*, *54*(10), 1139-1147. https://doi.org/10.1369/jhc.6A7005.2006

Lind-Holm Mogensen, F., Scafidi, A., Poli, A., & Michelucci, A. (2023). PARK7/DJ-1 in microglia: implications in Parkinson's disease and relevance as a therapeutic target. *J Neuroinflammation*, *20*(1), 95. https://doi.org/10.1186/s12974-023-02776-z

Liu, T., Sun, L., Zhang, Y., Wang, Y., & Zheng, J. (2022). Imbalanced GSH/ROS and sequential cell death. *J Biochem Mol Toxicol*, *36*(1), e22942. https://doi.org/10.1002/jbt.22942

Liu, X. M., Zhang, D., Wang, T. T., Sheng, J. Z., & Huang, H. F. (2014). Ion/water channels for embryo implantation barrier. *Physiology (Bethesda)*, *29*(3), 186-195. https://doi.org/10.1152/physiol.00039.2013

Liu, X. S., Luo, H. J., Yang, H., Wang, L., Kong, H., Jin, Y. E., Wang, F., Gu, M. M., Chen, Z., Lu, Z. Y., & Wang, Z. G. (2007). Palladin regulates cell and extracellular matrix interaction through maintaining normal actin cytoskeleton architecture and stabilizing beta1-integrin. *J Cell Biochem*, *100*(5), 1288-1300. https://doi.org/10.1002/jcb.21126

Livak, K. J., & Schmittgen, T. D. (2001). Analysis of relative gene expression data using real-time quantitative PCR and the 2(-Delta Delta C(T)) Method. *Methods*, *25*(4), 402-408. https://doi.org/10.1006/meth.2001.1262

Lockwood, C. J., Murk, W. K., Kayisli, U. A., Buchwalder, L. F., Huang, S. J., Arcuri, F., Li, M., Gopinath, A., & Schatz, F. (2010). Regulation of interleukin-6 expression in human decidual cells and its potential role in chorioamnionitis. *Am J Pathol*, *177*(4), 1755-1764. https://doi.org/10.2353/ajpath.2010.090781

Loid, M., Obukhova, D., Kask, K., Apostolov, A., Meltsov, A., Tserpelis, D., van den Wijngaard, A., Altmae, S., Yahubyan, G., Baev, V., Saare, M., Peters, M., Minajeva, A., Adler, P., Acharya, G., Krjutskov, K., Nikolova, M., Vilella, F., Simon, C., . . . Salumets, A. (2024). Aging promotes accumulation of senescent and multiciliated cells in human endometrial epithelium. *Hum Reprod Open*, *2024*(3), hoae048. https://doi.org/10.1093/hropen/hoae048

Lucas, E. S., Dyer, N. P., Murakami, K., Lee, Y. H., Chan, Y. W., Grimaldi, G., Muter, J., Brighton, P. J., Moore, J. D., Patel, G., Chan, J. K., Takeda, S., Lam, E. W., Quenby, S., Ott, S., & Brosens, J. J. (2016). Loss of Endometrial Plasticity in Recurrent Pregnancy Loss. *Stem Cells*, *34*(2), 346-356. https://doi.org/10.1002/stem.2222

Lucas, E. S., Vrljicak, P., Muter, J., Diniz-da-Costa, M. M., Brighton, P. J., Kong, C. S., Lipecki, J., Fishwick, K. J., Odendaal, J., Ewington, L. J., Quenby, S., Ott, S., & Brosens, J. J. (2020). Recurrent pregnancy loss is associated with a pro-senescent decidual response during the peri-implantation window. *Commun Biol*, *3*(1), 37. https://doi.org/10.1038/s42003-020-0763-1

Luo, D., Zhang, Y., Bai, Y., Liu, X., Gong, Y., Zhou, B., Zhang, L., Luo, L., & Zhou, R. (2014). Prostasin gene polymorphism at rs12597511 is associated with severe preeclampsia in Chinese Han women. *Chin Med J (Engl)*, *127*(11), 2048-2052. https://www.ncbi.nlm.nih.gov/pubmed/24890150

Ma, X. J., Fu, Y. Y., Li, Y. X., Chen, L. M., Chai, K., & Wang, Y. L. (2009). Prostasin inhibits cell invasion in human choriocarcinomal JEG-3 cells. *Histochem Cell Biol*, *132*(6), 639-646. https://doi.org/10.1007/s00418-009-0652-7

Macklon, N. S., & Brosens, J. J. (2014). The human endometrium as a sensor of embryo quality. *Biol Reprod*, *91*(4), 98. https://doi.org/10.1095/biolreprod.114.122846

Manohar, K., Gupta, R. K., Gupta, P., Saha, D., Gare, S., Sarkar, R., Misra, A., & Giri, L. (2021). FDA approved L-type channel blocker Nifedipine reduces cell death in hypoxic A549 cells through modulation of mitochondrial calcium and superoxide generation. *Free Radic Biol Med*, *177*, 189-200. https://doi.org/10.1016/j.freeradbiomed.2021.08.245

Marques, P., Madeira, T., & Gama, A. (2022). Menstrual cycle among adolescents: girls' awareness and influence of age at menarche and overweight. *Rev Paul Pediatr*, *40*, e2020494. https://doi.org/10.1590/1984-0462/2022/40/2020494

Martyn, K. D., Frederick, L. M., von Loehneysen, K., Dinauer, M. C., & Knaus, U. G. (2006). Functional analysis of Nox4 reveals unique characteristics compared to other NADPH oxidases. *Cell Signal*, *18*(1), 69-82. https://doi.org/10.1016/j.cellsig.2005.03.023

Massimiani, M., Lacconi, V., La Civita, F., Ticconi, C., Rago, R., & Campagnolo, L. (2019). Molecular Signaling Regulating Endometrium-Blastocyst Crosstalk. *Int J Mol Sci*, *21*(1). https://doi.org/10.3390/ijms21010023

Maybin, J. A., & Critchley, H. O. (2015). Menstrual physiology: implications for endometrial pathology and beyond. *Hum Reprod Update*, *21*(6), 748-761. https://doi.org/10.1093/humupd/dmv038

Mihm, M., Gangooly, S., & Muttukrishna, S. (2011). The normal menstrual cycle in women. *Anim Reprod Sci*, *124*(3-4), 229-236. https://doi.org/10.1016/j.anireprosci.2010.08.030

Miller, D. W., Ahmad, R., Hague, S., Baptista, M. J., Canet-Aviles, R., McLendon, C., Carter, D. M., Zhu, P. P., Stadler, J., Chandran, J., Klinefelter, G. R., Blackstone, C., & Cookson, M. R. (2003). L166P mutant DJ-1, causative for recessive Parkinson's disease, is degraded through the ubiquitin-proteasome system. *J Biol Chem*, *278*(38), 36588-36595. https://doi.org/10.1074/jbc.M304272200

Morelli, M., Scumaci, D., Di Cello, A., Venturella, R., Donato, G., Faniello, M. C., Quaresima, B., Cuda, G., Zullo, F., & Costanzo, F. (2014). DJ-1 in endometrial cancer: a possible biomarker to improve differential diagnosis between subtypes. *Int J Gynecol Cancer*, *24*(4), 649-658. https://doi.org/10.1097/IGC.0000000000000102

Munne, S., Bahce, M., Sandalinas, M., Escudero, T., Marquez, C., Velilla, E., Colls, P., Oter, M., Alikani, M., & Cohen, J. (2004). Differences in chromosome susceptibility to aneuploidy and survival to first trimester. *Reprod Biomed Online*, *8*(1), 81-90. https://doi.org/10.1016/s1472-6483(10)60501-9

Munro, M. G., Critchley, H. O. D., Fraser, I. S., & Committee, F. M. D. (2018). The two FIGO systems for normal and abnormal uterine bleeding symptoms and classification of causes of abnormal uterine bleeding in the reproductive years: 2018 revisions. *Int J Gynaecol Obstet*, *143*(3), 393-408. https://doi.org/10.1002/ijgo.12666

Muter, J., Lynch, V. J., McCoy, R. C., & Brosens, J. J. (2023). Human embryo implantation. *Development*, *150*(10). https://doi.org/10.1242/dev.201507

Nagakubo, D., Taira, T., Kitaura, H., Ikeda, M., Tamai, K., Iguchi-Ariga, S. M., & Ariga, H. (1997). DJ-1, a novel oncogene which transforms mouse NIH3T3 cells in cooperation with ras. *Biochem Biophys Res Commun*, *231*(2), 509-513. https://doi.org/10.1006/bbrc.1997.6132

Nataj Majd, M., Moini, A., Samimi Sadeh, S., & Bastanhagh, E. (2022). The effect of Nifedipine on embryo transfer outcomes: A randomized clinical trial. *Int J Reprod Biomed*, *20*(12), 1013-1018. https://doi.org/10.18502/ijrm.v20i12.12562

Neves, M., Graos, M., Anjo, S. I., & Manadas, B. (2022). Modulation of signaling pathways by DJ-1: An updated overview. *Redox Biol*, *51*, 102283. https://doi.org/10.1016/j.redox.2022.102283

Ng, K. K. L., Rozen, G., Stewart, T., Agresta, F., & Polyakov, A. (2019). Does nifedipine improve outcomes of embryo transfer?: Interim analysis of a randomized, double blinded, placebo-controlled trial. *Medicine (Baltimore)*, *98*(4), e14251. https://doi.org/10.1097/MD.0000000000014251

Ng, N. S., & Ooi, L. (2021). A Simple Microplate Assay for Reactive Oxygen Species Generation and Rapid Cellular Protein Normalization. *Bio Protoc*, *11*(1), e3877. https://doi.org/10.21769/BioProtoc.3877

Nguyen, M. T., & Lee, W. (2022). MiR-320-3p Regulates the Proliferation and Differentiation of Myogenic Progenitor Cells by Modulating Actin Remodeling. *Int J Mol Sci*, *23*(2). https://doi.org/10.3390/ijms23020801

Nicholson, L., Lindsay, L., & Murphy, C. R. (2018). Change in distribution of cytoskeleton-associated proteins, lasp-1 and palladin, during uterine receptivity in the rat endometrium. *Reprod Fertil Dev*, *30*(11), 1482-1490. https://doi.org/10.1071/RD17530

Nikas, G., & Aghajanova, L. (2002). Endometrial pinopodes: some more understanding on human implantation? *Reprod Biomed Online*, *4 Suppl 3*, 18-23. https://doi.org/10.1016/s1472-6483(12)60111-4

Nirgude, S., & Choudhary, B. (2021). Insights into the role of GPX3, a highly efficient plasma antioxidant, in cancer. *Biochem Pharmacol*, *184*, 114365. https://doi.org/10.1016/j.bcp.2020.114365

Nitti, M., Marengo, B., Furfaro, A. L., Pronzato, M. A., Marinari, U. M., Domenicotti, C., & Traverso, N. (2022). Hormesis and Oxidative Distress: Pathophysiology of Reactive Oxygen Species and the Open Question of Antioxidant Modulation and Supplementation. *Antioxidants (Basel)*, *11*(8). https://doi.org/10.3390/antiox11081613

Ochoa-Bernal, M. A., & Fazleabas, A. T. (2020). Physiologic Events of Embryo Implantation and Decidualization in Human and Non-Human Primates. *Int J Mol Sci*, *21*(6). https://doi.org/10.3390/ijms21061973

Ogasawara, M., Aoki, K., Okada, S., & Suzumori, K. (2000). Embryonic karyotype of abortuses in relation to the number of previous miscarriages. *Fertil Steril*, *73*(2), 300-304. https://doi.org/10.1016/s0015-0282(99)00495-1

Okada, H., Tsuzuki, T., & Murata, H. (2018). Decidualization of the human endometrium. *Reprod Med Biol*, *17*(3), 220-227. https://doi.org/10.1002/rmb2.12088

Okumura, T., Raja Xavier, J. P., Pasternak, J., Yang, Z., Hang, C., Nosirov, B., Singh, Y., Admard, J., Brucker, S. Y., Kommoss, S., Takeda, S., Staebler, A., Lang, F., & Salker, M. S. (2024). Rel Family Transcription Factor NFAT5 Upregulates COX2 via HIF-1alpha Activity in Ishikawa and HEC1a Cells. *Int J Mol Sci*, *25*(7). https://doi.org/10.3390/ijms25073666

Olivennes, F., Cunha-Filho, J. S., Fanchin, R., Bouchard, P., & Frydman, R. (2002). The use of GnRH antagonists in ovarian stimulation. *Hum Reprod Update*, *8*(3), 279-290. https://doi.org/10.1093/humupd/8.3.279

Otey, C. A., Dixon, R., Stack, C., & Goicoechea, S. M. (2009). Cytoplasmic Ig-domain proteins: cytoskeletal regulators with a role in human disease. *Cell Motil Cytoskeleton*, *66*(8), 618-634. https://doi.org/10.1002/cm.20385

Ould Amer, Y., & Hebert-Chatelain, E. (2018). Mitochondrial cAMP-PKA signaling: What do we really know? *Biochim Biophys Acta Bioenerg*, *1859*(9), 868-877. https://doi.org/10.1016/j.bbabio.2018.04.005

Palma, F. R., Gantner, B. N., Sakiyama, M. J., Kayzuka, C., Shukla, S., Lacchini, R., Cunniff, B., & Bonini, M. G. (2024). ROS production by mitochondria: function or dysfunction? *Oncogene*, *43*(5), 295-303. https://doi.org/10.1038/s41388-023-02907-z

Pan-Castillo, B., Gazze, S. A., Thomas, S., Lucas, C., Margarit, L., Gonzalez, D., Francis, L. W., & Conlan, R. S. (2018). Morphophysical dynamics of human endometrial cells during

decidualization. *Nanomedicine*, *14*(7), 2235-2245. https://doi.org/10.1016/j.nano.2018.07.004

Pantcheva, P., Elias, M., Duncan, K., Borlongan, C. V., Tajiri, N., & Kaneko, Y. (2014). The role of DJ-1 in the oxidative stress cell death cascade after stroke. *Neural Regen Res*, *9*(15), 1430-1433. https://doi.org/10.4103/1673-5374.139458

Pecchillo Cimmino, T., Ammendola, R., Cattaneo, F., & Esposito, G. (2023). NOX Dependent ROS Generation and Cell Metabolism. *Int J Mol Sci*, *24*(3). https://doi.org/10.3390/ijms24032086

Pecci, A., Ogara, M. F., Sanz, R. T., & Vicent, G. P. (2022). Choosing the right partner in hormone-dependent gene regulation: Glucocorticoid and progesterone receptors crosstalk in breast cancer cells. *Front Endocrinol (Lausanne)*, *13*, 1037177. https://doi.org/10.3389/fendo.2022.1037177

Peng, L., Chelariu-Raicu, A., Ye, Y., Ma, Z., Yang, H., Ishikawa-Ankerhold, H., Rahmeh, M., Mahner, S., Jeschke, U., & von Schonfeldt, V. (2021). Prostaglandin E2 Receptor 4 (EP4) Affects Trophoblast Functions via Activating the cAMP-PKA-pCREB Signaling Pathway at the Maternal-Fetal Interface in Unexplained Recurrent Miscarriage. *Int J Mol Sci*, *22*(17). https://doi.org/10.3390/ijms22179134

Perez-Riverol, Y., Bai, J., Bandla, C., Garcia-Seisdedos, D., Hewapathirana, S., Kamatchinathan, S., Kundu, D. J., Prakash, A., Frericks-Zipper, A., Eisenacher, M., Walzer, M., Wang, S., Brazma, A., & Vizcaino, J. A. (2022). The PRIDE database resources in 2022: a hub for mass spectrometry-based proteomics evidences. *Nucleic Acids Res*, *50*(D1), D543-D552. https://doi.org/10.1093/nar/gkab1038

Perona, R. M., & Wassarman, P. M. (1986). Mouse blastocysts hatch in vitro by using a trypsin-like proteinase associated with cells of mural trophectoderm. *Dev Biol*, *114*(1), 42-52. https://doi.org/10.1016/0012-1606(86)90382-9

Pluchino, N., Drakopoulos, P., Wenger, J. M., Petignat, P., Streuli, I., & Genazzani, A. R. (2014). Hormonal causes of recurrent pregnancy loss (RPL). *Hormones (Athens)*, *13*(3), 314-322. https://doi.org/10.14310/horm.2002.1505

Quenby, S., Gallos, I. D., Dhillon-Smith, R. K., Podesek, M., Stephenson, M. D., Fisher, J., Brosens, J. J., Brewin, J., Ramhorst, R., Lucas, E. S., McCoy, R. C., Anderson, R., Daher, S., Regan, L., Al-Memar, M., Bourne, T., MacIntyre, D. A., Rai, R., Christiansen, O. B., . . . Coomarasamy, A. (2021). Miscarriage matters: the epidemiological, physical, psychological, and economic costs of early pregnancy loss. *Lancet*, *397*(10285), 1658-1667. https://doi.org/10.1016/S0140-6736(21)00682-6

Quenby, S., Vince, G., Farquharson, R., & Aplin, J. (2002). Recurrent miscarriage: a defect in nature's quality control? *Hum Reprod*, *17*(8), 1959-1963. https://doi.org/10.1093/humrep/17.8.1959

Quesnel, A., Martin, L. D., Tarzi, C., Lenis, V. P., Coles, N., Islam, M., Angione, C., Outeiro, T. F., Khundakar, A. A., & Filippou, P. S. (2024). Uncovering potential diagnostic and pathophysiological roles of alpha-synuclein and DJ-1 in melanoma. *Cancer Med*, *13*(1), e6900. https://doi.org/10.1002/cam4.6900

Rai, P., & Shivaji, S. (2011). The role of DJ-1 in the pathogenesis of endometriosis. *PLoS One*, *6*(3), e18074. https://doi.org/10.1371/journal.pone.0018074

Ramathal, C. Y., Bagchi, I. C., Taylor, R. N., & Bagchi, M. K. (2010). Endometrial decidualization: of mice and men. *Semin Reprod Med*, *28*(1), 17-26. https://doi.org/10.1055/s-0029-1242989

Ruan, Y. C., Guo, J. H., Liu, X., Zhang, R., Tsang, L. L., Dong, J. D., Chen, H., Yu, M. K., Jiang, X., Zhang, X. H., Fok, K. L., Chung, Y. W., Huang, H., Zhou, W. L., & Chan, H. C. (2012). Activation of the epithelial Na+ channel triggers prostaglandin E(2) release and

production required for embryo implantation. *Nat Med*, *18*(7), 1112-1117. https://doi.org/10.1038/nm.2771

Ruane, P. T., Paterson, I., Reeves, B., Adlam, D., Berneau, S. C., Renshall, L., Brosens, J. J., Kimber, S. J., Brison, D. R., Aplin, J. D., & Westwood, M. (2024). Glucose influences endometrial receptivity to embryo implantation through O-GlcNAcylation-mediated regulation of the cytoskeleton. *Am J Physiol Cell Physiol*, *327*(3), C634-C645. https://doi.org/10.1152/ajpcell.00559.2023

Ruder, E. H., Hartman, T. J., Blumberg, J., & Goldman, M. B. (2008). Oxidative stress and antioxidants: exposure and impact on female fertility. *Hum Reprod Update*, *14*(4), 345-357. https://doi.org/10.1093/humupd/dmn011

S M Cook, T. E. S., K M Chynoweth, M Wigton, R W Simmonds, K M Lang. (2006). Practical implementation of dynamic methods for measuring atomic force microscope cantilever spring constants. *Nanotechnology*, *17*, 2135-2145.

Salamonsen, L. A., & Nie, G. (2002). Proteases at the endometrial-trophoblast interface: their role in implantation. *Rev Endocr Metab Disord*, *3*(2), 133-143. https://doi.org/10.1023/a:1015407012559

Salker, M., Teklenburg, G., Molokhia, M., Lavery, S., Trew, G., Aojanepong, T., Mardon, H. J., Lokugamage, A. U., Rai, R., Landles, C., Roelen, B. A., Quenby, S., Kuijk, E. W., Kavelaars, A., Heijnen, C. J., Regan, L., Macklon, N. S., & Brosens, J. J. (2010). Natural selection of human embryos: impaired decidualization of endometrium disables embryo-maternal interactions and causes recurrent pregnancy loss. *PLoS One*, *5*(4), e10287. https://doi.org/10.1371/journal.pone.0010287

Salker, M. S., Christian, M., Steel, J. H., Nautiyal, J., Lavery, S., Trew, G., Webster, Z., Al-Sabbagh, M., Puchchakayala, G., Foller, M., Landles, C., Sharkey, A. M., Quenby, S., Aplin, J. D., Regan, L., Lang, F., & Brosens, J. J. (2011). Deregulation of the serum- and glucocorticoid-inducible kinase SGK1 in the endometrium causes reproductive failure. *Nat Med*, *17*(11), 1509-1513. https://doi.org/10.1038/nm.2498

Salker, M. S., Hosseinzadeh, Z., Alowayed, N., Zeng, N., Umbach, A. T., Webster, Z., Singh, Y., Brosens, J. J., & Lang, F. (2016). LEFTYA Activates the Epithelial Na+ Channel (ENaC) in Endometrial Cells via Serum and Glucocorticoid Inducible Kinase SGK1. *Cell Physiol Biochem*, *39*(4), 1295-1306. https://doi.org/10.1159/000447834

Salker, M. S., Nautiyal, J., Steel, J. H., Webster, Z., Sucurovic, S., Nicou, M., Singh, Y., Lucas, E. S., Murakami, K., Chan, Y. W., James, S., Abdallah, Y., Christian, M., Croy, B. A., Mulac-Jericevic, B., Quenby, S., & Brosens, J. J. (2012). Disordered IL-33/ST2 activation in decidualizing stromal cells prolongs uterine receptivity in women with recurrent pregnancy loss. *PLoS One*, *7*(12), e52252. https://doi.org/10.1371/journal.pone.0052252

Salker, M. S., Schierbaum, N., Alowayed, N., Singh, Y., Mack, A. F., Stournaras, C., Schaffer, T. E., & Lang, F. (2016). LeftyA decreases Actin Polymerization and Stiffness in Human Endometrial Cancer Cells. *Sci Rep*, *6*, 29370. https://doi.org/10.1038/srep29370

Salker, M. S., Singh, Y., Durairaj, R. R. P., Yan, J., Alauddin, M., Zeng, N., Steel, J. H., Zhang, S., Nautiyal, J., Webster, Z., Brucker, S. Y., Wallwiener, D., Anne Croy, B., Brosens, J. J., & Lang, F. (2018). LEFTY2 inhibits endometrial receptivity by downregulating Orai1 expression and store-operated Ca(2+) entry. *J Mol Med (Berl)*, *96*(2), 173-182. https://doi.org/10.1007/s00109-017-1610-9

Salker, M. S., Zhou, Y., Singh, Y., Brosens, J., & Lang, F. (2015). LeftyA sensitive cytosolic pH regulation and glycolytic flux in Ishikawa human endometrial cancer cells. *Biochem Biophys Res Commun*, *460*(3), 845-849. https://doi.org/10.1016/j.bbrc.2015.03.120

Schindelin, J., Arganda-Carreras, I., Frise, E., Kaynig, V., Longair, M., Pietzsch, T., Preibisch, S., Rueden, C., Saalfeld, S., Schmid, B., Tinevez, J. Y., White, D. J., Hartenstein, V., Eliceiri,

K., Tomancak, P., & Cardona, A. (2012). Fiji: an open-source platform for biological-image analysis. *Nat Methods*, *9*(7), 676-682. https://doi.org/10.1038/nmeth.2019

Schumann, C., Taratula, O., Khalimonchuk, O., Palmer, A. L., Cronk, L. M., Jones, C. V., Escalante, C. A., & Taratula, O. (2015). ROS-induced nanotherapeutic approach for ovarian cancer treatment based on the combinatorial effect of photodynamic therapy and DJ-1 gene suppression. *Nanomedicine*, *11*(8), 1961-1970. https://doi.org/10.1016/j.nano.2015.07.005

Scumaci, D., Olivo, E., Fiumara, C. V., La Chimia, M., De Angelis, M. T., Mauro, S., Costa, G., Ambrosio, F. A., Alcaro, S., Agosti, V., Costanzo, F. S., & Cuda, G. (2020). DJ-1 Proteoforms in Breast Cancer Cells: The Escape of Metabolic Epigenetic Misregulation. *Cells*, *9*(9). https://doi.org/10.3390/cells9091968

Shahin, S., Singh, V. P., Shukla, R. K., Dhawan, A., Gangwar, R. K., Singh, S. P., & Chaturvedi, C. M. (2013). 2.45 GHz microwave irradiation-induced oxidative stress affects implantation or pregnancy in mice, Mus musculus. *Appl Biochem Biotechnol*, *169*(5), 1727-1751. https://doi.org/10.1007/s12010-012-0079-9

Shannon, N., Gravelle, R., & Cunniff, B. (2022). Mitochondrial trafficking and redox/phosphorylation signaling supporting cell migration phenotypes. *Front Mol Biosci*, *9*, 925755. https://doi.org/10.3389/fmolb.2022.925755

Shi, S., Carattino, M. D., Hughey, R. P., & Kleyman, T. R. (2013). ENaC regulation by proteases and shear stress. *Curr Mol Pharmacol*, *6*(1), 28-34. https://doi.org/10.2174/18744672112059990027

Shmygol, A., & Brosens, J. J. (2021). Proteinase Activated Receptors Mediate the Trypsin-Induced Ca(2 +) Signaling in Human Uterine Epithelial Cells. *Front Cell Dev Biol*, *9*, 709902. https://doi.org/10.3389/fcell.2021.709902

Shu, K., Xiao, Z., Long, S., Yan, J., Yu, X., Zhu, Q., & Mei, T. (2013). Expression of DJ-1 in endometrial cancer: close correlation with clinicopathological features and apoptosis. *Int J Gynecol Cancer*, *23*(6), 1029-1035. https://doi.org/10.1097/IGC.0b013e3182959182

Singh, Y., Chen, H., Zhou, Y., Foller, M., Mak, T. W., Salker, M. S., & Lang, F. (2015). Differential effect of DJ-1/PARK7 on development of natural and induced regulatory T cells. *Sci Rep*, *5*, 17723. https://doi.org/10.1038/srep17723

Smith, N., & Wilson, M. A. (2017). Structural Biology of the DJ-1 Superfamily. *Adv Exp Med Biol*, *1037*, 5-24. https://doi.org/10.1007/978-981-10-6583-5_2

Soares, S. R., Troncoso, C., Bosch, E., Serra, V., Simon, C., Remohi, J., & Pellicer, A. (2005). Age and uterine receptiveness: predicting the outcome of oocyte donation cycles. *J Clin Endocrinol Metab*, *90*(7), 4399-4404. https://doi.org/10.1210/jc.2004-2252

Stevens Brentjens, L., Habets, D., Den Hartog, J., Al-Nasiry, S., Wieten, L., Morre, S., Van Montfoort, A., Romano, A., & van Golde, R. (2022). Endometrial factors in the implantation failure spectrum: protocol of a MUltidisciplinary observational cohort study in women with Repeated Implantation failure and recurrent Miscarriage (MURIM Study). *BMJ Open*, *12*(6), e056714. https://doi.org/10.1136/bmjopen-2021-056714

Sucurovic, S., Nikolic, T., Brosens, J. J., & Mulac-Jericevic, B. (2017). Spatial and Temporal Analyses of FGF9 Expression During Early Pregnancy. *Cell Physiol Biochem*, *42*(6), 2318-2329. https://doi.org/10.1159/000480004

Sucurovic, S., Nikolic, T., Brosens, J. J., & Mulac-Jericevic, B. (2020). Analysis of heart and neural crest derivatives-expressed protein 2 (HAND2)-progesterone interactions in peri-implantation endometriumdagger. *Biol Reprod*, *102*(5), 1111-1121. https://doi.org/10.1093/biolre/ioaa013

Sugawara, J., Tazuke, S. I., Suen, L. F., Powell, D. R., Kaper, F., Giaccia, A. J., & Giudice, L. C. (2000). Regulation of insulin-like growth factor-binding protein 1 by hypoxia and 3',5'-

cyclic adenosine monophosphate is additive in HepG2 cells. *J Clin Endocrinol Metab*, *85*(10), 3821-3827. https://doi.org/10.1210/jcem.85.10.6866

Sun, Y., Sun, X., Zhao, L., Zhang, Z., Wang, Y., Dai, Z., Zhao, X., & Pu, X. (2020). DJ-1 deficiency causes metabolic abnormality in ornidazole-induced asthenozoospermia. *Reproduction*, *160*(6), 931-941. https://doi.org/10.1530/REP-20-0097

Sun, Z. G., Shi, H. J., Gu, Z., Wang, J., & Shen, Q. X. (2007). A single intrauterine injection of the serine protease inhibitor 4-(2-aminoethyl)benzenesulfonyl fluoride hydrochloride reversibly inhibits embryo implantation in mice. *Contraception*, *76*(3), 250-255. https://doi.org/10.1016/j.contraception.2007.05.084

Szabo, R., Wu, Q., Dickson, R. B., Netzel-Arnett, S., Antalis, T. M., & Bugge, T. H. (2003). Type II transmembrane serine proteases. *Thromb Haemost*, *90*(2), 185-193. https://doi.org/10.1160/TH03-02-0071

Tabibzadeh, S. (2011). Isolation, characterization, and function of EBAF/LEFTY B: role in infertility. *Ann N Y Acad Sci*, *1221*, 98-102. https://doi.org/10.1111/j.1749-6632.2010.05944.x

Tabibzadeh, S., & Hemmati-Brivanlou, A. (2006). Lefty at the crossroads of "stemness" and differentiative events. *Stem Cells*, *24*(9), 1998-2006. https://doi.org/10.1634/stemcells.2006-0075

Tang, M., Mazella, J., Zhu, H. H., & Tseng, L. (2005). Ligand activated relaxin receptor increases the transcription of IGFBP-1 and prolactin in human decidual and endometrial stromal cells. *Mol Hum Reprod*, *11*(4), 237-243. https://doi.org/10.1093/molehr/gah149

Tang, M., Naidu, D., Hearing, P., Handwerger, S., & Tabibzadeh, S. (2010). LEFTY, a member of the transforming growth factor-beta superfamily, inhibits uterine stromal cell differentiation: a novel autocrine role. *Endocrinology*, *151*(3), 1320-1330. https://doi.org/10.1210/en.2009-1081

Tang, M., Taylor, H. S., & Tabibzadeh, S. (2005). In vivo gene transfer of lefty leads to implantation failure in mice. *Hum Reprod*, *20*(7), 1772-1778. https://doi.org/10.1093/humrep/deh849

Tao, X., & Tong, L. (2003). Crystal structure of human DJ-1, a protein associated with early onset Parkinson's disease. *J Biol Chem*, *278*(33), 31372-31379. https://doi.org/10.1074/jbc.M304221200

Teklenburg, G., Salker, M., Heijnen, C., Macklon, N. S., & Brosens, J. J. (2010). The molecular basis of recurrent pregnancy loss: impaired natural embryo selection. *Mol Hum Reprod*, *16*(12), 886-895. https://doi.org/10.1093/molehr/gaq079

Toner, J. P., Grainger, D. A., & Frazier, L. M. (2002). Clinical outcomes among recipients of donated eggs: an analysis of the U.S. national experience, 1996-1998. *Fertil Steril*, *78*(5), 1038-1045. https://doi.org/10.1016/s0015-0282(02)03371-x

Trempe, J. F., & Fon, E. A. (2013). Structure and Function of Parkin, PINK1, and DJ-1, the Three Musketeers of Neuroprotection. *Front Neurol*, *4*, 38. https://doi.org/10.3389/fneur.2013.00038

Turesheva, A., Aimagambetova, G., Ukybassova, T., Marat, A., Kanabekova, P., Kaldygulova, L., Amanzholkyzy, A., Ryzhkova, S., Nogay, A., Khamidullina, Z., Ilmaliyeva, A., Almawi, W. Y., & Atageldiyeva, K. (2023). Recurrent Pregnancy Loss Etiology, Risk Factors, Diagnosis, and Management. Fresh Look into a Full Box. *J Clin Med*, *12*(12). https://doi.org/10.3390/jcm12124074

Tyanova, S., Temu, T., Sinitcyn, P., Carlson, A., Hein, M. Y., Geiger, T., Mann, M., & Cox, J. (2016). The Perseus computational platform for comprehensive analysis of (prote)omics data. *Nat Methods*, *13*(9), 731-740. https://doi.org/10.1038/nmeth.3901

Uhlen, M., Bjorling, E., Agaton, C., Szigyarto, C. A., Amini, B., Andersen, E., Andersson, A. C., Angelidou, P., Asplund, A., Asplund, C., Berglund, L., Bergstrom, K., Brumer, H., Cerjan,

D., Ekstrom, M., Elobeid, A., Eriksson, C., Fagerberg, L., Falk, R., . . . Ponten, F. (2005). A human protein atlas for normal and cancer tissues based on antibody proteomics. *Mol Cell Proteomics*, *4*(12), 1920-1932. https://doi.org/10.1074/mcp.M500279-MCP200

Ulloa, L., & Tabibzadeh, S. (2001). Lefty inhibits receptor-regulated Smad phosphorylation induced by the activated transforming growth factor-beta receptor. *J Biol Chem*, *276*(24), 21397-21404. https://doi.org/10.1074/jbc.M010783200

Vander Borght, M., & Wyns, C. (2018). Fertility and infertility: Definition and epidemiology. *Clin Biochem*, *62*, 2-10. https://doi.org/10.1016/j.clinbiochem.2018.03.012

Vento-Tormo, R., Efremova, M., Botting, R. A., Turco, M. Y., Vento-Tormo, M., Meyer, K. B., Park, J. E., Stephenson, E., Polanski, K., Goncalves, A., Gardner, L., Holmqvist, S., Henriksson, J., Zou, A., Sharkey, A. M., Millar, B., Innes, B., Wood, L., Wilbrey-Clark, A., . . . Teichmann, S. A. (2018). Single-cell reconstruction of the early maternal-fetal interface in humans. *Nature*, *563*(7731), 347-353. https://doi.org/10.1038/s41586-018-0698-6

Wang, H. V., & Moser, M. (2008). Comparative expression analysis of the murine palladin isoforms. *Dev Dyn*, *237*(11), 3342-3351. https://doi.org/10.1002/dvdy.21755

Wang, J., Zhan, H., Wang, Y., Zhao, L., Huang, Y., & Wu, R. (2024). Current advances in understanding endometrial epithelial cell biology and therapeutic applications for intrauterine adhesion. *Stem Cell Res Ther*, *15*(1), 379. https://doi.org/10.1186/s13287-024-03989-6

Wang, W., Zhao, H., & Chen, B. (2020). DJ-1 protects retinal pericytes against high glucose-induced oxidative stress through the Nrf2 signaling pathway. *Sci Rep*, *10*(1), 2477. https://doi.org/10.1038/s41598-020-59408-2

Wang, X., Sun, Y., Shi, H., & Xin, A. (2024). Establishment of an Embryo Implantation Model In Vitro. *J Vis Exp*(208). https://doi.org/10.3791/66873

Weimar, C. H., Kavelaars, A., Brosens, J. J., Gellersen, B., de Vreeden-Elbertse, J. M., Heijnen, C. J., & Macklon, N. S. (2012). Endometrial stromal cells of women with recurrent miscarriage fail to discriminate between high- and low-quality human embryos. *PLoS One*, *7*(7), e41424. https://doi.org/10.1371/journal.pone.0041424

Whirledge, S. D., Oakley, R. H., Myers, P. H., Lydon, J. P., DeMayo, F., & Cidlowski, J. A. (2015). Uterine glucocorticoid receptors are critical for fertility in mice through control of embryo implantation and decidualization. *Proc Natl Acad Sci U S A*, *112*(49), 15166-15171. https://doi.org/10.1073/pnas.1508056112

Whitby, S., Zhou, W., & Dimitriadis, E. (2020). Alterations in Epithelial Cell Polarity During Endometrial Receptivity: A Systematic Review. *Front Endocrinol (Lausanne)*, *11*, 596324. https://doi.org/10.3389/fendo.2020.596324

Whitcomb, D. C., Gorry, M. C., Preston, R. A., Furey, W., Sossenheimer, M. J., Ulrich, C. D., Martin, S. P., Gates, L. K., Jr., Amann, S. T., Toskes, P. P., Liddle, R., McGrath, K., Uomo, G., Post, J. C., & Ehrlich, G. D. (1996). Hereditary pancreatitis is caused by a mutation in the cationic trypsinogen gene. *Nat Genet*, *14*(2), 141-145. https://doi.org/10.1038/ng1096-141

Wilson, M. A. (2011). The role of cysteine oxidation in DJ-1 function and dysfunction. *Antioxid Redox Signal*, *15*(1), 111-122. https://doi.org/10.1089/ars.2010.3481

Wilson, M. A., Collins, J. L., Hod, Y., Ringe, D., & Petsko, G. A. (2003). The 1.1-A resolution crystal structure of DJ-1, the protein mutated in autosomal recessive early onset Parkinson's disease. *Proc Natl Acad Sci U S A*, *100*(16), 9256-9261. https://doi.org/10.1073/pnas.1133288100

Wu, G., Li, C., Tao, J., Liu, Z., Li, X., Zang, Z., Fu, C., Wei, J., Yang, Y., Zhu, Q., Zhang, J. Q., Shen, M., & Liu, H. (2022). FSH mediates estradiol synthesis in hypoxic granulosa cells by activating glycolytic metabolism through the HIF-1alpha-AMPK-GLUT1 signaling pathway. *J Biol Chem*, *298*(5), 101830. https://doi.org/10.1016/j.jbc.2022.101830

Xiang, Y., Fu, L., Xiang, H. X., Zheng, L., Tan, Z. X., Wang, L. X., Cao, W., Xu, D. X., & Zhao, H. (2021). Correlations among Pulmonary DJ-1, VDR and Nrf-2 in patients with Chronic Obstructive Pulmonary Disease: A Case-control Study. *Int J Med Sci*, *18*(11), 2449-2456. https://doi.org/10.7150/ijms.58452

Xie, D., Chen, C. C., Ptaszek, L. M., Xiao, S., Cao, X., Fang, F., Ng, H. H., Lewin, H. A., Cowan, C., & Zhong, S. (2010). Rewirable gene regulatory networks in the preimplantation embryonic development of three mammalian species. *Genome Res*, *20*(6), 804-815. https://doi.org/10.1101/gr.100594.109

Xu, X., Leng, J. Y., Gao, F., Zhao, Z. A., Deng, W. B., Liang, X. H., Zhang, Y. J., Zhang, Z. R., Li, M., Sha, A. G., & Yang, Z. M. (2014). Differential expression and anti-oxidant function of glutathione peroxidase 3 in mouse uterus during decidualization. *FEBS Lett*, *588*(9), 1580-1589. https://doi.org/10.1016/j.febslet.2014.02.043

Yang, T., Yan, J., Han, Q., Zhang, Q., & Liao, Q. (2020). Expression and significance of Parkinson disease protein 7 in placental, serum and umbilical cord blood in preeclampsia. *Ginekol Pol*, *91*(12), 764-768. https://doi.org/10.5603/GP.a2020.0131

Yang, W., Nurbaeva, M. K., Schmid, E., Russo, A., Almilaji, A., Szteyn, K., Yan, J., Faggio, C., Shumilina, E., & Lang, F. (2014). Akt2- and ETS1-dependent IP3 receptor 2 expression in dendritic cell migration. *Cell Physiol Biochem*, *33*(1), 222-236. https://doi.org/10.1159/000356664

Ye, J., Coulouris, G., Zaretskaya, I., Cutcutache, I., Rozen, S., & Madden, T. L. (2012). Primer-BLAST: a tool to design target-specific primers for polymerase chain reaction. *BMC Bioinformatics*, *13*, 134. https://doi.org/10.1186/1471-2105-13-134

Yin, X., Pavone, M. E., Lu, Z., Wei, J., & Kim, J. J. (2012). Increased activation of the PI3K/AKT pathway compromises decidualization of stromal cells from endometriosis. *J Clin Endocrinol Metab*, *97*(1), E35-43. https://doi.org/10.1210/jc.2011-1527

Yu, H. F., Duan, C. C., Yang, Z. Q., Wang, Y. S., Yue, Z. P., & Guo, B. (2019). HB-EGF Ameliorates Oxidative Stress-Mediated Uterine Decidualization Damage. *Oxid Med Cell Longev*, *2019*, 6170936. https://doi.org/10.1155/2019/6170936

Yu, H. F., Yang, Z. Q., Xu, M. Y., Huang, J. C., Yue, Z. P., & Guo, B. (2022). Yap is essential for uterine decidualization through Rrm2/GSH/ROS pathway in response to Bmp2. *Int J Biol Sci*, *18*(6), 2261-2276. https://doi.org/10.7150/ijbs.67756

Yu, N., Kwak-Kim, J., & Bao, S. (2023). Unexplained recurrent pregnancy loss: Novel causes and advanced treatment. *J Reprod Immunol*, *155*, 103785. https://doi.org/10.1016/j.jri.2022.103785

Zhang, C., Guo, Y., Yang, Y., Du, Z., Fan, Y., Zhao, Y., & Yuan, S. (2023). Oxidative stress on vessels at the maternal-fetal interface for female reproductive system disorders: Update. *Front Endocrinol (Lausanne)*, *14*, 1118121. https://doi.org/10.3389/fendo.2023.1118121

Zhang, L., Wang, J., Wang, J., Yang, B., He, Q., & Weng, Q. (2020). Role of DJ-1 in Immune and Inflammatory Diseases. *Front Immunol*, *11*, 994. https://doi.org/10.3389/fimmu.2020.00994

Zhang, Q., & Yan, J. (2016). Update of Wnt signaling in implantation and decidualization. *Reprod Med Biol*, *15*(2), 95-105. https://doi.org/10.1007/s12522-015-0226-4

Zheng, X. L., Kitamoto, Y., & Sadler, J. E. (2009). Enteropeptidase, a type II transmembrane serine protease. *Front Biosci (Elite Ed)*, *1*(1), 242-249. https://doi.org/10.2741/E23

Zhou, J., Qi, C., Fang, X., Wang, Z., Zhang, S., Li, D., & Song, J. (2021). DJ-1 modulates Nrf2-mediated MRP1 expression by activating Wnt3a/beta-catenin signalling in A549 cells exposed to cigarette smoke extract and LPS. *Life Sci*, *276*, 119089. https://doi.org/10.1016/j.lfs.2021.119089

Zhou, T. T., Wang, X. Y., Huang, J., Deng, Y. Z., Qiu, L. J., Liu, H. Y., Xu, X. W., Ma, Z. X., Tang, L., & Chen, H. P. (2020). Mitochondrial Translocation of DJ-1 Is Mediated by Grp75:

Implication in Cardioprotection of Resveratrol Against Hypoxia/Reoxygenation-Induced Oxidative Stress. *J Cardiovasc Pharmacol*, *75*(4), 305-313. https://doi.org/10.1097/FJC.0000000000000805

Zhu, D., Wei, X., Zhou, X. Y., Deng, L. B., Xiong, S. Y., Chen, J. P., Chen, G. Q., Zou, G., & Sun, L. M. (2023). Chromosomal abnormalities in recurrent pregnancy loss and its association with clinical characteristics. *J Assist Reprod Genet*, *40*(7), 1713-1720. https://doi.org/10.1007/s10815-023-02816-w

Zhu, X., Wang, J., Li, L., Deng, L., Wang, J., Liu, L., Zeng, R., Wang, Q., & Zheng, Y. (2018). GPX3 suppresses tumor migration and invasion via the FAK/AKT pathway in esophageal squamous cell carcinoma. *Am J Transl Res*, *10*(6), 1908-1920. https://www.ncbi.nlm.nih.gov/pubmed/30018730

9. Appendix

9.1 Supplementary Figures

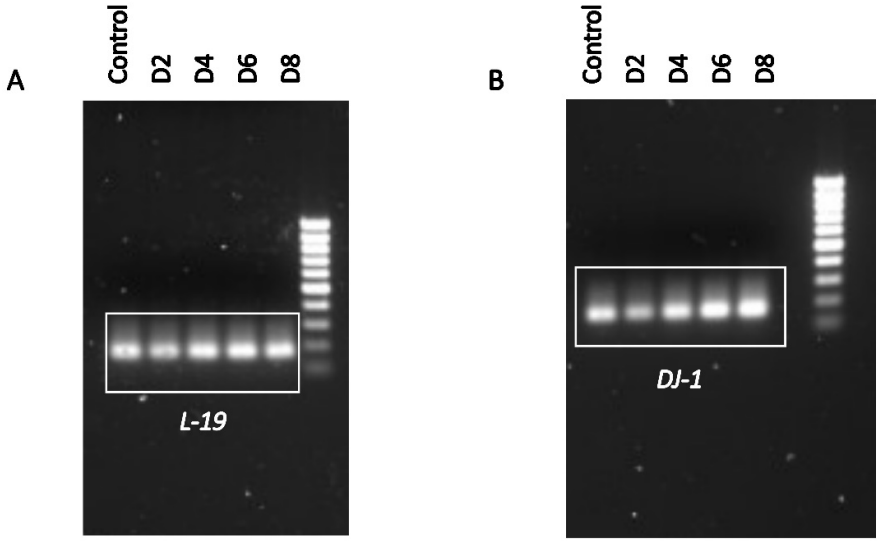

Supplementary Figure 9-1: Full agarose gel electrophoresis for DJ-1 and L-19 in EnSCs.

*Original agarose gel electrophoresis for **Figure 3-2A** showing amplification of qRT-PCR product of **(A)** L-19 and **(B)** DJ-1 of EnSCs treated with 0.5 µM 8-Br-cAMP and 1 µM MPA for 2, 4, 6 or 8 days.*

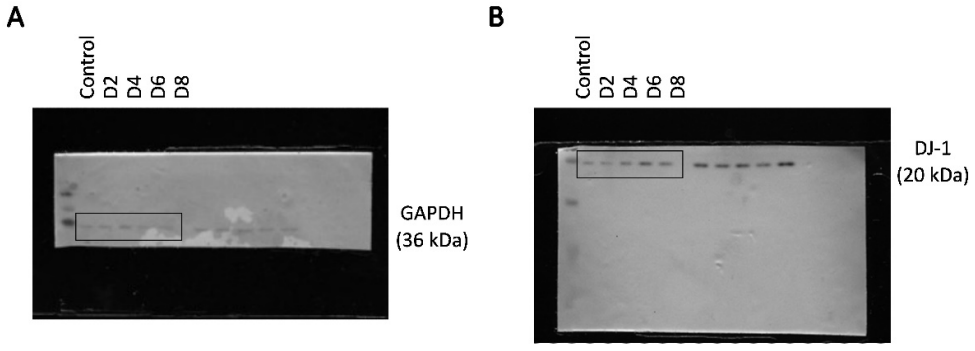

Supplementary Figure 9-2: Full unedited blot for DJ-1 and GAPDH in EnSCs.

*Original western blots for **Figure 3-2B** showing **(A)** anti-GAPDH, 36kDa and **(B)** anti-DJ-1, 20kDa in EnSCs treated with 0.5 µM 8-Br-cAMP and 1 µM MPA for 2, 4, 6 or 8 days.*

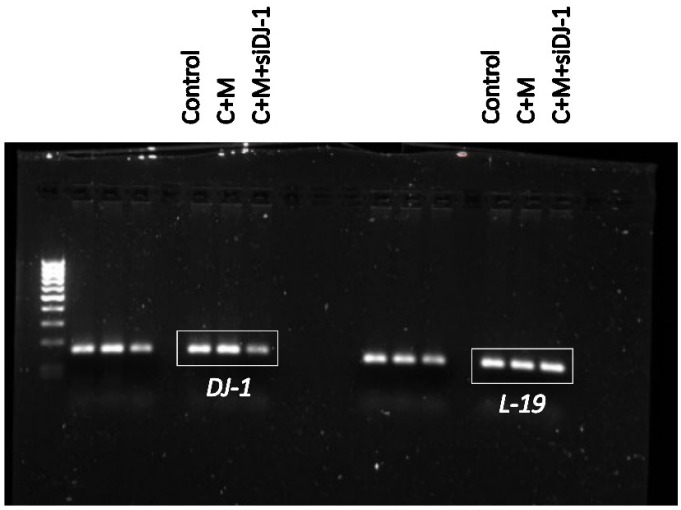

Supplementary Figure 9-3: Full agarose gel electrophoresis for DJ-1 and L-19 in EnSCs with siDJ-1.

*Original agarose gel electrophoresis for **Figure 3-6A** showing amplification of qRT-PCR product of DJ-1 and L-19 of EnSCs transfected by PARK7-targeting siRNA (siDJ-1) for 24 h, which was performed on the third day of a total of 6 day treatment with 0.5 µM 8-Br-cAMP and 1 µM MPA (C+M).*

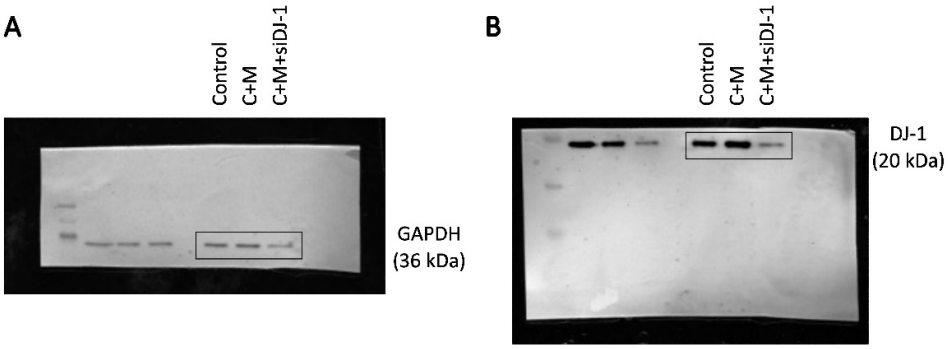

Supplementary Figure 9-4: Full unedited blot for DJ-1 and GAPDH in EnSCs with siDJ-1.

*Original western blots for **Figure 3-6B** showing **(A)** anti-GAPDH, 36kDa and **(B)** anti-DJ-1, 20kDa in EnSCs transfected by PARK7-targeting siRNA (siDJ-1) for 24 h, which was performed on the third day of a total of 6 day treatment with 0.5 µM 8-Br-cAMP and 1 µM MPA (C+M).*

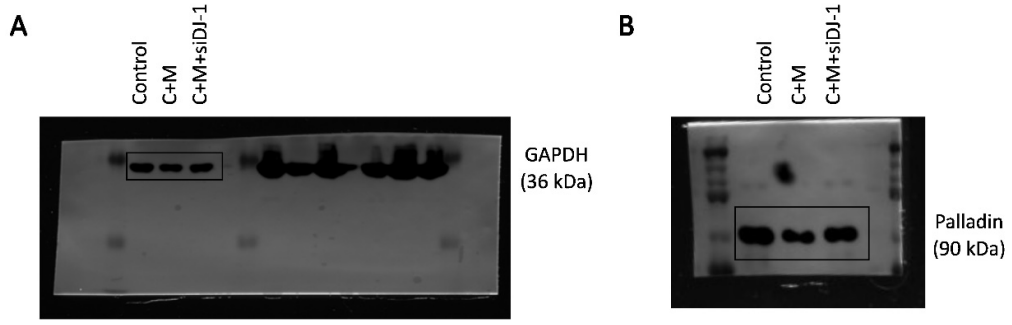

Supplementary Figure 9-5: Full unedited blot for Palladin and GAPDH in EnSCs with siDJ-1.

*Original western blots for **Figure 3-12B** showing **(A)** anti-GAPDH, 36kDa and **(B)** anti-Palladin, 90kDa in EnSCs transfected by PARK7-targeting siRNA (siDJ-1) for 24 h, which was performed on the third day of a total of 6 day treatment with 0.5 µM 8-Br-cAMP and 1 µM MPA (C+M).*

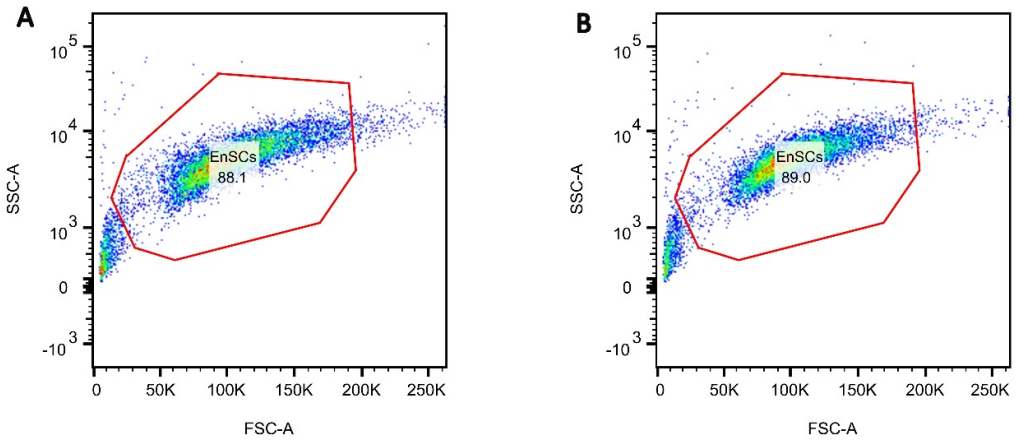

Supplementary Figure 9-6: Gating Strategy of Fluorescence-Activated Cell Sorting Analysis.

*Gating strategy for single cells, illustrated in EnSCs population. Forward (FSC-A) and side scatter (SSC-A) are adjusted to minimize events on the axes, resulting in a single-cell population including > 80 % of total cells (**a** C+M, **b** C+M+siDJ-1). Each dot or point on the plot represents an individual cell that has passed through the laser. Gating strategy has been applied on EnSCs population to exclude debris, dead cells and doublets.*

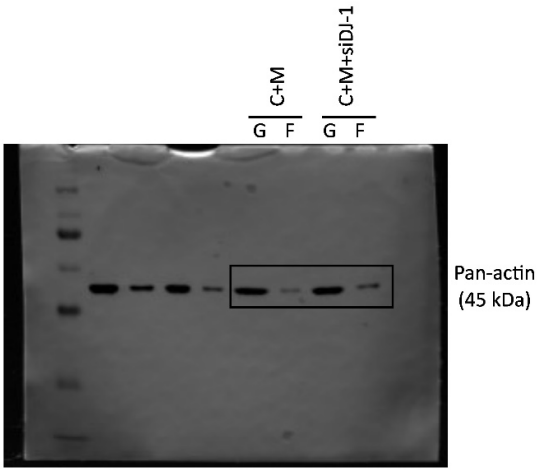

Supplementary Figure 9-7: Full unedited blot for G and F actin in EnSCs with siDJ-1.

*Original western blots for **Figure 3-16B** anti-Pan-actin, 45kDa in EnSCs transfected by PARK7-targeting siRNA (siDJ-1) for 24 h, which was performed on the third day of a total of 6 day treatment with 0.5 µM 8-Br-cAMP and 1 µM MPA (C+M).*

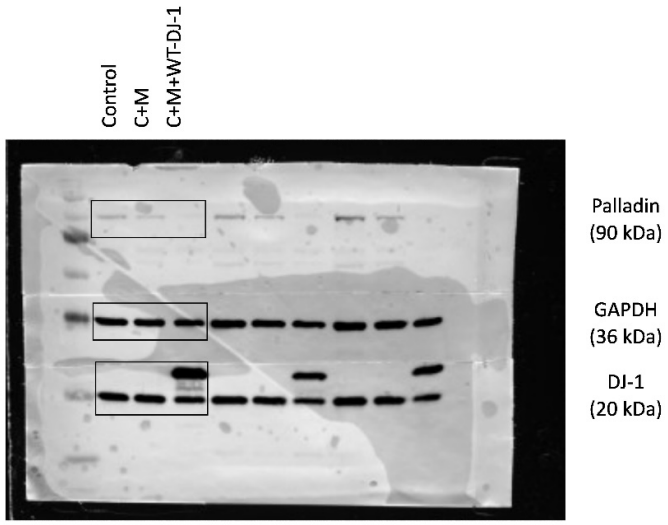

Supplementary Figure 9-8: Full unedited blot for DJ-1, Palladin and GAPDH in EnSCs with wt-DJ-1.

*Original western blots for **Figure 3-18A, C** showing anti-Palladin, 90kDa, anti-DJ-1, 20kDa and anti-GAPDH, 36kDa in EnSCs transfected by pGW1-Myc-DJ-1-wt (wt-DJ-1) for 24 h, which was performed on the third day of a total of 6 day treatment with 0.5 µM 8-Br-cAMP and 1 µM MPA (C+M).*

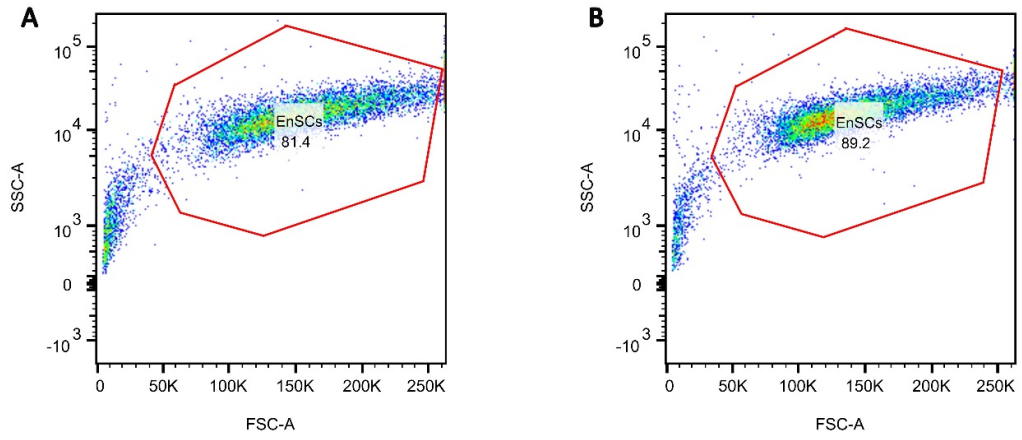

Supplementary Figure 9-9: Gating Strategy of Fluorescence-Activated Cell Sorting Analysis.

*Gating strategy for single cells, illustrated in EnSCs population. Forward (FSC-A) and side scatter (SSC-A) are adjusted to minimize events on the axes, resulting in a single-cell population including > 80 % of total cells (**a** C+M, **b** C+M+wt-DJ-1). Each dot or point on the plot represents an individual cell that has passed through the laser. Gating strategy has been applied on EnSCs population to exclude debris, dead cells and doublets.*

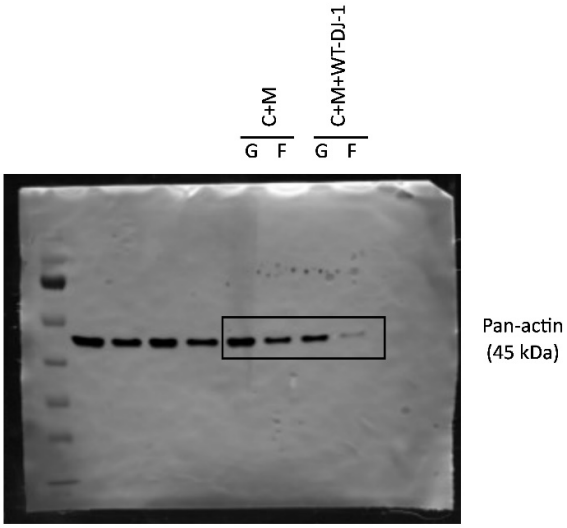

Supplementary Figure 9-10: Full unedited blot for G and F actin in EnSCs with wt-DJ-1.

*Original western blots for **Figure 3-22B** anti-Pan-actin, 45kDa in EnSCs transfected by pGW1-Myc-DJ-1-wt (wt-DJ-1) for 24 h, which was performed on the third day of a total of 6 day treatment with 0.5 µM 8-Br-cAMP and 1 µM MPA (C+M).*

9.2 Supplementary Tables

Supplementary Table 9-1: Patient Demographics and Characteristics RNA-seq

	Age	Live Birth	Number of Losses	BMI	LH+ Day
Controls	36.6 ± 1.36	0	0	24.6 ± 1.42	7.2 ± 0.13
RPL	37.5 ± 0.79	0.3± 0.15	4.9 ± 0.52	25.44 ± 1.02	7.9 ± 0.45

Data shown are arithmetic means ± SEM (n = 10 in each group)

Controls; unexplained = 5; male factor = 2; tubal disease = 1; endometriosis = 1; polycystic ovary syndrome = 1.

RPL: Recurrent Pregnancy Loss; BMI: Body Mass Index; LH+: days after the luteinizing hormone peak

Supplementary Table 9-2: Patient Demographics and Characteristics Used in Western Blots

	Age	Live Birth	Number of Losses	BMI	LH+ Day
Controls	35.2 ± 2.68	0	0	22.4 ± 2.07	9 ± 0.70
RPL	36.4± 3.28	0	4± 1.22	24.5± 3.10	8.2 ± 1.30

Data shown are arithmetic means ± SEM;

Controls (those not experiencing pregnancy losses) = 10 RPL; Recurrent Pregnancy Loss = 9;

BMI; Body Mass Index; LH+; days after the luteinizing hormone peak.

Supplementary Table 9-3: Upregulated Proteins in Decidualized EnSCs with or without DJ-1 Knockdown

Upregulated Gene names	-Log Student's T-test p-value non target KD_DJ-KD	Student's T-test Test statistic non target KD_DJ-KD	Student's T-test Difference/LOG2 FC
SERPINE2	1,405030577	-2,624425777	-0,974631786
MARCKSL1	1,632736062	-3,023394979	-0,939121246
ITGA5	1,469650905	-2,736075538	-0,582092762
PALLD	3,638092062	-7,824326679	-0,563687801
MMP14	1,409666173	-2,632398167	-0,479485989
EHD1	1,44477504	-2,847929735	-0,44367822
ERLIN2	1,654027191	-3,061560981	-0,434356689
AK3	2,932858195	-5,784870736	-0,379790783
ARMT1	2,080983827	-3,866569427	-0,376213074
SLC25A24	1,940897753	-3,593337836	-0,374184132
LMNA	1,939639891	-3,590927842	-0,337780476
PRMT1	1,514045084	-2,81345956	-0,325448036
S100A11	2,170776171	-4,047032195	-0,315128326
CTSL	1,367577724	-2,560210231	-0,305739403
S100A16	1,878897827	-3,475422634	-0,272423267
TP53I3	1,339608953	-2,51247375	-0,263301849
UBE2V1;TMEM189-UBE2V1	1,318409905	-2,476408429	-0,244933128
CSTB	1,948312559	-3,60755938	-0,244910717
LRPPRC	2,377412481	-4,479729994	-0,213801384
GLB1	1,679793428	-3,107968971	-0,202206612
ATP5O	1,535363029	-2,850829666	-0,192224979
SRI	2,78028695	-5,403440138	-0,163616657
PGM3	1,498082541	-2,785568084	-0,156730175
NONO	1,414808902	-2,641249196	-0,155093193
EDF1	1,497027524	-2,783727329	-0,136477947
PRDX1	1,363779573	-2,553717003	-0,135764599
REEP5	1,439470863	-2,683790715	-0,128194332

TUBA1B;TUBA1C;TUBA1A	1,961926547	-3,633738892	-0,11085701

Upregulated proteins (with -Log10 p-value > 1.3) in decidualized EnSCs with or without DJ-1 knockdown, ranked by Student's T-test difference.

Supplementary Table 9-4: Downregulated Proteins in Decidualized EnSCs with or without DJ-1 Knockdown

Downregulated Gene names	-Log Student's T-test p-value non target KD_DJ-KD	Student's T-test Test statistic non target KD_DJ-KD	Student's T-test Difference/LOG2 FC
PSMC4	1,39974303	2,615338824	0,13684845
CLTC	1,933245613	3,578688265	0,15719986
PSMA7	1,389744463	2,598174931	0,175521374
ETF1	1,387494955	2,594316771	0,183530807
PSMA1	2,204200387	4,115335179	0,206454754
PGRMC1	2,064071765	3,833058955	0,209489822
EIF3F	1,631608402	3,021378068	0,209855556
RUVBL2	1,311205642	2,464173979	0,231031418
IMPDH2	1,632125205	3,022302356	0,231866837
ASPH	1,83969325	3,401756624	0,247897148
SSB	1,456198672	2,712739222	0,250386715
RBBP4;RBBP7	1,715421974	3,172549041	0,253197193
EIF3A	1,742347223	3,221678182	0,267253876
PFDN2	1,638894545	3,034417884	0,276625633
SNX1	2,268062317	4,247608636	0,284954548
LRRC59	1,856256927	3,432797341	0,288261414
SRP9;DKFZp564M2223	1,453693262	2,708398548	0,289227486
CSE1L	2,035454236	3,77668996	0,290929317
SCAMP3	1,560868716	2,895728193	0,298167229
ACBD3	1,41803388	2,646803124	0,298781872
ABCE1	1,828869561	3,381537222	0,313004971
PSMB6	1,529635513	2,840775588	0,314351559
TMEM43	3,817922342	8,429175615	0,319987297
RPS25	4,362612889	10,51828013	0,320022106
PSMA4	1,473491546	2,742747502	0,324090004
VCP	3,365279878	6,976610677	0,337694645
KIF5B	1,367411614	2,559926182	0,340960979
MARS	1,728573469	3,196510423	0,344823837

KPNA4	1,64496608	3,605441429	0,34834671
ATP2A2	2,200577992	4,10790242	0,355434418
EIF4H	1,65444008	3,062302727	0,356203079
TFG	2,082162671	3,8689108	0,368225574
CCBL2	2,07864586	3,861927996	0,386444569
PDAP1	1,472437799	2,740916512	0,398446083
PSMB1	2,597936526	4,971187995	0,414880753
GLRX	2,427713358	4,589000059	0,42138052
SYNCRIP	2,770990184	5,38079684	0,439610481
KLC1	1,318148056	2,475963558	0,442950726
USP14	1,891362359	3,498987094	0,445399761
CLINT1	1,609622221	2,982143023	0,502355099
SPTBN1	1,414943049	2,641480165	0,573438644
GARS	2,120596624	3,945648026	0,575049877
SPTAN1	1,577522916	2,925158442	0,581540585
IDI1	1,454317021	2,709479061	0,669998646
STAT1	1,641216207	3,038576865	0,674937725
TMX3	2,874812424	5,637535352	0,734701157
TXNRD1	3,101347242	6,22879191	0,742181778
AKAP12	1,957386903	3,624999395	0,812675953
PYGL	1,527333378	2,836737298	0,84880209
PARK7	3,940141211	8,862895485	1,312864304

Downregulated proteins (with -Log10 p-value > 1.3) in decidualized EnSCs with or without DJ-1 knockdown, ranked by Student's T-test difference.

10. Declaration of Contributions

The work was carried out at the Research Institute for Women's Health at the University of Tübingen. The work presented herein was conducted under the guidance and supervision of of Prof. Sara Y. Brucker and Dr. Madhuri S. Salker.

With the exception of the steps mentioned below, all experiments and analyses were carried out independently by me: Immunofluorescence image acquisition was carried out with the assistance of Dr. Nisha Mohd Rafiq and Ms. Birgit Fehrenbacher. The mouse mating model was conducted at Department of Clinical Neurosciences, Hotchkiss Brain Institute, Cumming School of Medicine, University of Calgary by Dr. Alvin Joselin, Dr. Doo Soon Im and Dr. Gaurav Kaushik. The mouse implantation study was performed at Department of Physiology and Pathophysiology, Medical School, University of Rijeka by Dr. Biserka Mulac-Jericevic, Tatjana Daka and Tihana Vujnović. Human endometrial samples were collected at Reproductive Medicine Center, Department of Obstetrics and Gynecology, the First Affiliated Hospital of Anhui Medical University by Huanhuan Jiang. Embryo culture media was collected by Dr. Steffen Kull and Dr. Melanie Henes. Proteomics and the subsequent *in silico* analysis were performed by Anna Velic. Atomic force microscopy (AFM) for cell stiffness measurements was carried out by Emily Hellwich and Prof. Tilman Schäffer. Intracellular Calcium measurement was performed with the assistance of Dr. Jing Yan, Dr. Md. Alauddin and Prof. Florian Lang.

The statistical analysis presented in this thesis was performed independently by me.

The co-authors Dr. Madhuri Salker and Dr. Yogesh Singh supported me with their advice in the literature research, in the preparation and proofreading of the publication.

I hereby certify that I have written this thesis independently and have not used any sources other than those explicitly acknowledged and specified within the text.

11. Publications

The results of this thesis are part of an unpublished manuscript:

1. Yang Z, Yan J, Kull S, Alauddin Md. Brucker SY, Henes M, Lang F, Salker MS, **Embryo-derived trypsin-induced calcium entry is inhibited by endometrial infertility factor, LEFTY2.** Frontiers in Cell and Developmental Biology, Under Revision.

2. Yang Z, Hellwich E, Mohd Rafiq N, Joselin A, Soon Im D, Kaushik G, Singh Y, Mulac-Jericevic B, Jiang H, Brucker SY, Schäffer TE, Salker MS, **Loss of Parkinson's Disease Protein 7 upregulates ROS and cell migration and is associated with pregnancy loss**. BMC Molecular Medicine, Under Rivision.

Conferences:

1. Oral presentation at the 21. Arbeitskreis Molekularbiologie der Deutschen Gesellschaft für Reproduktionsmedizin (DGRM) (Weimar, Germany, 2022) and publication of the abstract in:

Yang Z, Singh Y, Brucker SY, Salker MS. **Loss of endometrial DJ-1 (PARK7) is associated with recurrent pregnancy loss.** Journal of Reproduktionsmedizin und Endokrinologie (2022).

2. Oral presentation at Netzwerktreffen Reproduktion (Augsburg, Germany, 2023).

3. Oral presentation at DFG-Sino meeting - Women's Reproductive Health (Tübingen, Germany, 2024).

Contributions to other manuscripts:

1. Okumura T, Raja Xavier JP, Pasternak J, **Yang Z**, Hang C, Nosirov B, Singh Y, Admard J, Brucker SY, Kommoss S, Takeda S, Staebler A, Lang F, Salker MS. **Rel Family**

Transcription Factor NFAT5 Upregulates COX2 via HIF-1α Activity in Ishikawa and HEC1a Cells. Int J Mol Sci. 2024 Mar 25;25(7):3666.

2. Štafl K, Trávníček M, Janovská A, Kučerová D, Pecnová Ľ, **Yang Z**, Stepanec V, Jech L, Salker MS, Hejnar J, Trejbalová K. **Receptor usage of Syncytin-1: ASCT2, but not ASCT1, is a functional receptor and effector of cell fusion in the human placenta.** Proc Natl Acad Sci U S A. 2024 Oct 29;121(44):e2407519121.

12. Acknowledgement

First and foremost, I extend my deepest appreciation to my supervisors, Prof. Sara Y. Brucker and Dr. Madhuri S. Salker. Their expert guidance, insightful feedback, and continuous support have been instrumental in shaping this thesis.

I would also like to extend my thanks to Dr. Yogesh Singh, whose invaluable advice on my publications and experiments has significantly enhanced the quality of my work.

Further, I am immensely grateful to Dr. Janet Raja Xavier and all the colleagues in Dr. Salker's group for teaching me essential laboratory techniques. Their collaboration, discussions, and willingness to share knowledge have enriched my research and made the process fulfilling.

Special thanks to my friends and my partner for their support and for being my source of joy and motivation. Their encouragement during challenging times have provided me with the strength and positivity to persevere.

Finally, I am profoundly grateful to my family for their support and encouragement during this academic journey. Their unwavering love, patience, and understanding have been my foundation.

To everyone who has contributed to this journey, I extend my deepest gratitude and heartfelt thanks.